平成 30 年度博士論文

Spatial distribution and mobility of metals and arsenic in river water and river bed sediments affected by copper mining activities in eastern Serbia

セルビア東部の銅鉱山開発活動の影響を受けた河川水および河川堆積物中の金属元素およびヒ素の分布と移動性

ステファン　ジョルジエフスキ

Stefan Đorđievski

博士工 9515252

秋田大学大学院

工学資源学研究科博士後期課程

資源学専攻

Abstract

Contamination of river water and river bed sediments caused by copper mining is a serious problem in many regions of the world. The main cause of contamination is generation of acid mine drainage (AMD) by weathering of sulfide minerals in overburden and flotation tailings. The processing of copper ores may generate additional quantities of wastewater. Flotation reagents that are used for mineral processing of copper ore may also cause adverse effects in aquatic environment. There are two copper mining areas in eastern Serbia, located around towns of Bor and Majdanpek. Mining operations in Bor and Majdanpek started in 1903 and 1961, respectively, and are still continuing. Numerous open pits, underground mines, overburden and flotation tailing ponds are present in both mining areas. However, copper smelter and refining facility is present only in Bor. The aim of this PhD thesis is to determine spatial distribution and mobility of metals and arsenic in river water and river bed sediments that were affected by mining activities in eastern Serbia.

Field survey for creation of geochemical maps was conducted in 2015 and early 2016. Total number of river water and river bed sediment samples was 198 and 181, respectively, with average sampling density of 1 sample per 42 and 46 km^2, respectively. Spatial distribution and mobility of 9 elements (Al, Mn, Fe, Ni, Cu, Zn, As, Cd, and Pb) in river water and river bed sediments were considered. Additional field surveys for determination of seasonal variation of concentrations of metals and arsenic were carried out in September 2016, February 2017, and August 2017.

Geochemical maps, histograms and cumulative probability (CP) diagrams were created for 9 elements in river water and river bed sediments from eastern Serbia. Variations of background and threshold concentrations were determined from histograms and CP diagrams. Spatial distribution of elements was determined from geochemical maps. Grouping of data points on histograms, CP diagrams and geochemical maps indicated patterns that were considered in detail. Minimum, median, mean, maximum, mean–2σ and mean+2σ values for 9 elements were calculated, and threshold values that separate background and anomalous concentrations were obtained from the brakes of slope on CP diagrams.

Concentration of Mn was decreased in river bed sediments that were in contact with acidic river water because of dissolution caused by acidic pH value. Higher concentrations of Ni were found in an area that consists of ultramafic rocks. High concentrations of Cu, Zn, As, Cd and Pb were found in river bed sediments downstream from Bor and Majdanpek copper mines; however, those concentrations were higher downstream from Bor copper mines. There

were no anomalous values of Al in river bed sediment. Higher concentrations of Fe were found in the region of Timok Magmatic Complex that consists of upper Cretaceous andesitic rocks. Concentration of Fe was also high in river bed sediments of Bor and Bela Rivers due to presence of Fe-rich minerals (pyrite, fayalite, magnetite) that originated from flotation tailings.

Water of rivers downstream from Bor copper mines was acidic. Geochemical maps of total and dissolved concentrations of metals and arsenic in river water showed that rivers downstream from Bor and Majdanpek copper mines were contaminated. Higher concentrations of metals and arsenic were more frequently found in water of rivers downstream from Bor copper mines. Metallurgical facilities in Bor had the largest impact on Bor River by discharging about 400 t of Cu per year through highly acidic wastewater (pH = 2.6). The highest measured concentrations of Cu in river water and sediments were 40 mg/L and 1.6%, respectively. Dissolution of calcite from limestone bedrock and a high concentration of bicarbonate ions in natural river water (about 250 mg/L) enhanced the neutralization of acidic river water and subsequent precipitation of metals and arsenic on the river bed. Decreases in the concentrations of Al, Fe, Cu, As, and Pb in river water were mainly due to precipitation on the river bed. On the other hand, dilution played an important role in the decreases in concentrations of Mn, Ni, Zn and Cd.

Instead of remediation of contaminated river bed sediments downstream from Bor mining area, natural attenuation of metals and arsenic should be monitored. However, in order to enhance the processes of natural attenuation, removal of sources of contaminanation is necessary.

Table of Contents

1. Introduction

1.1. Copper mining and environment

Contamination of water bodies caused by copper mining is a serious problem in many regions of the world (Rabadjieva et al. 2009; Oyarzún et al. 2013; Plathe et al. 2013). The main cause of contamination is generation of acid mine drainage (AMD) by weathering of sulfide minerals in mine wastes (Blowes et al., 2003). The processing of copper ores may generate additional quantities of wastewater with low pH and high contents of metals and arsenic. If it is not neutralized and decontaminated, these wastewaters pose a threat to the quality of natural river water and river sediments.

Two main types of mine wastes are generated by open-pit mining of copper ore: overburden (displaced waste rocks above the ore body) and flotation tailings (fine-grained gangue minerals that remain after recovery of valuable minerals from the ore). Production of copper concentrate by froth flotation generates large amounts of flotation tailings that are deposited in flotation tailing ponds. Failure of the flotation tailing dams may cause serious environmental consequences by uncontrolled spill of flotation tailings (Grimalt et al., 1999; Kossoff et al., 2014). Flotation of copper ores utilizes large quantities of flotation reagents. These organic compounds, such as polyethylene glycols, xanthates and mercaptobenzo-thiazole are released into flotation tailing ponds together with flotation tailings. They may leak into the groundwater and surface water, causing adverse effects (Hissner et al., 1999; Bararunyeretse et al., 2017; Đorđievski et al., 2017).

There are two copper mining areas in eastern Serbia, located around towns of Bor and Majdanpek. Mining operations in Bor and Majdanpek started in 1903 and 1961, respectively, and are still continuing. Numerous open pits, underground mines, overburden and flotation tailing ponds are present in both mining areas. However, copper smelter and refining facility is present only in Bor. Over 100 years of copper mining in this region has resulted in severe pollution of air, water and soil (Šerbula et al., 2017; Pejović et al., 2017; Alagić et al. 2015; Ranđelović et al., 2016). Elevated concentrations of metals and arsenic in river water and sediments downstream from these mines are already reported (Šerbula et al. 2016; Filimon et al., 2016). The aim of this PhD thesis is to determine spatial distribution and mobility of metals and arsenic in river water and river bed sediments that were affected by mining activity in eastern Serbia.

1.2. Variations of background and anomalous concentrations of metals and arsenic

Elevated concentrations of elements in river water and sediments may originate from mineral occurrences (natural process) or from the sources of pollution (anthropogenic factor). The range of concentrations measured in environmental matrices that do not have anthropogenic influence represent range of background concentrations. The concentration that divides background and range of anomalous concentrations is a threshold value. These values may be visualized using histograms, probability distribution diagrams, box plots and other statistical methods for representing structure of the data (Reimann et al., 2008). However, terms "geochemical background" and "threshold value" are not clearly and unambiguously defined in the literature, and are still the topic of discussion (Matschullat et al., 2000; Reimann and Garrett, 2005; Reimann et al., 2005; Reimann and Caritat, 2017).

Range of background concentrations and threshold values may vary from area to area. Thus, it is impossible to determine these values on the continental or global scale. Rather, background and threshold values should be determined on the regional scale (Reimann and Garret, 2005). Threshold values may be applied in environmental legislation as a maximum allowable concentration (MAC). Environmental matrices with element concentrations above MACs should be treated using some cleanup procedure in order to reduce elevated concentrations of elements. However, care should be taken because elevated concentrations may sometimes indicate natural mineral occurrences. In such cases, cleanup procedures may actually destroy natural environment with unique geochemical characteristics (Reimann and Caritat, 2017).

Geochemical maps are useful for visualization of spatial distribution of concentrations of elements in water, sediment, soil or other environmental matrices. Low and high concentrations are represented with different colors, and sampling points with concentration levels may be represented with different symbols on the map (dots, circles etc.). Geochemical maps with high and low sampling densities provide similar geochemical patterns, and similar background values of elements could be obtained using low-density maps, with lower cost compared to high density maps (Birke et al., 2015). Combination of statistical methods for showing the structure of data and geochemical maps may provide a better understanding of the variability of background range and threshold values (Reimann et al., 2008; Matschullat et al., 2000).

There were two continental-scale geochemical mapping projects in Europe. Field survey for FOREGS project was conducted between 1997 and 2001 in 26 European countries. In this project, a variety of parameters were measured in stream water, stream sediment, floodplain sediment (or alluvial soil), residual soil, and humus. Number of sampling points ranged from 385 to 852, depending on the type of samples (Salminen, 2005; De Vos and Tarvainen, 2006; Rodríguez-Lado et al., 2008; Buccianti, 2015). Another European geochemical mapping project was GEMAS project (geochemical mapping of agricultural soil), which aimed to determine concentrations of metals in agricultural and grazing soil of Europe. Field survey was carried out in 2008 and early 2009. Thirty-three (33) European countries participated in GEMAS project, with total 2108 samples of agricultural soil and 2024 samples of grazing land soil (Reimann et al., 2017). Republic of Serbia was included in GEMAS project, but not in the FOREGS project.

There was a project of geochemical mapping of soil in central Serbia that was conducted in several phases (Protić et al., 2005; Mrvić et al., 2009). Parameters that were measured included pH value of the soil, contents of metals, but also microbiological and organic parameters, such as 18 pesticides including atrazine and DDT (Protić et al., 2005). Mrivić et al. (2011a and 2011b) discussed contents of Ni and Cr in Braničevo, Bor and Zaječar provinces in eastern Serbia, as well as contents of other metals and arsenic only in Braničevo province. Pejović et al. (2017) conducted a study on variations of As contents in soil depending on climatic conditions and topographic exposure in the mountainous area northwest from Bor. However, no systematic geochemical survey regarding river water and river bed sediments in eastern Serbia was conducted. Eastern Serbia is a region with large impact of copper mining on the environment. Thus, it is important to distinguish between anthropogenic and natural concentrations of metals and arsenic. In this PhD thesis, areas with anthropogenic impact on river water and river bed sediments were located on the geochemical maps, and spatial distribution of metals and arsenic were discussed.

1.3. Mobility and natural attenuation of metals and arsenic in river water and river bed sediments

Mobility of metals in AMD-bearing river water is controlled by many factors such as mineralogy, geology, hydrology, biology and climate in the area as well as by seasonal variations of temperature, pH and Eh values in the river water (Nordstorm, 2011; Ogawa et al., 2012). Mobile species in aqueous phase may be present in particulate, colloidal and dissolved

forms (Casiot et al., 2009; Nystrand et al., 2012). Study of the distributions of these species in river water would provide an insight into the processes of dilution and precipitation of metals and arsenic throughout river systems.

Processes of natural attenuation are crucial for removal of potentially toxic elements and subsequent improvement in the ecological status of aquatic systems (Wilkin 2008; Elbaz-Poulichet et al., 2017). Dissolution of carbonate minerals in the catchments of acidified streams enhances the processes of natural attenuation by releasing calcium, magnesium and bicarbonate ions and by increasing pH and alkalinity of river water (España et al., 2005). An increase in the pH value of AMD-bearing river water favors formation of hydrous ferric oxides (HFO), which act as sorbents for metals and arsenic (Ogawa et al., 2012; Jia and Demopoulos, 2008). Concentrations of metals and arsenic in river water may be decreased by precipitation and immobilization in the river bed sediments. Metals from the contaminated sediments may be resuspended and redissolved as a result of floods, acidification and change of redox potential (Förstner 2004; Prica et al. 2010; Consani et al. 2017).

Nordstom (2011) and Wilkin (2008) gave extensive reviews on hydrogeochemical and natural attenuation processes that are playing an important role in reducing concentrations of metals in AMD-bearing river water. España et al. (2005) and Oyarzún et al. (2013) reported research on water chemistry in a catchment that lacked carbonate minerals to neutralize acidity of AMD discharges. In addition to the findings in those studies, our study showed mobility and natural attenuation processes of metals and arsenic in a catchment with widespread limestone bedrock, which enhances neutralization of AMD-bearing river water.

Several studies have been conducted on chemical characterization of wastewater effluents and river water around Bor copper mines (Korać and Kamberović, 2007; Milijašević et al., 2011; Brankov et al., 2012; Ishiyama et al., 2012; Stevanović et al., 2013; Gardić et al., 2015; Šerbula et al., 2016). Researchers have also studied bacterial communities in sediments from rivers in Bor mining area (Filimon et al., 2013; Filimon et al., 2016) and metal concentrations in fish species from Timok River as bio-indicators of aquatic pollution (Milošković et al. 2016). However, the mobility and natural attenuation of metals and arsenic in river water from Bor mines to the Danube River were not sufficiently examined in those studies. In order to clarify these processes, this PhD thesis determined variations in dissolved and particulate forms of metals and arsenic in river water, accumulation of metals and arsenic in river bed sediments, and hydrological and geological control of river water chemistry in rivers from Bor copper mines to the Danube River.

2. Study area

2.1. Geography of the study area

Study area is located in eastern Serbia (Fig. 2.1), and it includes watersheds of Timok River, Pek River and smaller tributaries of the transboundary Danube River (Fig. 2.2), with the total area of 8320 km^2. Watershed of Pek River (1230 km^2) is located completely within the borders of Serbia. Majority of the watershed of Timok River is located within the borders of Serbia (4500 km^2), except small areas in the east that belong to Bulgaria (100 km^2). Svrljig Timok River and Trgovište Timok River form White Timok River. White Timok River joins Black Timok River and form Timok River. Timok River flows into Danube River. Pek River is formed by junction of Small Pek River and Big Pek River, and it is also a tributary of Danube River. There are other smaller tributaries of Danube River in the study area: Poreč River, Jasenica River, etc.

Study area spreads across the territories of the following municipalities in eastern Serbia (Fig. 2.1): Veliko Gradište, Golubac, Kučevo (belonging to Braničevo province), Majdanpek, Kladovo, Negotin, Bor (belonging to Bor province), Zaječar, Boljevac, Knjaževac (belonging to Zaječar province) and Svrljig (belonging to Nišava province). The largest towns in the study area are Zaječar and Bor, with population of 38,000 and 34,000, respectively (2011 census).

Two copper mining areas are located around towns of Bor and Majdanpek (population of Majdanpek in 2011 was 7,700). Satellite images of Bor and Majdanpek mining areas are shown in Fig. 2.3. Smaller underground coal mines exist in the study area, as well as closed uranium mine near the village of Kalna. There are numerous limestone queries in the study area, and few quartz sand mines located near villages of Donja Bela Reka and Rgotina.

2.2. Bor copper mine

Mining operations in Bor started in 1903 and are still continuing. There are currently three active copper mines, open pit Veliki Krivelj, open pit Cerovo and underground mine Bor, and one closed mine, open pit Bor (Figs. 2.3 and 2.4 a). There are five flotation tailing ponds around the mines, and two of them are currently being used by two mineral processing plants in Bor and Veliki Krivelj. It was estimated that 700 Mt of mine waste is present in the overburden around open pits and in flotation tailing ponds (Figs. 2.3, 2.4b and 2.4c) (Bogdanović et al., 2011). These mines and mine wastes are acting as sources of AMD.

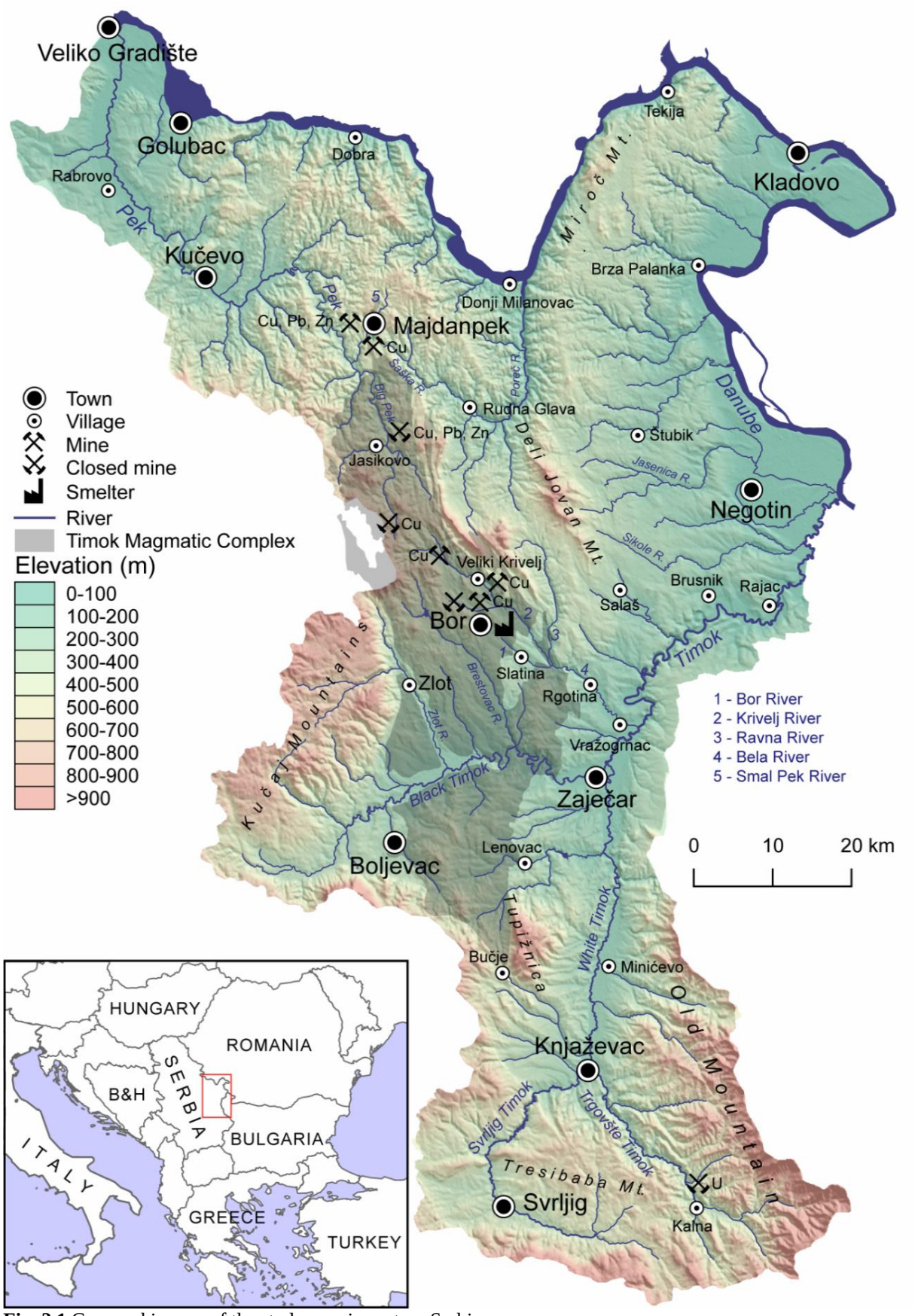

Fig. 2.1 Geographic map of the study area in eastern Serbia.

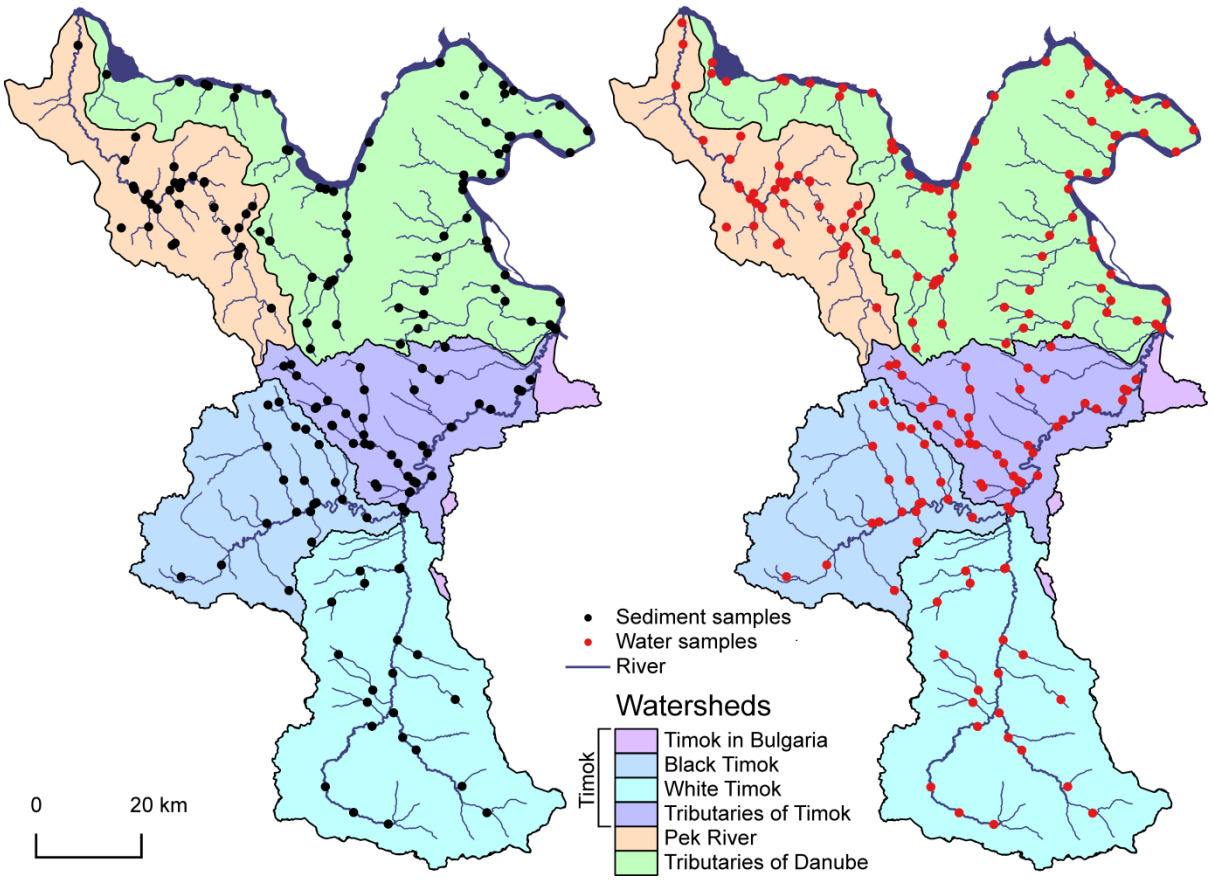

Fig. 2.2 Watershed areas of Timok River, Pek River and smaller tributaries of Danube River. Locations of sampling points of river bed sediment and river water samples are shown.

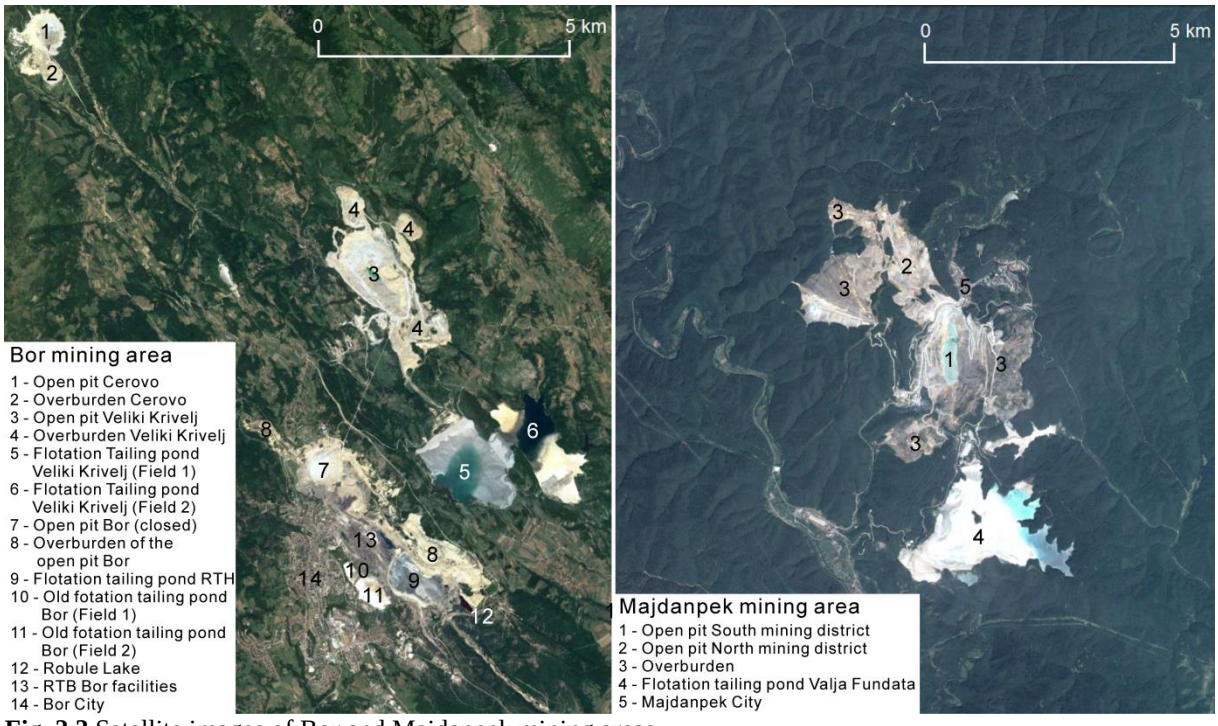

Fig. 2.3 Satellite images of Bor and Majdanpek mining areas

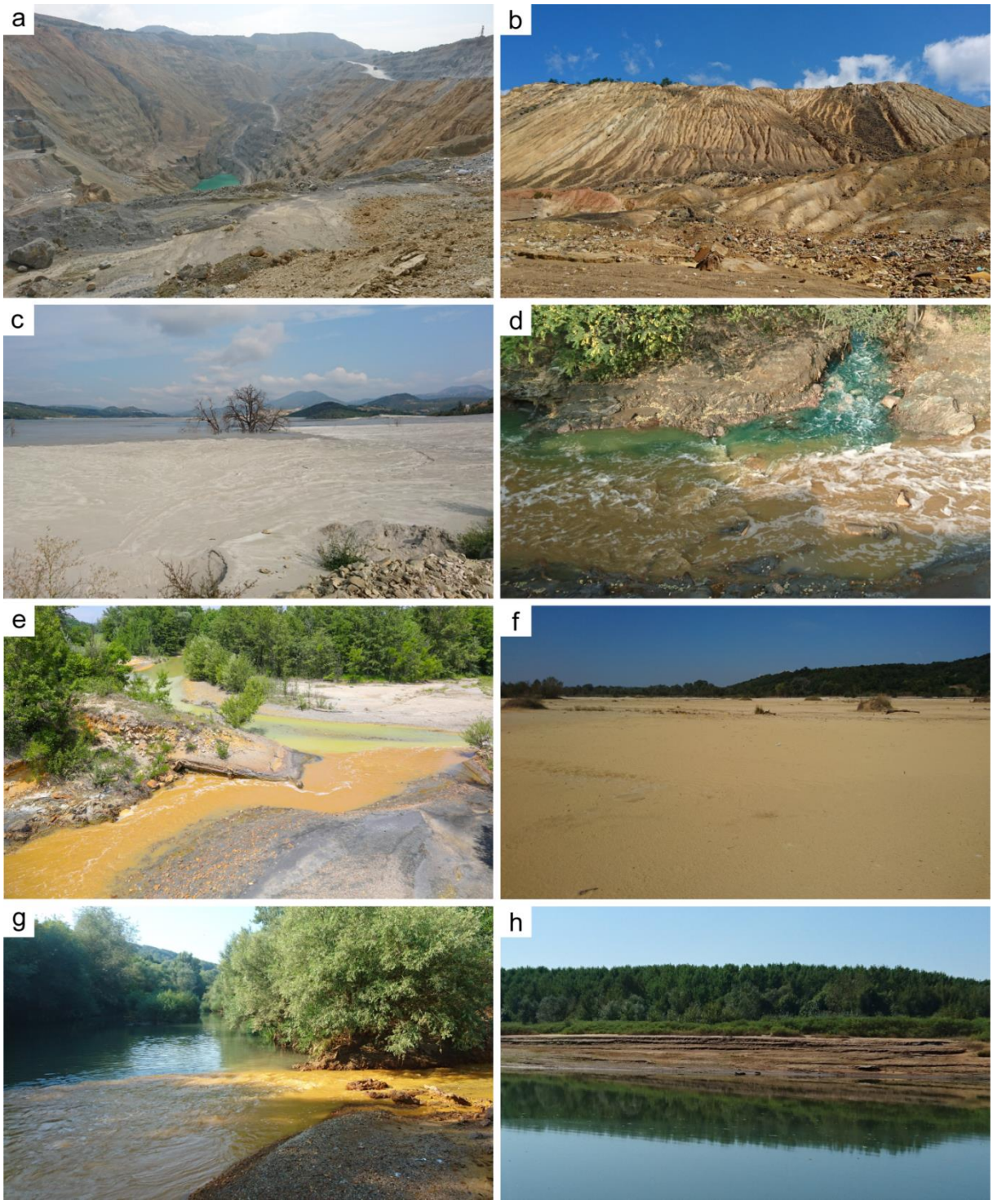

Fig. 2.4 Photographs showing environmental hotspots around Bor mining area. **a** Open pit Veliki Krivelj. **b** Overburden near S1. **c** Flotation tailing pond Veliki Krivelj. **d** Merging of greenish metallurgical wastewater (S3) into Bor River. **e** Confluence of Bor River (front) and Krivelj River (back). **f** Deposit of flotation tailings at the confluence of Bela River and Timok River. **g** Confluence of Bela River and Timok River. **h** Confluence of Timok River and Danube River

One of the largest mine waste dumps in Bor mining area is so called "Oštreljski Planir" (Fig. 2.4 b). This mine waste dump was formed by disposal of overburden from Bor open pit in the period from 1975 to 1980. Đorđievski et al. (2016) determined chemical and mineralogical composition of eight randomly chosen samples from Ošreljski planir by using x-ray fluorescence (XRF) and x-ray powder diffraction (XRD) analyses. It was found that concentrations of Cu, Fe, S and As in samples from waste dump were in range 0.02%–41.8%, 0.03%–21.5%, 2.3%–32.7%, and up to 3.6%, respectively. Very high concentrations of Cu and As were found only locally. Copper sulfide minerals (covellite, chalcopyrite and enargite) were detected in samples from the waste dump. The following gangue minerals were also detected in samples: quartz, albite, kaolinite, gypsum, siderite and pyrite.

Besides the copper mines and mine wastes, a copper smelter and metallurgical processing plants release highly acidic metallurgical wastewater into Bor River (Fig. 2.4d). Fine-grained flotation tailings have also been released into Bor River since the 1950s due to accidents in a mineral processing plant in Bor (Paunović, 2010; Bogdanović et al., 2014). These flotation tailings were transported by the water of Bor River and Bela River into Timok River. In the gorge of Timok River, a hydroelectric power plant named "Sokolovica" was constructed in 1948 by building a 17-m-high dam. The lake located upstream from the dam was filled by the flotation tailings, and flotation tailings were transported further downstream in spite of the dam. As a result, about 2000 ha of fertile soil in the floodplains of Timok River were covered by flotation tailings (Fig. 2.4f and 2.4h) (Bogdanović et al., 2014).

True-color Landsat satellite images of floodplains of Timok River in the area from Brusnik Village to the confluence with Danube River are shown in Fig. 2.5. The images were recorded in summer seasons of 1986, 1994, 2003 and 2014 during the days with minimal cloud cover. After Brusnik Village, the valley of Timok River becomes wider, which favors flooding and deposition of flotation tailings on floodplains. Area covered by flotation tailings is clearly distinguishable from the forests, grasslands and agricultural land due to the high reflection of the sunlight on flotation tailings (white area on the images). The images cover 28 years period, and if these images are visually compared, it can be seen that vegetation was recovered on the floodplains of Timok River by the year of 2014. During that period, no major release of flotation tailings from mineral processing plant in Bor has occurred. Natural recovery of vegetation on floodplains of Timok River may be considered as one form of natural attenuation of contaminants that originate from mining activity (Wilikin, 2008). Characteristics of newly-grown vegetation on floodplains of Timok River are described by Nikolić et al. (2016).

Bor copper deposits are located in the upper Cretaceous Timok Magmatic Complex (Fig. 2.1), which belongs to Banat-Timok-Srednogorie arc located in Romania, Serbia and Bulgaria. The main orebodies are located along the fault with a northwest-southeast direction. The upper and lower parts of the deposits consist of massive sulfide ores and porphyry copper ores, respectively. The ore minerals in the massive sulfide orebodies consist of enargite, chalcocite, covellite, bornite and chalcopyrite, and the ore minerals in the porphyry copper orebodies consist of pyrite, chalcopyrite, magnetite and molybdenite (Koželj, 2002). Sulfide minerals are exposed to weathering in the open pits, overburden and flotation tailing ponds, and they act as a source of AMD (Đorđievski et al., 2016; Stevanović et al., 2011). Although the majority of massive sulfide orebodies have been excavated, a large mining potential still exists in the region due to new discovered high-grade deposits (Jelenković et al., 2016). In addition to igneous rocks, Jurassic and Cretaceous limestone rocks are also abundant in the catchment of Timok River, especially in its western part. The region is well-known for its karst landscapes and aquifers that are being used for water supply (Stevanović and Dragišić, 1998; Stevanović et al., 2007).

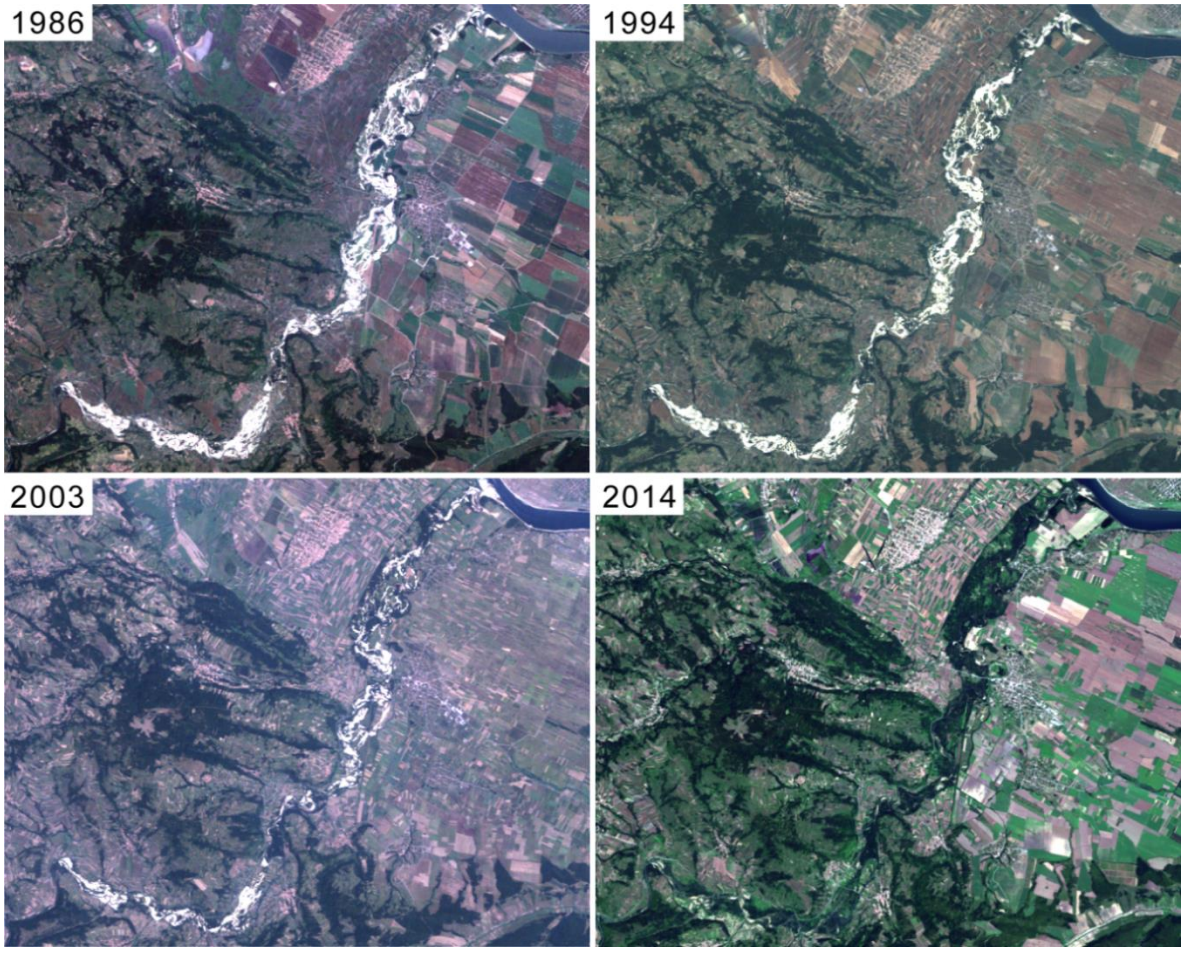

Fig. 2.5 Landsat satellite images of floodplains of Timok River from 1986, 1994, 2003 and 2014 (area from Brusnik Village to the confluence with Danube River)

Bor mining area belongs to the drainage system of Timok River, which is the tributary of the transboundary Danube River (Fig. 2.1). Areas with lower altitude in the watershed of Timok River receive about 600 mm of precipitation per year, while the mountainous areas receive up to 1500 mm (Đurović and Živković, 2013). A hydrograph of Black Timok River (tributary of Timok River) is shown in Fig. 2.6. This hydrograph represents the flow regime of rivers in the study area. As the figure shows, there are drastic changes in discharge of rivers during the year. The greatest discharge occurs during the snowmelt season in March and April, and the period of smallest discharge is during August and September. The greatest discharge of Black Timok River in 2015 was recorded on 6th March, and the smallest discharge was recorded on 13th August (66.2 and 0.58 $m^3 s^{-1}$, respectively). The hydrological data presented here were obtained from the Hydro-meteorological Service of the Republic of Serbia.

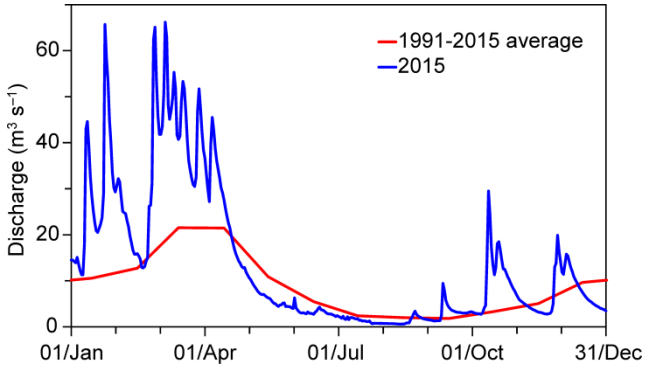

Fig. 2.6 Hydrograph of Black Timok River (tributary of Timok River) near the town of Zaječar. The red line represents average monthly discharge in the period 1991–2015. The blue line represents daily discharge in 2015

2.3. Majdanpek copper mine

Majdanpek copper mine is located in the northernmost part of the Timok Magmatic Complex (Fig. 2.1). Ore deposits are located in the Late Cretaceous andesitic dike complex that is 5 km long and 300 m wide. The dyke intruded into the north-south trading fracture zone in Proterozoic to Cambrian metamorphic rocks, Triassic clastic rocks and Jurassic limestone (Armstong et al., 2005). Before the exploitation of porphyry copper ores in Majdanpek started in 1961, limonite and pyrite ores were mined for iron production. Current mining activities in Majdanpek are carried out in two open pits – South Mining District (South Revir, Fig. 2.5 b) and North Mining District (North Revir). Stockwork and disseminated styles of porphyry copper mineralization are present in South mining District. Main ore minerals are chalcopyrite, pyrite, magnetite and molybdenite. On the other hand, North mining district consists of several porphyry and massive sulfide orebodies, including polymetallic sulfidic Cu-Zn-Pb orebodies (Armstong et al., 2005). Copper concentrate from Majdanpek is produced in mineral processing plant in Majdanpek and transported to smelter in Bor by railway.

Overburden in Majdanpek is deposited on several locations around the open pits. Flotation tailings from the mineral processing plant in Majdanpek are deposited in the flotation tailing pond Valja Fundata located on the underlaying karst terrain. An accident occurred in 1974 in flotation tailing pond Valja Fundata due to the leak of flotation tailings through the limestone caves into the Pek River (Lekovski et al., 2013). Environmental issues exist in the Majdanpek due to the dust that is raised by the wind from the open pit South mining district and surrounding overburden (Mikić et al., 2015).

The Majdanpek mine is located mainly in the watershed of Pek River, and one smaller part of Majdanpek Mine is located in the watershed of Šaška River. The wastewater from Majdanpek mine is released into Small Pek River. Small Pek River passes through Majdanpek City and around open pit South mining district (Fig. 2.7 a and b). The bottom of the open pit South mining district is filled by near-neutral AMD (pH = 6.84, Marković et al., 2015). In order to access the deepest portion of the open pit, AMD has to be pumped out and purified before releasing into the Small Pek River, and this issue is a serious environmental problem (Marković et al., 2015). Small Pek River and Big Pek River join and form Pek River that flows through town of Kučevo and merges with Danube River near the town of Veliko Gradište (Figs. 2.1 and 2.7 c). Danube River is a border between Sebia and Romania, and it is also northen border of the study area (Figs. 2.1 and 2.7 d).

Fig. 2.7 Photographs showing rivers in Majdanpek mining area. **a** Small Pek River in Majdanpek City. **b** Small Pek River passing around open pit South mining district. **c** Pek River 2 km downstream from Kučevo Town. **d** Danube River near Donji Milanovac Town

3. Materials and methods

3.1. Field surveys

Field survey for creation of geochemical maps was conducted in summer of 2015 and early 2016. Sampling and sample preparation were carried out by the author and stuff of Mining and Metallurgy Institute Bor (Serbia). Total number of water and sediment samples was 198 and 181, respectively, with average sampling density of 1 sample per 42 and 46 km^2, respectively. Sampling points were not evenly distributed across the study area (Fig. 2.2). For example, no samples were taken in the northern part of the study area around the Miroč Mountain. On the other hand, area with the high sampling density is located upstream from the town of Kučevo (Fig. 2.2).

Discharge of the rivers was calculated by measuring the average speed of river water using a digital chronometer and by measuring the average depth and width of the river at the sampling points (Fig. 3.1 a). However, direct measurement of discharge of Timok River was not possible. Thus, the discharge value for Timok River at P7 was calculated by summation of discharges of two major upstream tributaries (White Timok River and Black Timok River), and discharge of Timok River at P8, P9 and P10 was calculated by adding the discharge of Bela River (P6) to the discharge of Timok River at P7. Discharge of the Danube River was not measured.

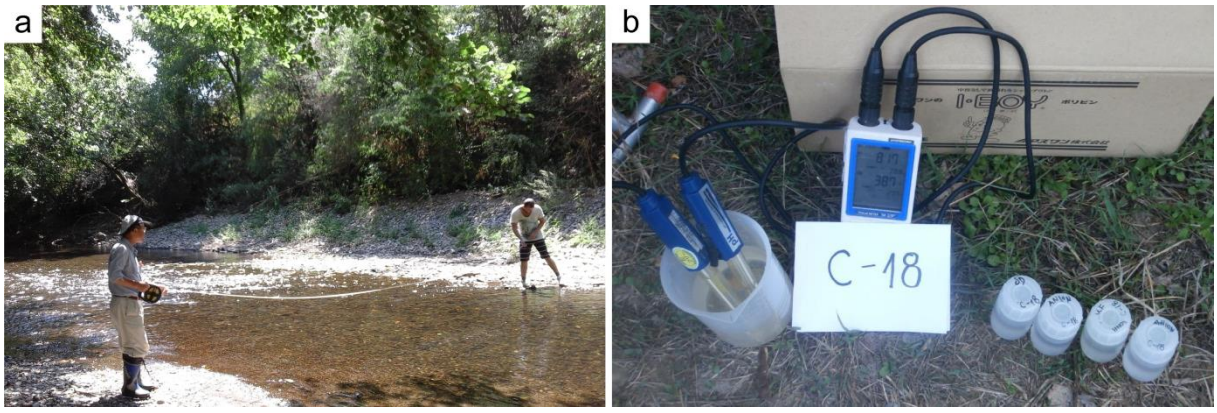

Fig. 3.1 Field measurements in 2015. **a** Measurement of discharge (flow rate) of Black Timok River. **b** Measurement of pH and Eh value, and collection of water samples in polypropylene bottles

Values of pH and Eh were measured in the field using a combined handheld Ion/pH meter, model IM-23P (Fig. 3.1 b). Unfiltered and filtered water samples were collected in 50-ml polypropylene bottles, and filtration of water was carried out in the field using cellulose acetate hydrophilic filters with a pore size of 0.20 μm. Unfiltered and filtered river water

samples for analysis of metals and arsenic were immediately acidified by addition of 2.5 ml concentrated nitric acid. Filtered samples for analysis of anions were not acidified with nitric acid. Sediment samples on the river bed were collected in plastic bags using a shovel at random positions under the river water, and the samples were dried at room temperature and sieved to obtain <180-μm fractions.

Additional field surveys were carried out in September 2016, February 2017, and August 2017 in area downstream from Bor copper mines. Measurements of pH, Eh and discharge were carried out using same procedure as that during the field survey for creation of geochemical maps. Electrical conductivity (EC) was additionally measured using field conductometer. Three types of river water samples were collected at 10 sampling points: Unfiltered samples, filtered samples (<0.2 μm) and ultrafiltered samples (<3000 Da, which is approximately <6 nm). Ultrafiltration was carried out in laboratory of Mining and Metallurgy Institute Bor immediately after the collection of filtered river water samples in the field. Filtered samples that were supposed to be ultrafiltered were transported in refrigerator from the field to the laboratory. Ultrafiltered samples contained dissolved species, filtered samples contained dissolved and colloidal species, and unfiltered samples contained particulate, colloidal and dissolved species. Concentration of elements in colloidal form was calculated by subtraction of concentration of elements in filtered and concentration of elements in ultrafiltered water samples. Concentration of elements in particulate form was calculated by subtraction of concentration of elements in unfiltered and filtered water samples. In September 2016, a sample of ochreous precipitates was collected at the confluence of Bela River and Timok River. In August 2017, samples of efflorescent sulfate salts were collected near the sources of AMD in Bor mining area.

3.2. Analyses of samples

Chemical analyses of water and sediment samples for creation of geochemical maps were carried out in Activation Laboratories Ltd., Canada. In water samples, metals and arsenic were analyzed using inductively coupled plasma mass spectrometry (ICP-MS), and anions were analyzed using ion chromatography (IC). Sediment samples were dissolved by total digestion, and metals in the obtained solutions were analyzed using ICP-MS, except for Fe and As, which were analyzed by using instrumental neutron activation analysis (INAA).

Accuracy of the measurements of metals and arsenic in water and sediment samples was assessed by analysis of stock solutions and certified reference materials, respectively.

Concentrations of metals, arsenic and anions in method blanks were below limits of detection (LOD). Differences between measured and certified values (accuracy) and limits of detection of metals, arsenic and anions are shown in Tables 6.2, 6.3 and 6.4.

Filtered samples consisted of particles with sizes <0.20 μm, which may include dissolved and colloidal species (Tang et al., 2001; Waeles et al., 2015). For simplicity, this fraction is reffered as dissolved, even though it may also contain colloidal species. Metals in unfiltered samples are present as particulate, colloidal and dissolved forms. Concentrations of metals in particulate form were calculated by subtraction of concentrations in unfiltered and filtered samples.

River water samples that were collected during the field surveys in September 2016, February 2017, and August 2017 were analyzed at Akita University. Concentrations of Al, Mn, Ni, Cu, Zn, As, Cd, and Pb were measured by ICP-MS, and Fe was measured by Flame Atomic Absorption Spectrometry (FAAS).

X-ray diffraction (XRD) analysis of powdered river bed sediment samples was carried out in Mining and Metallurgy Institute Bor using Rigaku MiniFlex600 diffractometer equipped with a Cu anode X-ray tube and D/teX Ultra 250 silicon strip detector. Same fractions (<180 μm) of same sediment samples (RS1-RS10) were used for XRD and chemical analyses. X-ray diffraction (XRD) measurements of powdered efflorescent sulfate salts and ochreous muds were carried out using a Rigaku MiniFlex II diffractometer equipped with a Cu anode X-ray tube and secondary monochromator at Akita University.

3.3. Data processing

If plotted on histogram, geochemical data will show distribution close to the log-normal distribution (Reimann and Filzmoser, 2000). In ideal case, log-transformed set of geochemical data will give histogram that resembles bell shape. However, this is not the case for most of the real geochemical data sets. Several geochemical processes may take place in one study area, and each of these processes may give separate sets of values with log-normal distributions. Such data set shows multimodal distribution, having several interfering bell-shape distributions on one histogram. Extreme concentrations may appear in the dataset from the area that has some pollution or mineral occurrences. These values may sometimes be several orders of magnitude larger than the majority of the values from the dataset. If data is plotted on histogram in linear scale, the data set with extreme values will show one large column on the left side of the histogram, corresponding to the background values, and several

smaller columns in the middle and on the right side, corresponding to the anomalous values. However, if the data set is plotted on the logarithmic scale, the histogram will acquire bell-shape on the left side, with several smaller columns on the right side. Therefore, it is more practical to use log-transformed geochemical data set (or data set plotted on logarithmic scale) for interpretation of the data structure.

Histograms and cumulative probability (CP) diagrams in combination with geochemical maps were used in this PhD thesis to examine distribution of metals and arsenic concentrations in river bed sediments and river water (Figs. 4.1, 5.1, 5.2, and 4.3). Concentrations of metals and arsenic were plotted on histograms in logarithmic scale versus number of samples that belong to particular concentration range. Concentration of each data point was plotted on CP diagram versus its percentile shown in probability scale. In order to calculate percentile of each data point, concentrations for each element were first sorted from smallest to largest, and then order numbers of each data point were divided by total number of samples + 1, and multiplied by 100% (Percentile = order number / (total number + 1) · 100%). Histograms and CP diagrams were created using combination of Microsoft Excel and Origin software.

If the data set that shows log-normal distribution is plotted on the CP diagram, the data points would be arranged along the straight line. If the data set that shows log-normal distribution, and have few extreme values (anomalous values, outliers) is plotted on CP diagram, the upper part of the straight line would bend. In that case, extreme values will depart from the straight line because these values do not belong to the log-normal distribution. However, if the data set shows multimodal distribution (having several log-normal distributions originating from different geochemical processes), the plot on the CP diagram would be more complicated. Generally, each log-normal distribution in the dataset would be represented by straight line, and brake in slope of the curve would indicate the boundary between two distributions. On CP diagrams in Figs. 4.1, 5.1 and 5.2, data points that belong to background range are shown in black color and data points that belong to different distributions are shown in different colors (blue, orange, and red). The brake of slope on CP curve is used in this PhD thesis for determination of the threshold value between background range of concentrations and extreme concentrations of metals and arsenic in river bed sediments and river water. This method was suggested as one of the most appropriate methods for determination of variation of background and threshold values of concentrations of metals in environmental samples (Reimann and Caritat, 2017; Reimann et al., 2017). Other

methods that could be employed for determination of background range and threshold values are: mean + 2σ, median + 2 median absolute deviations (MAD), Tukey boxplots, 95^{th} or 98^{th} percentiles, etc. (Reimann and Caritat, 2017; Matschullat et al., 2000).

Geochemical maps are created in QGIS software using two methods: proportional circles and inverse distance weighting (IDW) interpolation. Basemap of the geochemical maps is consisted of the river network, and the boundaries of interpolated area correspond to the boundaries of the study area. Log-transformed data was used for the interpolation, and the values in the legend are then back-transformed from logarithms into the original values. Interpolation of the area predicts concentration values at places where samples were not taken. In that way, it is possible to have an idea of a general tendency in the metal concentrations in some area. However, this method has some limitations, because these predictions are very often biased, and may lead to false conclusions about the concentrations in some areas, especially for maps with low-density sampling. Because of that, proportional circles are added on the geochemical maps in this PhD study in order to make clear about the exact position and concentration value at each sampling point. Circles with smaller radius correspond to smaller concentrations, and circles with larger radius correspond to larger concentrations. Colors of the circles are related to the colors of the data points on the CP diagrams and columns on the histogram for each element. In that way, each data point from the CP diagram that belongs (for example) to the red group is plotted on the geochemical map in the same color. Simultaneous grouping of the points with the same color on the map, CP diagram and histogram indicates some pattern that needs more detailed consideration.

Standard deviations (σ), minimum, median and maximum values, as well as mean (average) values for each element were calculated in Microsoft Excel spreadsheet. Some researchers suggested that mean + 2σ may be employed for calculation of threshold value between background range and anomalous values in the dataset; however, in some cases results obtained by this method are disputed by other researchers (Reimann et al., 2005). In this PhD thesis, mean + 2σ values were calculated using both log-transformed and original concentration values, and obtained values are compared with thresholds that were obtained from the CP diagrams. Mean (average) values were also calculated using both log-transformed and original concentration values.

4. Variations of background and anomalous concentrations of metals and arsenic in river bed sediments

Statistical summary of concentrations of metals and arsenic in river bed sediments are shown in Table 4.1. Minimum, median, mean and maximum values of concentrations of 9 elements (Al, Mn, Fe, Ni, Cu, Zn, As, Cd and Pb) are shown, as well as standard deviations (σ), mean–2σ, mean+2σ, and threshold values obtained from CP diagrams (CP1 and CP2). Additionaly, mean, σ, mean–2σ and mean+2σ were calculated using log-transformed data, and then the values were back-transformed into the original values. Minimum, median and maximum values are same when they were calculated from original data and log-transformed data. Mean–2σ values that were calculated from original data are negative for all elements except for Al. Because the concentration of an element in river bed sediment cannot be negative, this calculation may not be appropriate. When mean–2σ calculation was performed using log-transformed data, no negative values were obtained (Table 4.1).

Geochemical maps, histograms and CP diagrams for 9 elements (Al, Mn, Fe, Ni, Cu, Zn, As, Cd, and Pb) in river bed sediments from eastern Serbia are shown in Fig. 4.1. Median, mean (calculated both using original and log-transformed concentrations) and statistically calculated threshold valus using log-transformed concentrations (mean–2σ and mean+2σ) are shown in histograms and CP diagrams.

Table 4.1 Statistical summary of concentrations of metals and arsenic in river bed sediment

		Unit	min	median	mean	max	σ	mean–2σ	Mean+2σ	CP1	CP2
Al	orig	%	2.5	6.0	5.8	9.4	1.2	3.5	8.2	n.d.	n.d.
	log				5.7		1.2	3.7	8.9		
Mn	orig	mg/kg	69	1060	1186	6810	813	-441	2812	500*	4000
	log				972		1.9	260	3634		
Fe	orig	%	0.9	4.7	6.6	31	5.6	-4.6	17.9	7	n.d.
	log				5.1		2.0	1.3	20		
Ni	orig	mg/kg	4.6	30	39	619	51	-64	142	65	n.d.
	log				30		1.9	7.9	112		
Cu	orig	mg/kg	3.1	50	990	26400	3114	-5238	7219	90	4000
	log				92		6.8	2.0	4195		
Zn	orig	mg/kg	12	88	338	4080	704	-1071	1747	150	1000
	log				124		3.3	12	1329		
As	orig	mg/kg	2.1	12	63	1600	173	-282	409	23	300
	log				17		3.6	1.3	227		
Cd	orig	mg/kg	0.05	0.20	0.88	25	2.5	-4.1	5.8	0.55	n.d.
	log				0.27		3.8	0.02	3.9		
Pb	orig	mg/kg	7.8	22	55	719	97	-138	248	31	100
	log				30		2.5	4.9	184		

orig – values obtained from original data; log – values obtained from log-transformed data

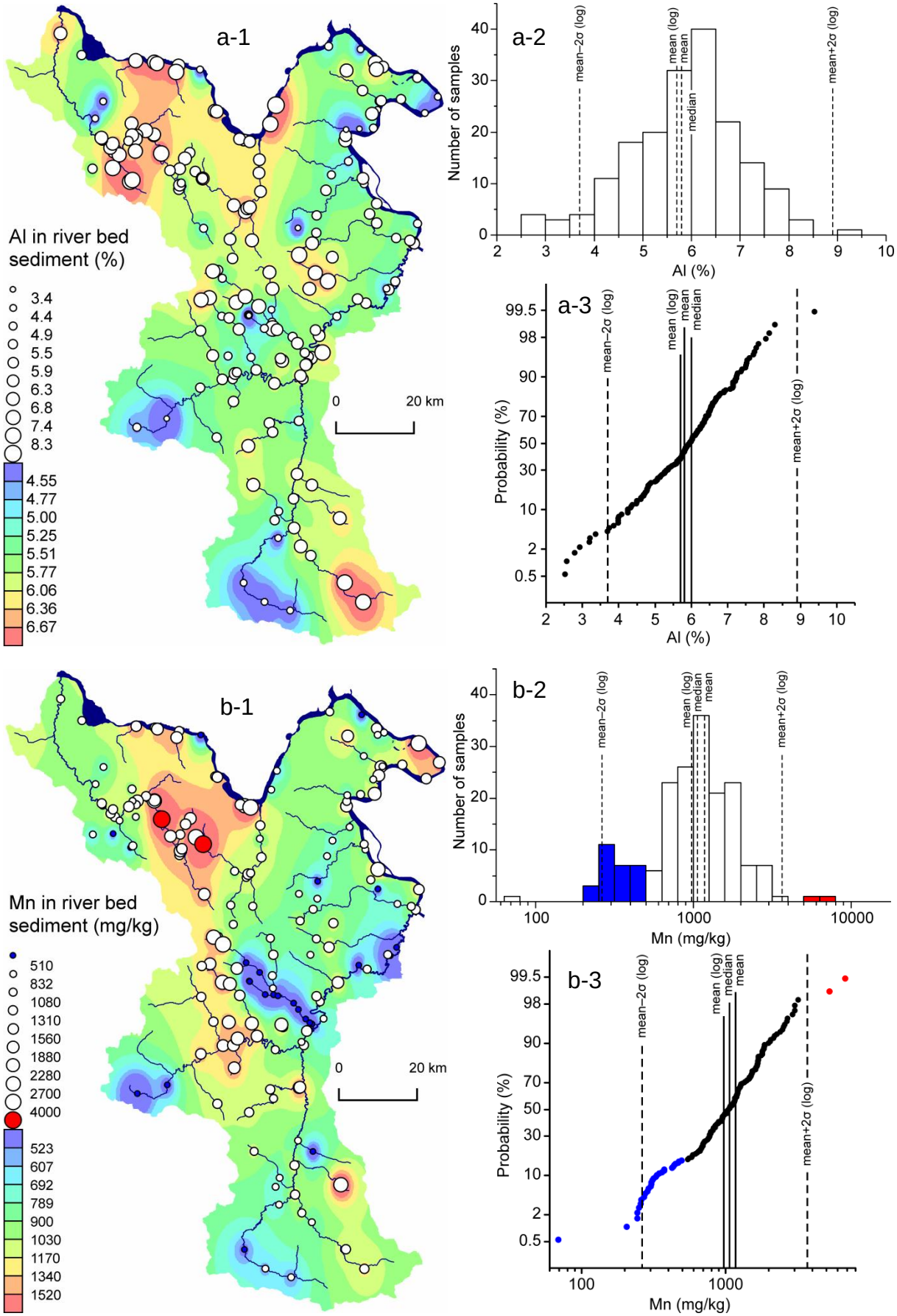

Fig. 4.1 Geochemical maps, histograms and CP diagrams for 9 elements in river bed sediments from eastern Serbia. **a** Al. **b** Mn. **c** Fe. **d** Ni. **e** Cu. **f** Zn. **g** As. **h** Cd. **i** Pb

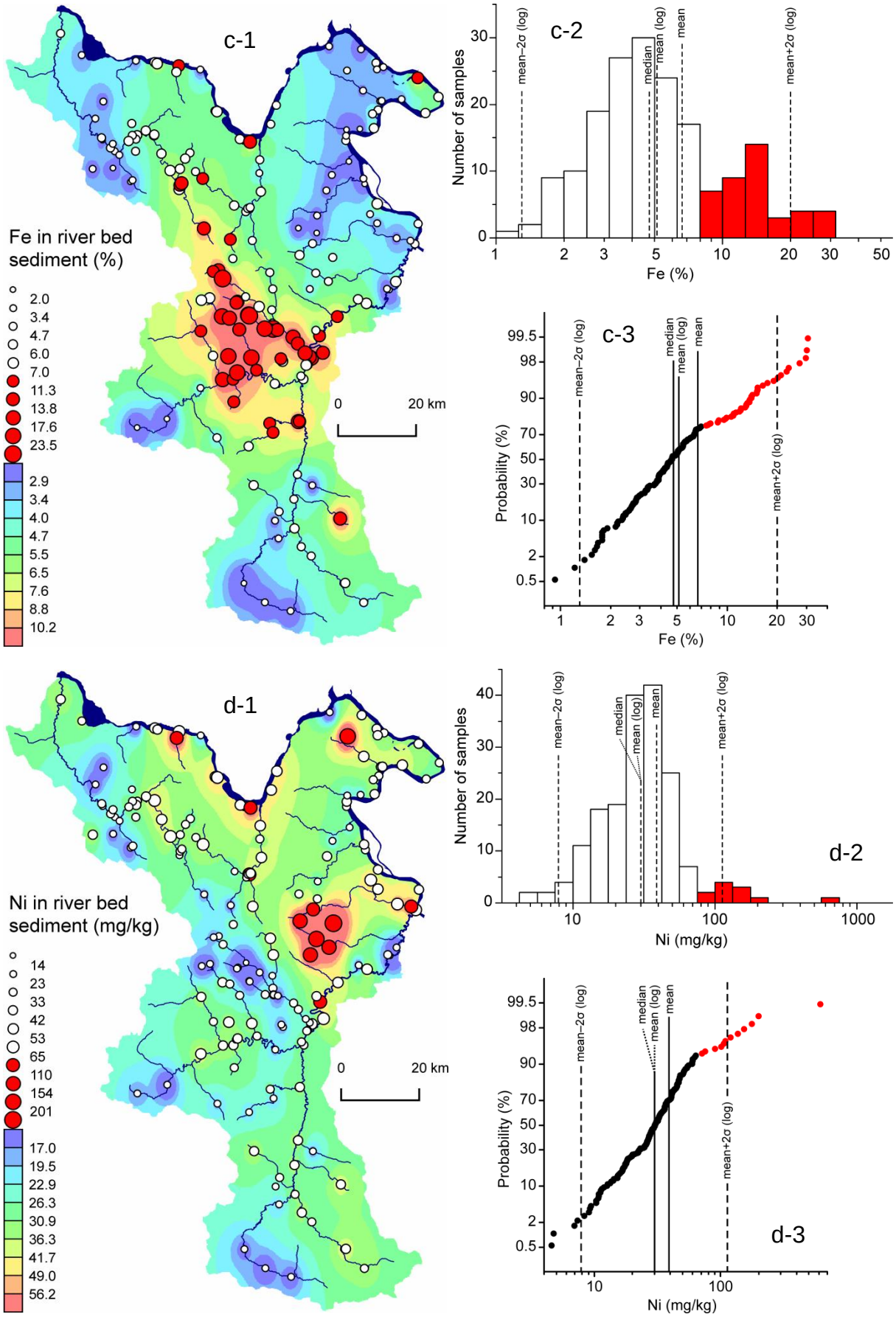

Fig. 4.1 (continued)

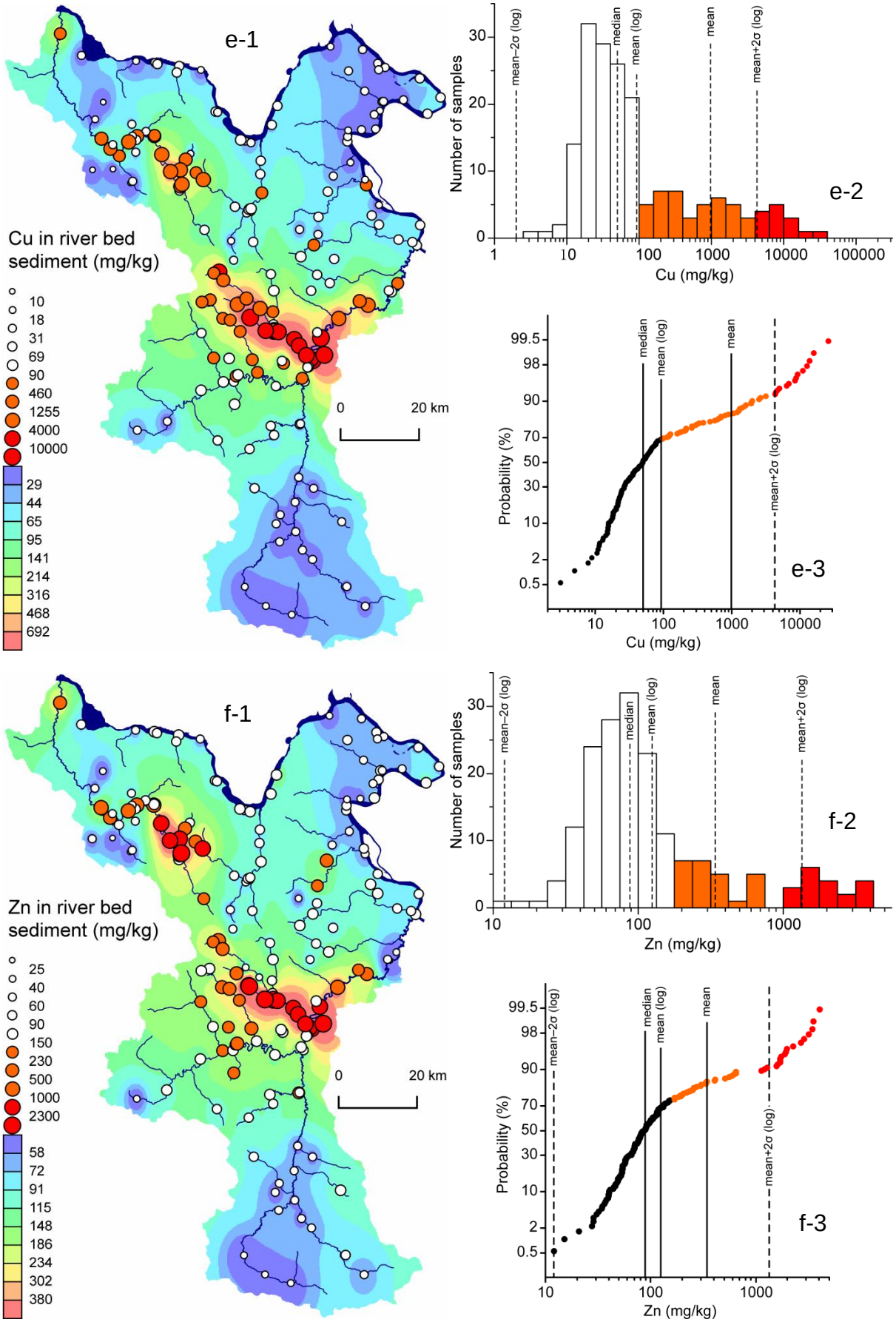

Fig. 4.1 (continued)

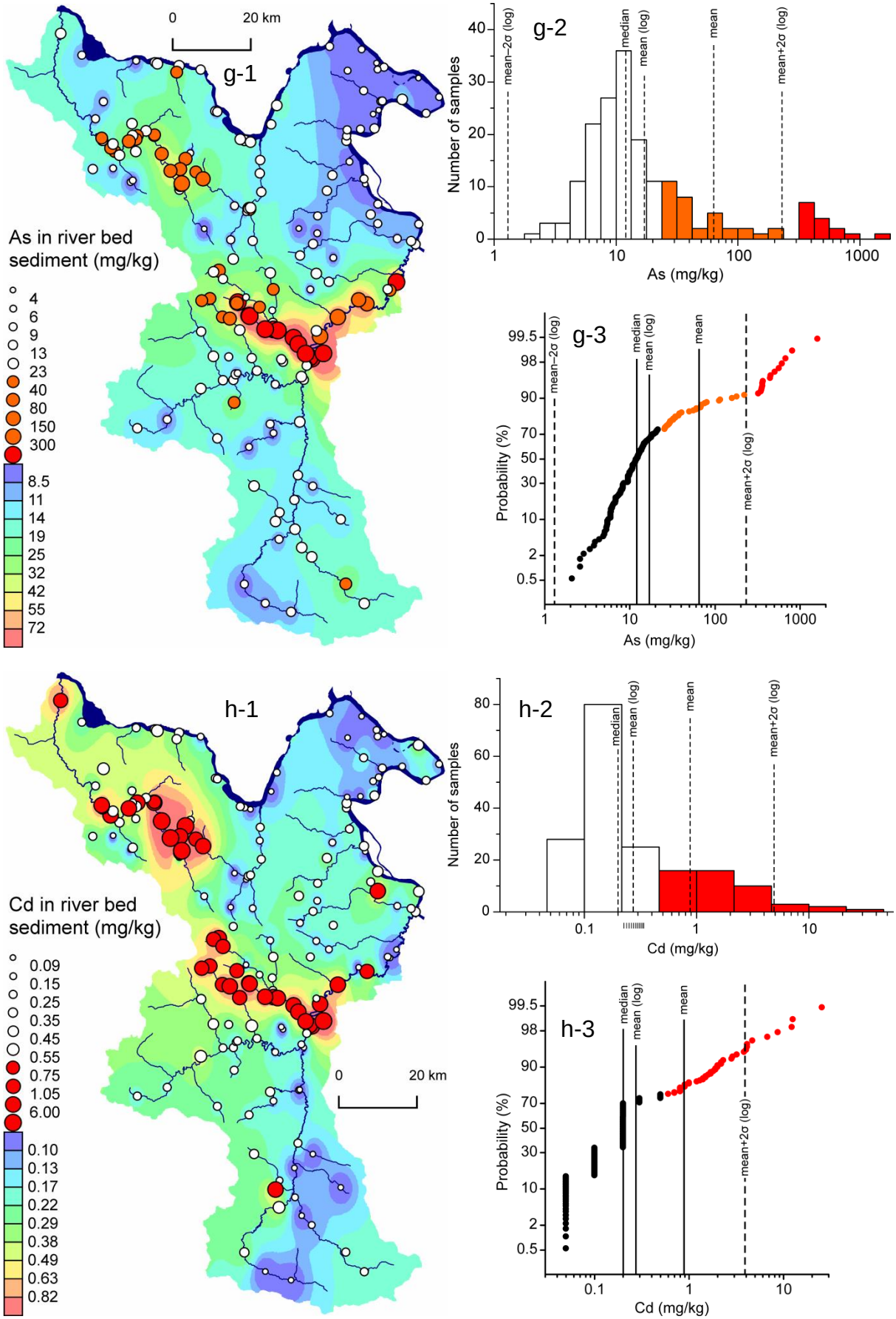

Fig. 4.1 (continued)

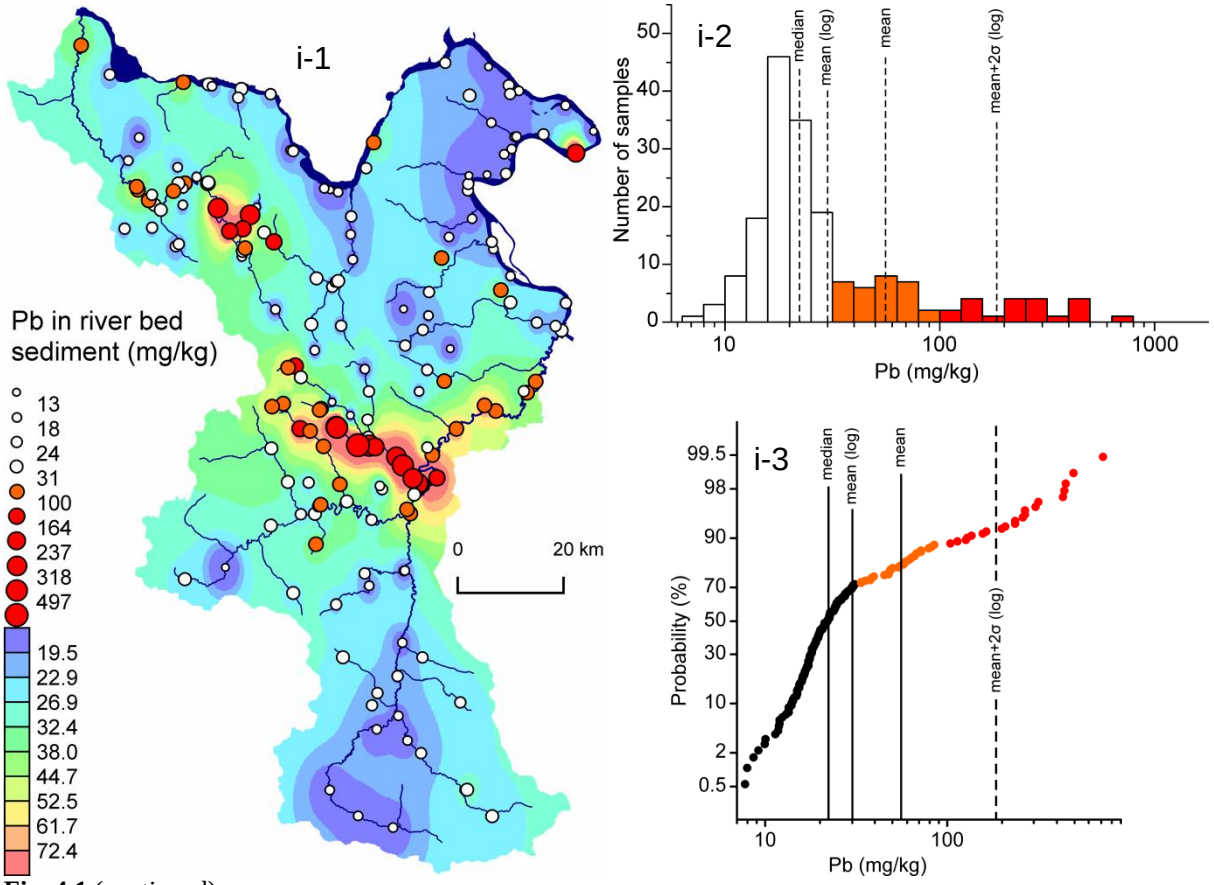

Fig. 4.1 (continued)

Aluminium (Al)

Horizontal axis on histogram and CP diagram for Al is shown in linear scale (Fig. 4.1) because distribution of concentrations of this element in river bed sediments is close to normal (not close to log-normal distribution). If concentrations of Al were plotted on logarithmic scale, histogram would have been skewed on the right side, and curve on CP diagram would have been less straight. Whether concentrations of Al were plotted on linear or logarithmic scale, the CP curve would not show any distinct brake in slope. This indicates that there are no significant outliers for Al in river bed sediment, except few lowest and highest values that are randomly distributed in the geochemical map.

Manganese (Mn)

There are two upper outlayer values for manganese in river bed sediments located in Pek River and Šaška River near Majdanpek (5320 and 6810 mg/kg, respectively). Based on the break on the CP diagram, upper threshold for Mn is around 4000 mg/kg (Fig. 4.1 and Table 4.1). Mean + 2σ value for Mn that was calculated from log-transformed data (3634 mg/kg) was similar to the value that was estimated from the CP diagram. However, Mn

showed distinct brake of slope on CP diagram at lower concentration values. Based on the brake of slope on CP diagram, lower threshold for Mn was 500 mg/kg. Values below 500 mg/kg are shown in blue color on CP diagram, histogram and geochemical map of Mn. Grouping of the values below 500 mg/kg in the geochemical map was located along Bor River, Krivelj River and Bela River, downstream from the Bor copper mines. The data suggests that acidic water of these rivers leached out manganese from the river bed sediment. There were also randomly distributed sampling points with concentration of Mn lower than 500 mg/kg. Low concentration of manganese in these randomly distributed points was due to some other unknown geochemical process. Other elements in river bed sediments from eastern Serbia did not show the distributions of concentrations as Mn.

Iron (Fe)

CP diagram of Fe in river bed sediment shows distinct brake in slope at 7%. Concentrations of Fe in river bed sediment that were higher than 7% are shown in red color on histogram, CP diagram and geochemical map. This upper threshold value was close to the arithmetic mean for Fe content in river bed sediment (6.6%). Mean + 2σ (log) was much higher (20%) than the threshold value determined using the break of slope on CP diagram. Sampling points with Fe content higher than 7% are present in the area of Timok Magmatic Complex, and along the area of Bor River and Bela River. Grouping in the area of Timok Magmatic Complex is thought to be due to natural geological processes. However, grouping along Bor River and Bela River is thought to be due to the high content of Fe-bearing minerals in river bed sediment (pyrite, magnetite, and fayalite) that were released from the mineral processing plant in Bor, and mechanically transported downstream by the river water.

Nickel (Ni)

Area with high Ni content in river bed sediment is located at the eastern slopes of Deli Jovan Mountain. This anomaly is thought to be related to the ultramafic rocks that are present in that area (not related to the pollution). CP diagram of Ni shows brake in slope at 65 mg/kg. Few sampling points that exceed 65 mg/kg are randomly distributed in the study area. This is an example of distribution of element showing no pollution-related anomalous concentrations.

Copper (Cu)

Two threshold values are determined for Cu using CP diagram, namely 90 mg/kg and 4000 mg/kg. Values that exceeded 4000 mg/kg are located downstream from Bor copper mines (along Bor River, Bela River and in the Timok River after the confluence with Bela River). Values that exceeded 90 mg/kg are located in wider area downstream from Bor and Majdanpek copper mines, but also along Brestovac River which did not have an impact of mining activity. It is difficult to determine whether some of the anomalous Cu values were geology-related or not. River bed sediments of Pek River and Šaška River (downstream from Majdanpek) are polluted by Cu, but not as much as rivers downstream from Bor copper mines. Value of mean + 2σ (4195 mg/kg) is close to the threshold determined using CP diagram (4000 mg/kg). Several distributions are distinguished in the histogram for Cu in river bed sediment. Background values are around 30 mg/kg (mode of the backround distribution), and the highest values shown in red color are grouped around 8000 mg/kg (about 270-times higher). This result shows that river bed sediments downstream from Bor and Majdanpek copper mines are strongly contaminated with Cu.

Zinc (Zn), arsenic (As), cadmium (Cd) and lead (Pb)

Spatial distributions of anomalous values of Zn, As, Cd and Pb in river bed sediment were similar to that of Cu. As a general tendency, river bed sediments downstream from Bor and Majdanpek copper mines were contaminated with these metals. Higher concentrations were usually found downstream from Bor copper mines. Concentration ranges of bars in histogram for Cd are wider, and there is large number of data points in CP diagram with same concentration value due to excessive rounding at lower concentrations. Because of that, CP diagram for Cd was not so useful for determination of threshold value.

5. Variations of background and anomalous values of pH and Eh, and concentrations of anions, metals and arsenic in river water

5.1. Variations of pH and Eh values in river water

Statistical summary of pH and Eh values of river water are shown in Table 5.1. Geochemical maps, histograms and CP diagrams of pH and Eh values of river water in eastern Serbia are shown in Fig. 5.1. The area with acidic pH values (pH<6) is located only along Bor River, Krivelj River and Bela River downstream from Bor copper mines. Water of Timok River after the confluence with Bela River had neutral pH value. pH values of water from other rivers in the study were close to neutral, including the rivers downstream from Majdanpek copper mines. Thus, AMD from Majdanpek copper mines gave weak influence on pH value of Small Pek River, Pek River and Šaška River. The largest number of samples had pH value from 7 to 8.5. AMD-bearing river water had pH values in range from 4 to 5.5. Wastewater effluents had the lowest pH value in the study area (pH = 2.5–3.0). The area with the highest Eh values is located around Bor copper mines. The largest number of samples had Eh value in range from 500 to 700 mV.

Table 5.1 Statistical summary of pH and Eh values of river water

	Unit	min	median	mean	max	σ	mean–2σ	mean+2σ
pH	-	2.61	7.98	7.66	9.01	1.11	5.43	9.89
Eh	mV	268	588	599	910	81.5	436	762

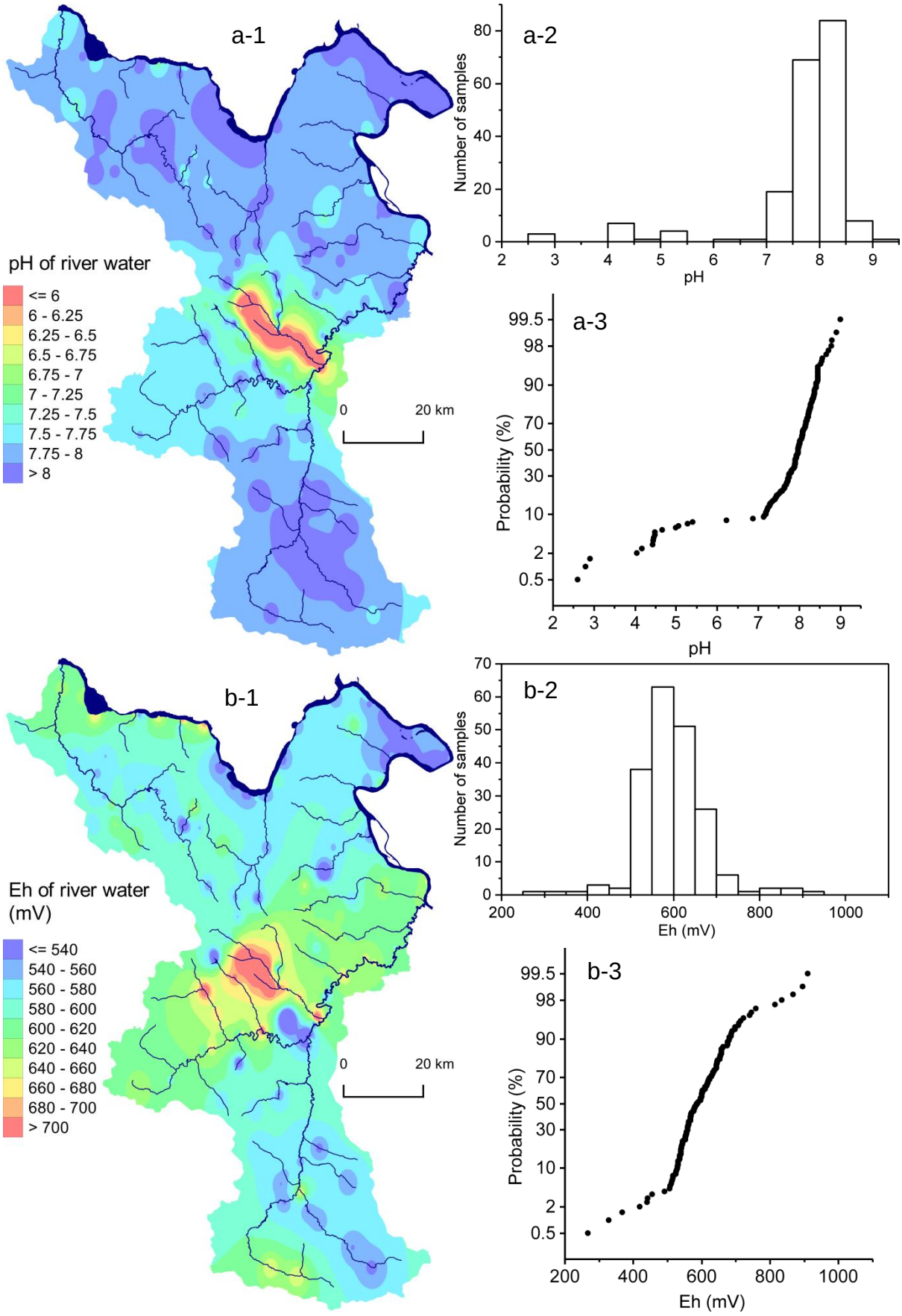

Fig. 5.1 Geochemical maps, histograms and CP diagrams of pH and Eh values of river water from eastern Serbia

5.2. Variations of concentrations of chlorides and sulfates in river water

Statistical summary of concentrations of chlorides and sulfates in river water is shown in Table 5.2. Minimum, median, mean, maximim, standard deviation (σ), mean–2σ, and mean+2σ values were calculated. Additinolay, mean, σ, mean–2σ, and mean+2σ were calculated from log-transformed data, and then obtained values were back-transformed to original values (Table 5.2). Geochemical maps, histograms and CP diagrams of chlorides and sulfates in river water are shown in Fig. 5.2. Threshold values for chlorides and sulfates were estimated from CP diagrams and results are shown in Table 5.2. Anomalous concentrations of chlorides and sulfates were those above 40 mg/L and 200 mg/L, respectively. There were 4 and 27 sampling points with anomalous concentrations of chlorides and sulfates, respectively. Sampling points with anomalous concentrations of sulfates were mostly grouped along rivers downstream from Bor copper mines.

Table 5.2 Statistical summary of concentrations of chlorides and sulfates in river water

		unit	min	median	mean	max	σ	mean–2σ	mean+2σ	CP
Cl	orig	mg/L	0.91	9.20	9.76	334	6.44	-3.13	22.6	40
	log				8.70		2.51	1.38	54.9	
SO4	orig	mg/L	7.28	42.9	73.0	5240	113	-153	299	200
	log				62.3		3.76	4.40	880	

orig – values obtained from original data; log – values obtained from log-transformed data

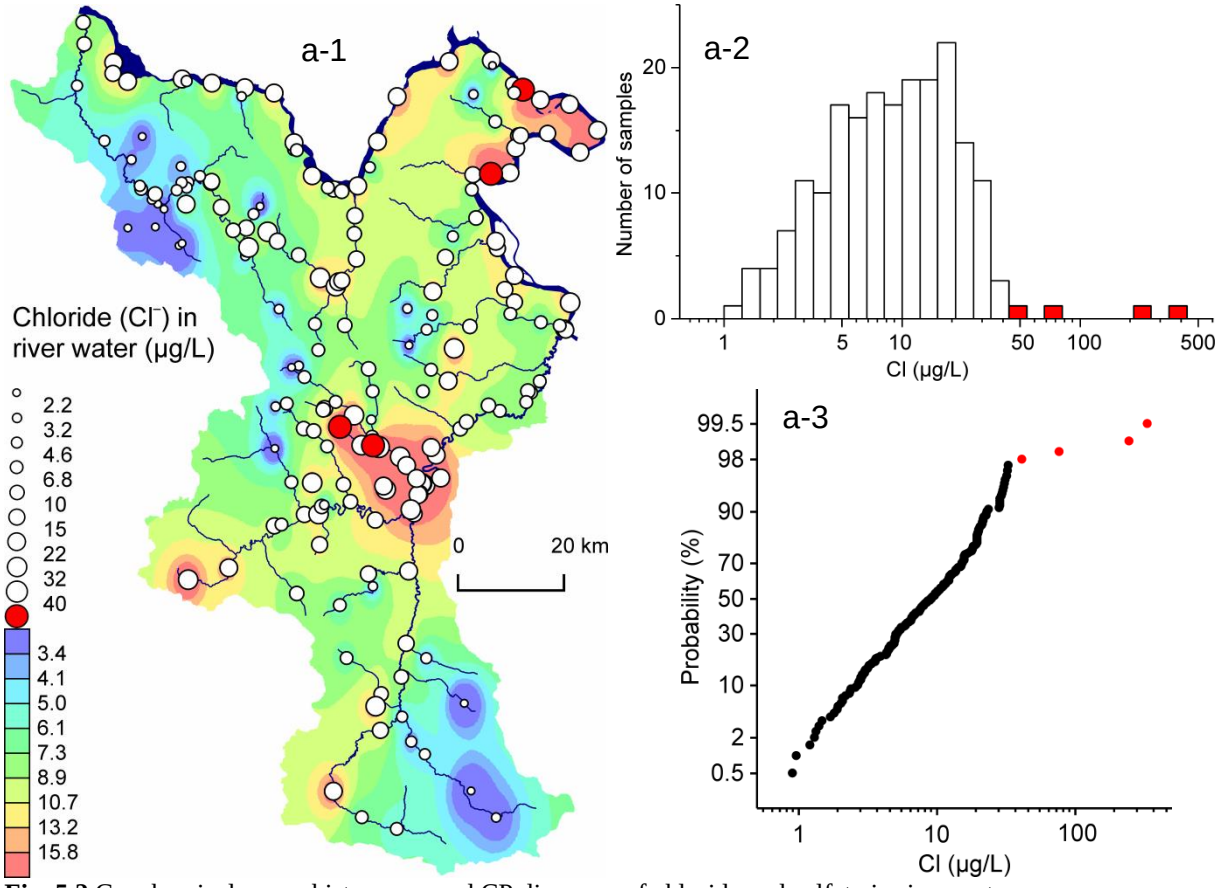

Fig. 5.2 Geochemical maps, histograms and CP diagrams of chloride and sulfate in river water

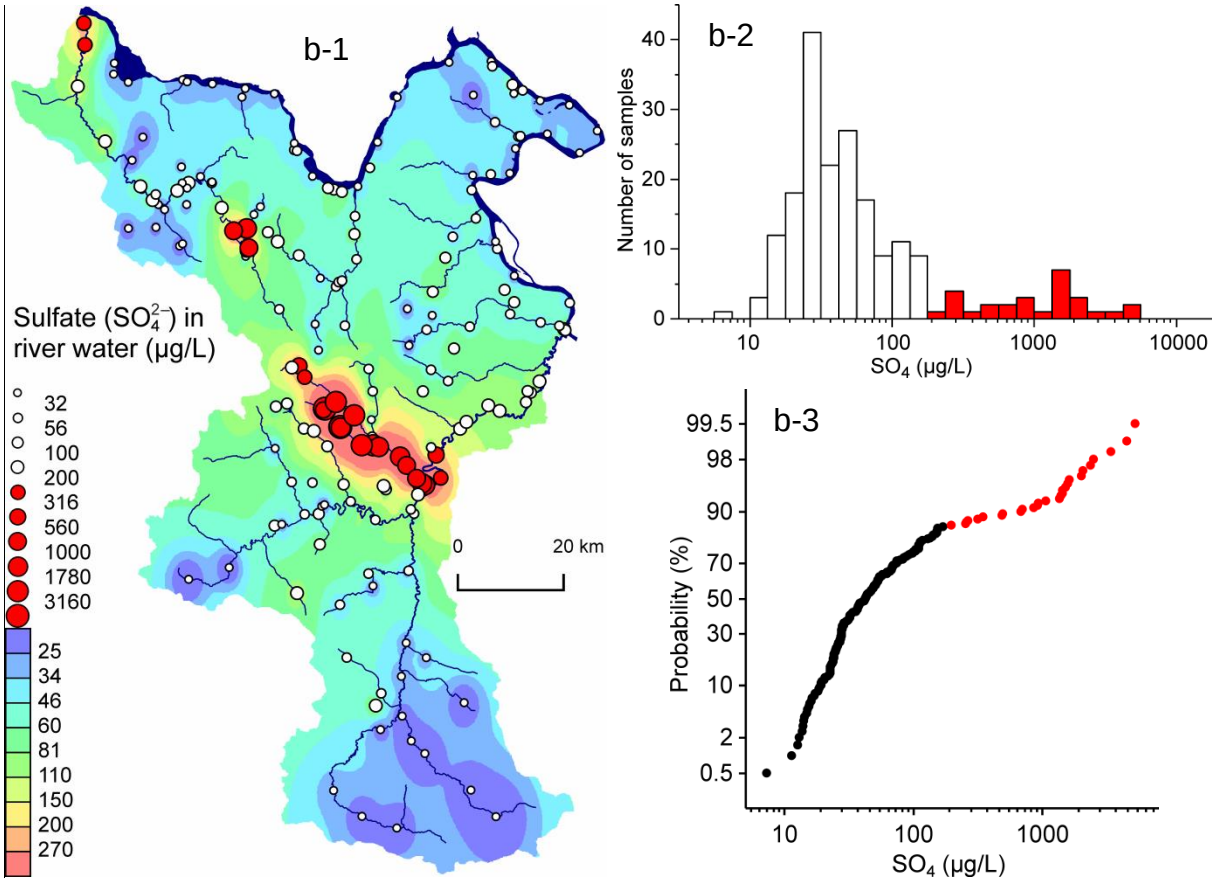

Fig. 5.2 (continued)

5.3. Variations of concentrations of metals and arsenic in river water

Statistical summary of concentrations of metals and arsenic in unfiltered river water (total concentrations), is shown in Table 5.3. The parameters that were calculated include minimum, median (50^{th} percentile), mean (average), maximum, standard deviation (σ), mean–2σ, mean+2σ and thresholds obtained from CP diagrams. Additinolay, mean, σ, mean–2σ, and mean+2σ were calculated from log-transformed data, and then obtained values were back-transformed to original values (Table 5.3). Minimum, median and maximum values were same when they were calculated from original concentration values and log-transformed values. Values of mean–2σ were negative when they were calculated from original concentration values. Thus, it is more appropriate to use log-transformed values to calculate mean–2σ and mean+2σ values. For all elements except Ni and Pb, two threshold values were estimated by using CP diagrams. Values that were higher than the lower threshold value (CP1) represent values with moderate pollution. Values that exceeded higher threshold (CP2) represent values with strong pollution.

Table 5.3 Statistical summary of concentrations of metals and arsenic in unfiltered river water (total concentrations of metals and arsenic)

		Unit	min	median	mean	max	σ	mean–2σ	Mean+2σ	CP1	CP2
Al	orig	µg/L	6	165	4121	223000	19240	-34359	42601	1000	10000
	log				215		7.9	3.5	13442		
Mn	orig	µg/L	0.4	33	1123	33200	4108	-7093	9339	100	2000
	log				55		8.9	0.7	4339		
Fe	orig	µg/L	10	220	17401	819000	86952	-156502	191304	1100	10000
	log				353		10	3.8	33192		
Ni	orig	µg/L	0.2	0.9	41	2240	193	-346	427	10	-
	log				1.6		8.2	0.02	107		
Cu	orig	µg/L	0.8	3.8	3771	127000	16873	-29974	37516	15	1000
	log				12		17	0.04	3432		
Zn	orig	µg/L	0.5	4.3	386	18900	1866	-3346	4117	15	200
	log				9.3		8.8	0.1	724		
As	orig	µg/L	0.15	2.1	102	7350	617	-1132	1337	9	15
	log				2.9		5.9	0.1	102		
Cd	orig	µg/L	0.005	0.01	3.5	224	19	-35	42	0.1	3
	log				0.03		14	0.0002	5.7		
Pb	orig	µg/L	0.005	0.3	10	473	47	-84	104	2	-
	log				0.4		9.0	0.005	32		

orig – values obtained from original data; log – values obtained from log-transformed data

Statistical summary of concentrations of metals and arsenic in filtered river water (dissolved concentrations) is shown in Table 5.4. Same parameters as for unfiltered river water samples were calculated. Statistically calculated values for unfiltered and filtered water samples are different. Threshold values that were obtained from CP diagrams for unfiltered and filtered samples are different for Al, Fe, Zn and As.

Table 5.4 Statistical summary of concentrations of metals and arsenic in filtered river water (concentrations of metals and arsenic in dissolved from)

		Unit	min	median	mean	max	σ	mean–2σ	Mean+2σ	CP1	CP2
Al	orig	µg/L	2	30	3039	194000	17102	-31165	37242	100	1000
	log				40		8.1	0.6	2608		
Mn	orig	µg/L	0.1	13	979	32900	3751	-6522	8480	100	2000
	log				26		12	0.2	4006		
Fe	orig	µg/L	10	50	9162	581000	61099	-113035	131360	500	-
	log				70		7.7	1.2	4145		
Ni	orig	µg/L	0.2	1.6	46	2590	216	-386	477	10	-
	log				2.7		6.5	0.1	111		
Cu	orig	µg/L	0.2	3.4	3390	133000	16107	-28823	35604	15	1000
	log				8.1		16	0.03	2088		
Zn	orig	µg/L	0.3	7.8	335	18900	1590	-2846	3516	200	-
	log				12		8	0.2	781		
As	orig	µg/L	0.03	1.5	52	7170	526	-1000	1104	5	-
	log				1.7		3.8	0.1	25		
Cd	orig	µg/L	0.005	0.05	3.6	219	20	-35	43	0.1	3
	log				0.07		12	0.001	9.5		
Pb	orig	µg/L	0.005	0.3	3.7	224	20	-37	45	2	-
	log				0.31		7.5	0.01	17		

orig – values obtained from original data; log – values obtained from log-transformed data

Geochemical maps, histograms and probability distribution diagrams of metals and arsenic in unfiltered and filtered river water (total and dissolved concentrations) from eastern Serbia are shown in Fig. 5.3. Geochemical maps and histograms for unfiltered samples (total concentrations) and filtered samples (dissolved concentrations) are shown separately. However, CP plots of total and dissolved concentrations of metals and arsenic are shown in one diagram for better comparison. Background range is shown in black color, and values that exceeded thresholds that were obtained from CP diagrams are shown in orange and red colors on histograms and CP diagrams. Median, mean, mean (log), mean–2σ and Mean+2σ values are shown on histograms and CP diagrams for comparison with threshold values obtained using brakes of slope from CP diagram.

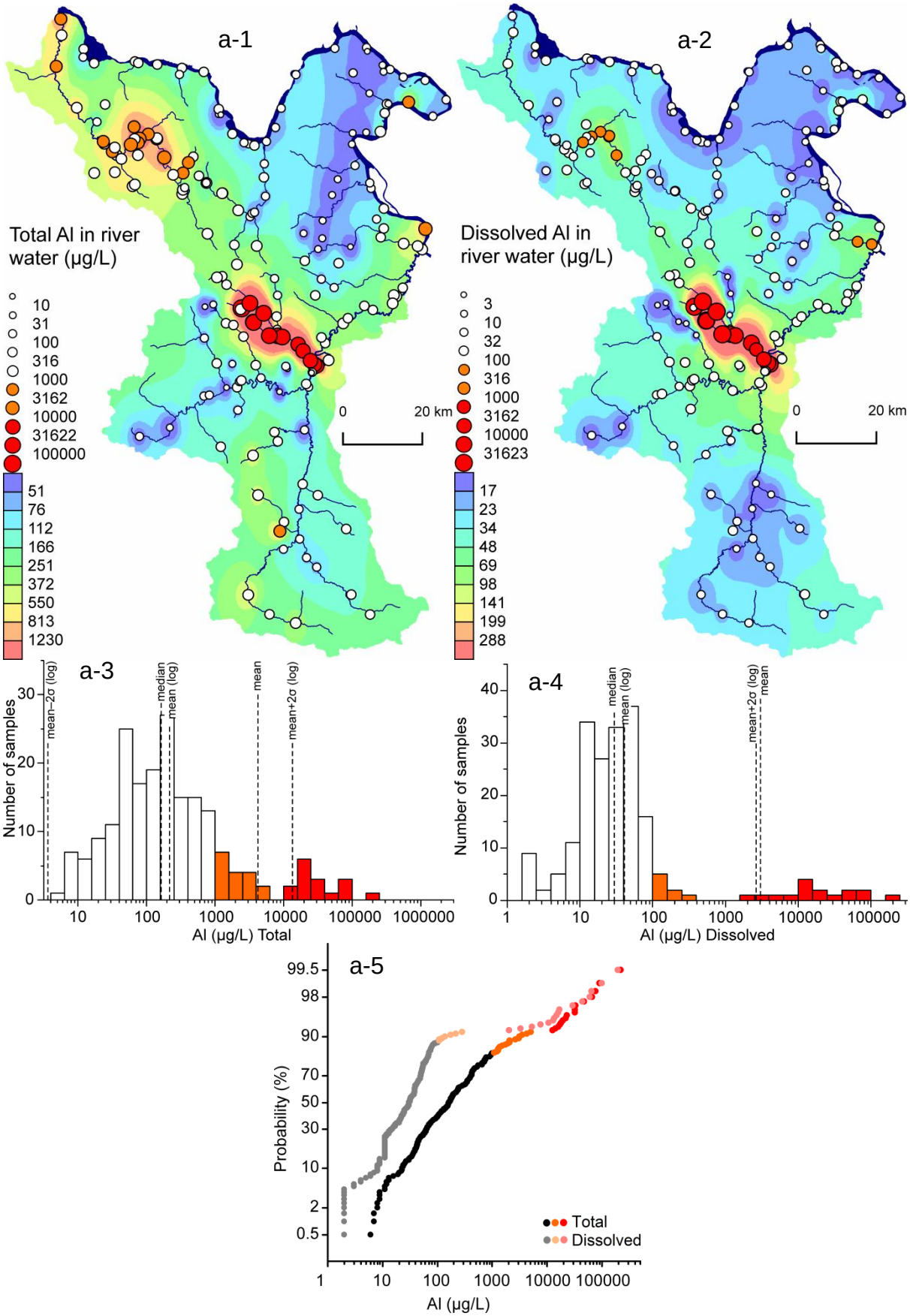

Fig 5.3 Geochemical maps, histograms and CP diagrams of total and dissolved concentrations of 9 elements in river water from eastern Serbia. **a** Al. **b** Mn. **c** Fe. **d** Ni. **e** Cu. **f** Zn. **g** As. **h** Cd. **i** Pb

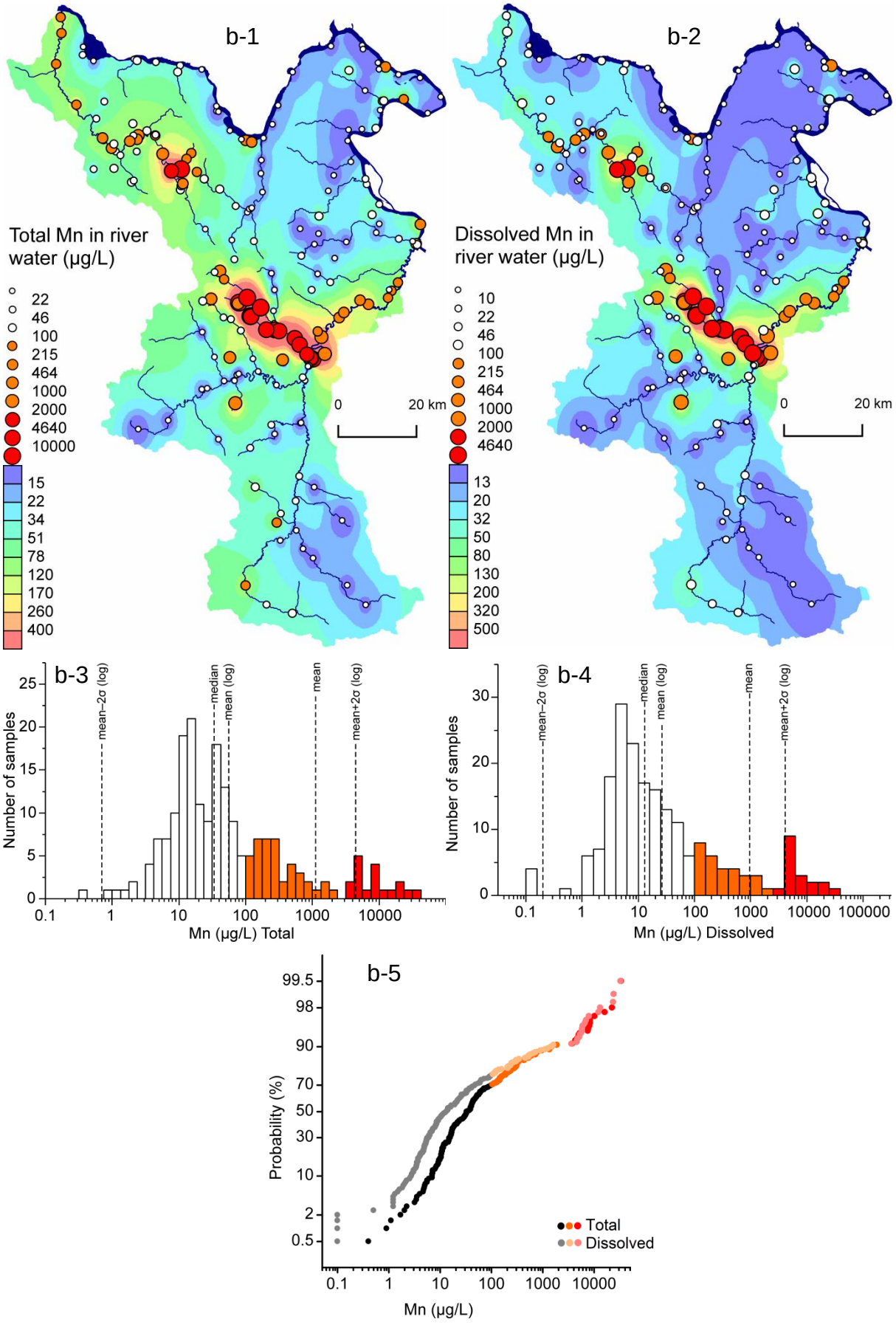

Fig 5.3 (contuined)

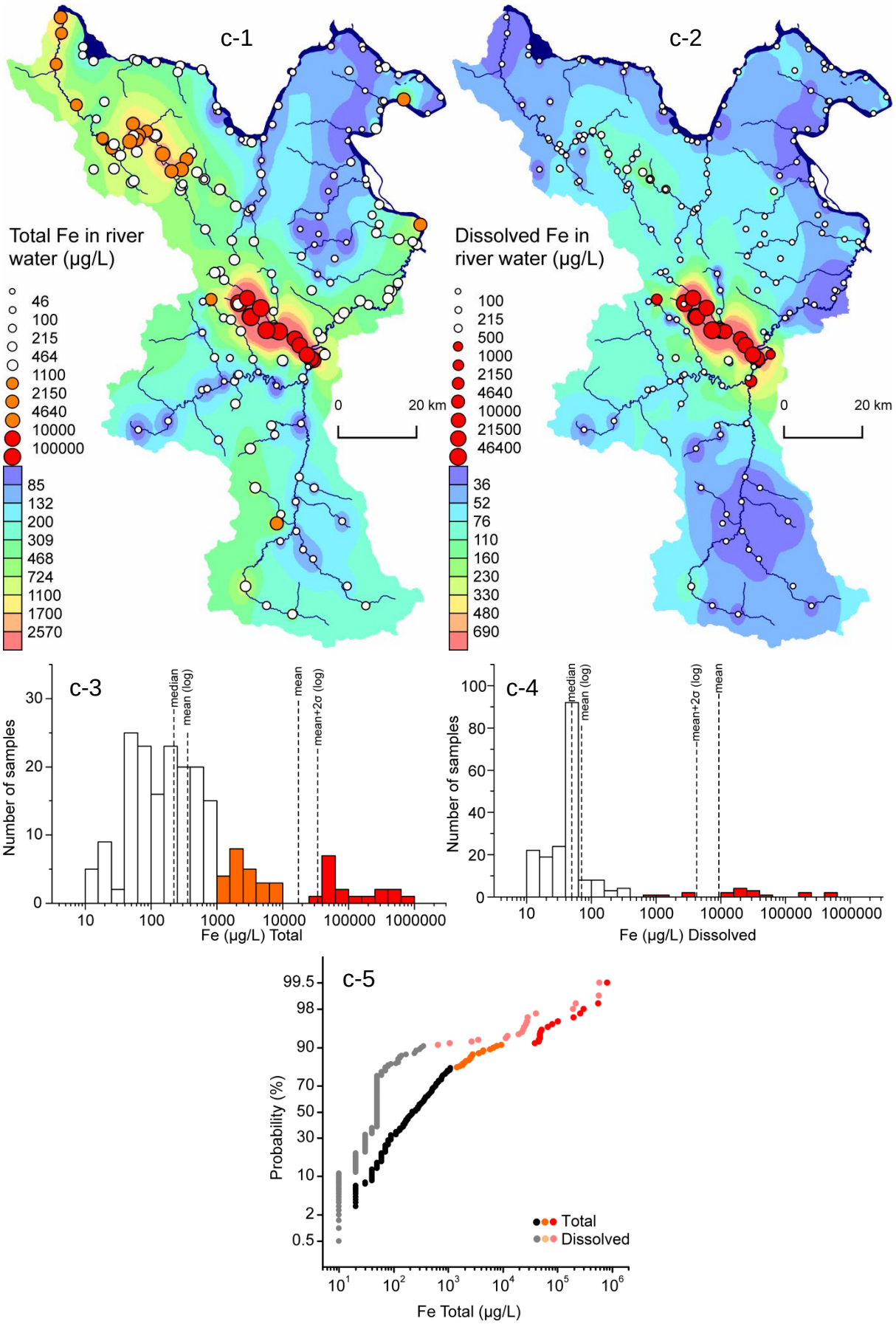

Fig 5.3 (contuined)

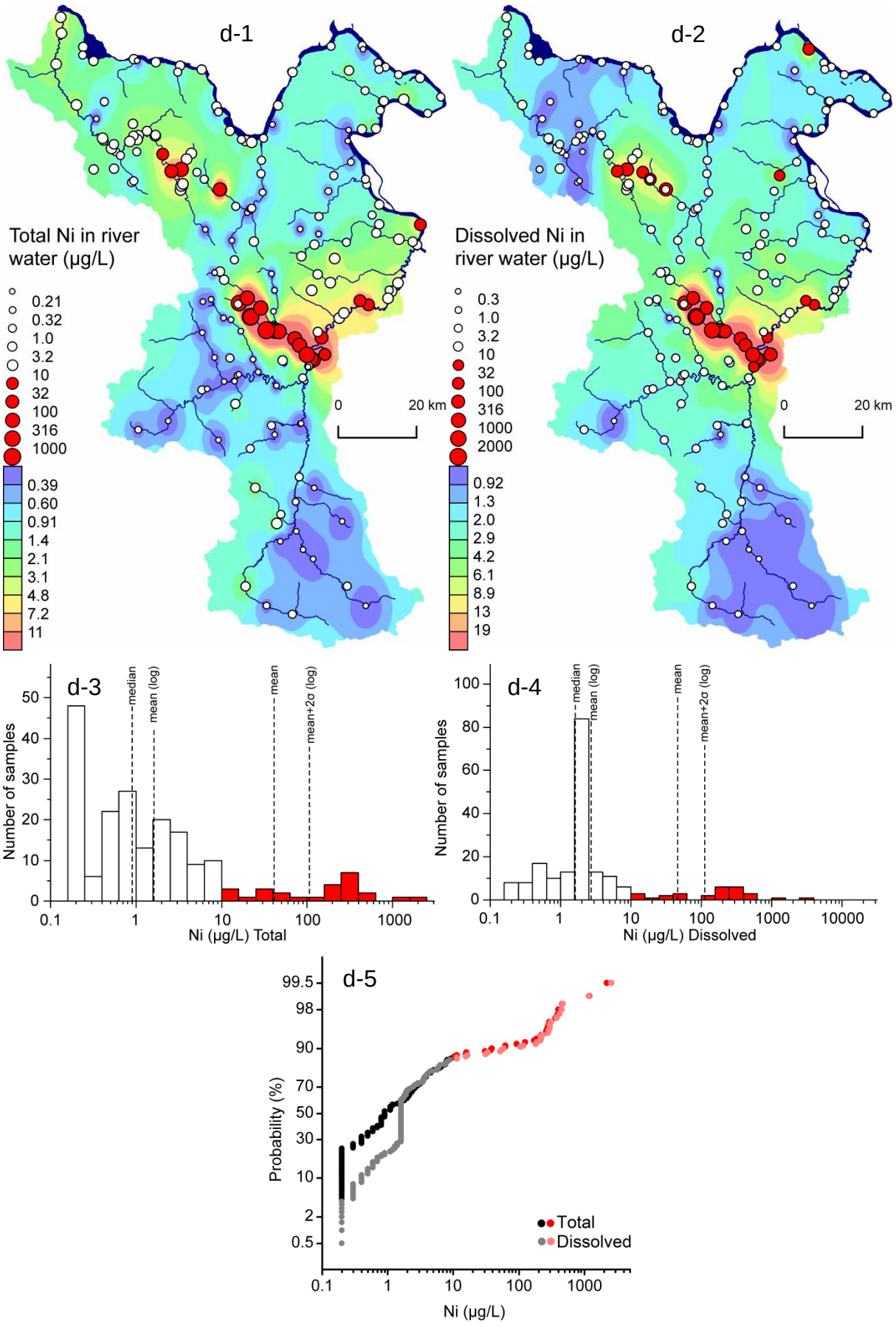

Fig 5.3 (contuined)

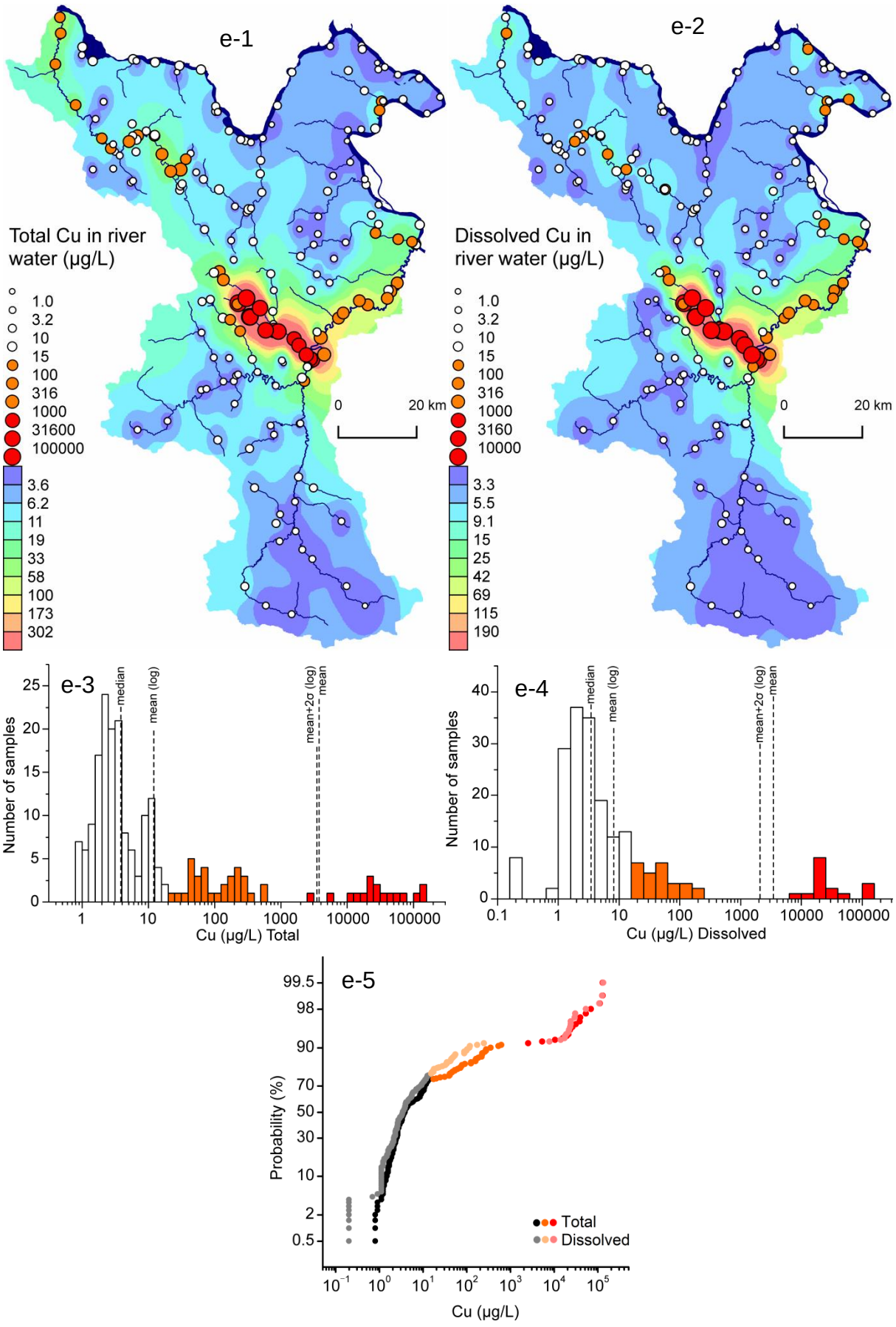

Fig 5.3 (contuined)

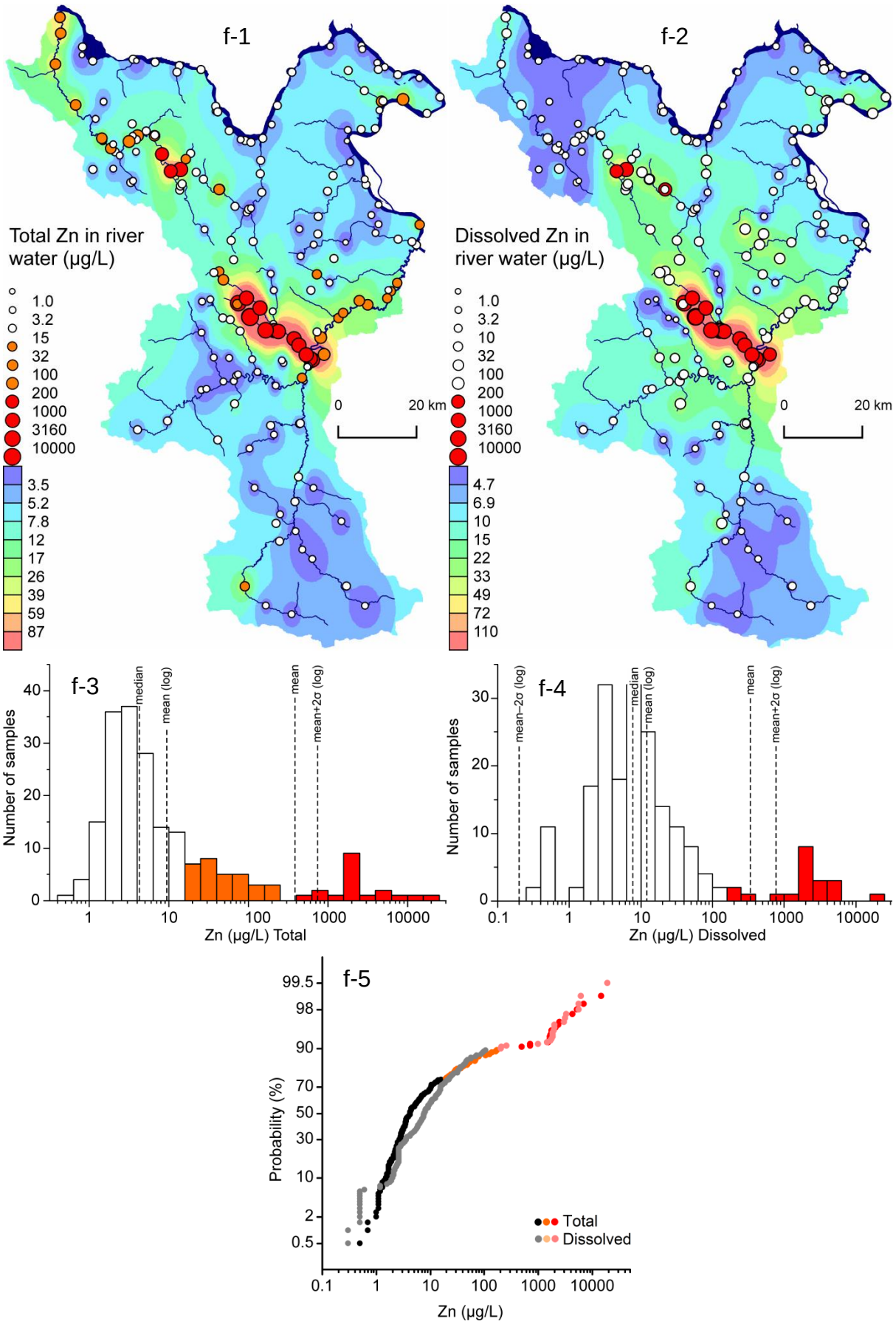

Fig 5.3 (contuined)

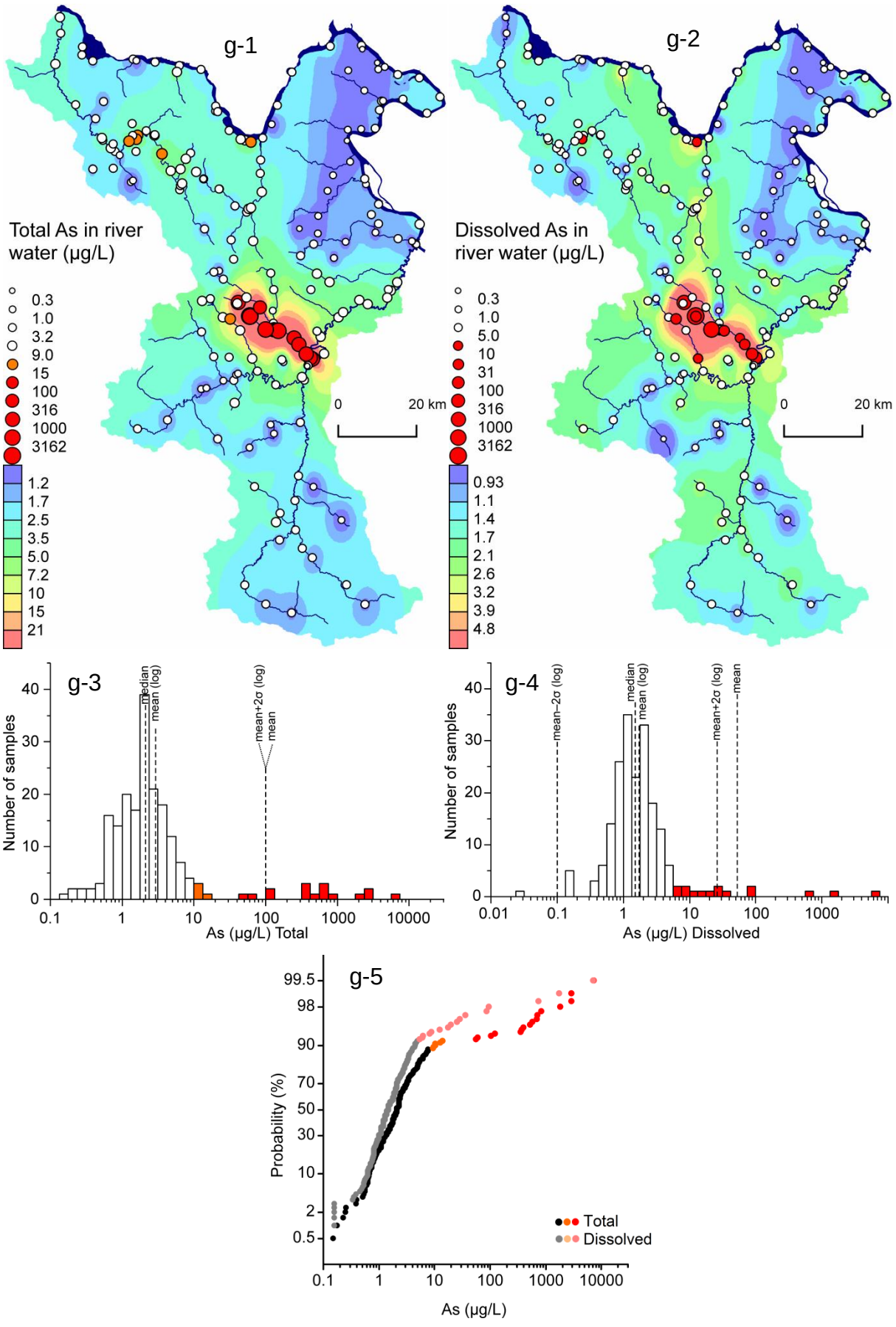

Fig 5.3 (contuined)

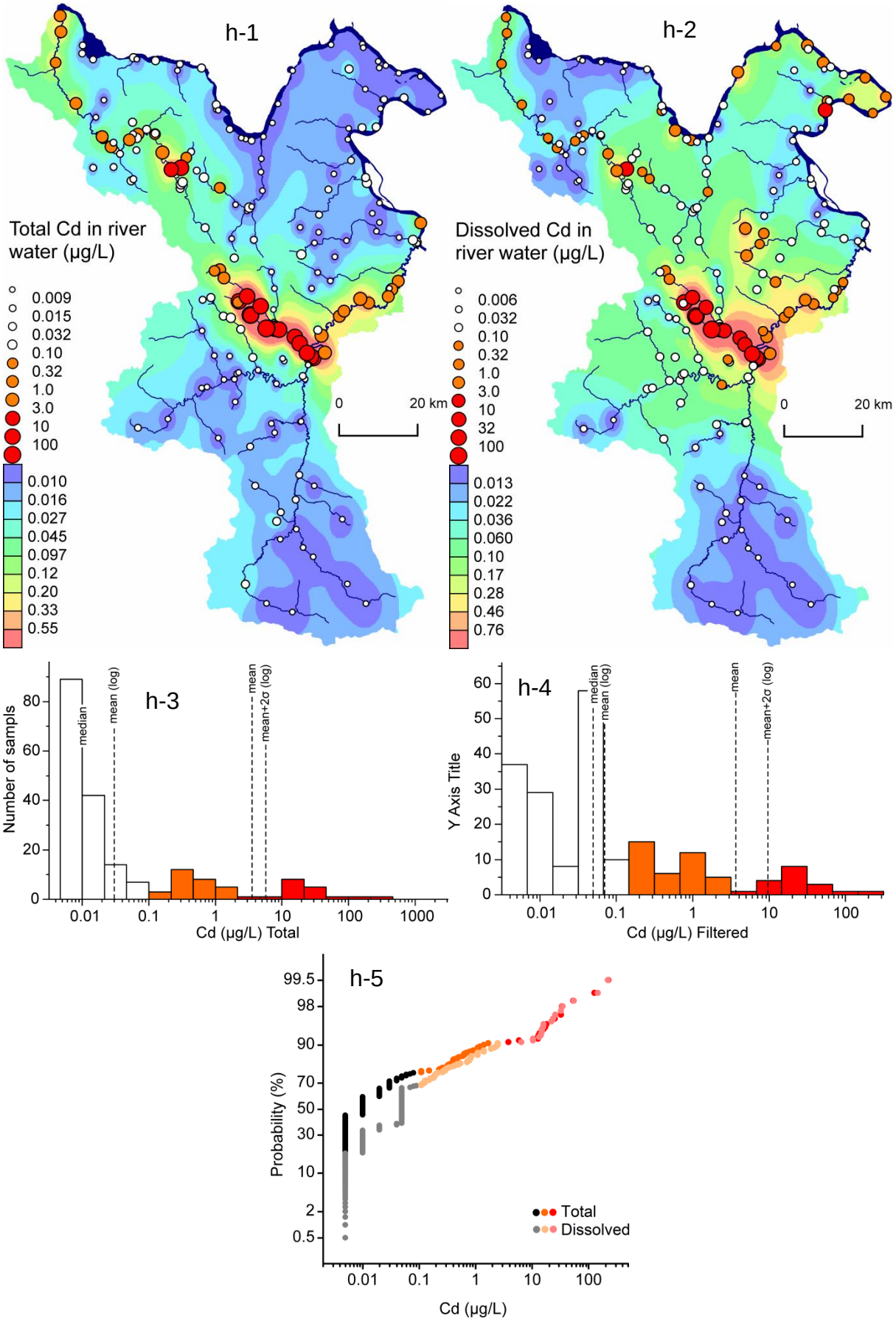

Fig 5.3 (contuined)

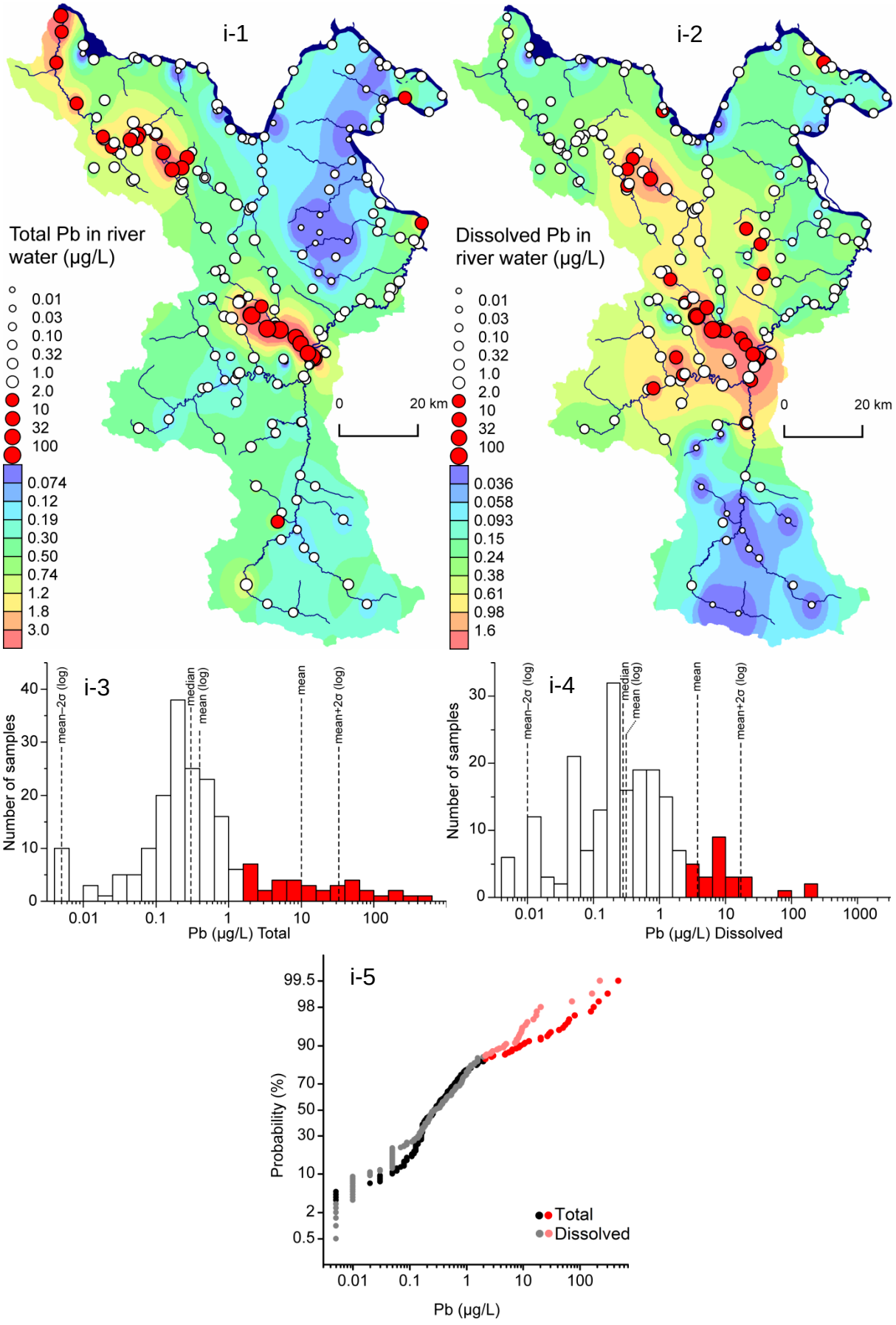

Fig 5.3 (contuined)

As a general tendency, river water downstream from Bor and Majdanpek copper mines was contaminated with metals and arsenic. In Bor mining area, contaminated rivers were Bor River, Krivelj River, Bela River and Timok River. In Majdanpek mining area contaminated rivers were Small Pek River, Pek River and Šaška River. The highest concentrations of metals and arsenic were found along Bor River, Krivelj River and Bela River. Concentrations that indicated moderate pollution were found along Timok River, Small Pek River, Pek River and Šaška River. However, extreme concentrations of Mn, Zn and Cd were also found in Small Pek River. Water of upper reach of Šaška River was moderately contaminated with metals and arsenic. Timok River was not contaminated with Al, Fe, As and Pb, since these elements were removed from river water after the confluence of Bela River and Timok River.

The difference in concentrations between total and dissolved species can be seen on CP diagrams. Generally, if points that show total concentrations are close to the points that show dissolved concentrations, then the concentrations of particulate forms of that element are not large. In case of aluminum, CP curves of total and dissolved concentrations are not close for lower concentrations. However, for higher concentrations, these curves became close. It means that quantity of particulate forms of Al decrease when Al is present in river water in high concentrations. It is reasonable, since higher concentrations of Al indicate low pH of river water, and therefore, Al is dominantly present in dissolved form. In case of arsenic, CP curves are close at lower concentrations, then they separate at higher concentrations, and finally they became close for the highest concentrations. Lower concentrations of As have alkaline pH value, and at those pH values, As tends to stay in dissolved form. AMD-bearing river water with acidic pH values contain particulate hydrous ferric oxides, which act as sorbents for arsenic. Arsenic is adsorbed at those pH values, and that is the reason why curves on CP diagrams for higher concentrations are separated. The extreme concentrations of arsenic are present in wastewater effluents with very low pH value, where no hydrous ferric oxides are present to sorb arsenic. Therefore, arsenic is present in dissolved form, and CP curve of total and dissolved arsenic becomes close for the highest concentrations.

6. Mobility and natural attenuation of metals and arsenic in the drainage system of Timok River from Bor copper mines to Danube River

6.1. Sampling sites

In the studied area, we chose 5 wastewater effluent samples (E1–E5), 10 river water samples (RW1–RW10) and 10 river bed sediment samples (RS1–RS10) for detailed consideration of mobility and natural attenuation of metals and arsenic. Data of chemical composition of river water and sediments from these sampling points is same as the data that was used for creation of geochemical maps of river water and river bed sediments (Appendices 2, 3, 4, and 5). These sampling points were chosen for detailed consideration because rivers downstream from Bor copper mines had the highest concentrations of metals and arsenic in eastern Serbia. Sampling points were chosen in order to examine 1) major sources of wastewater (E1–E5); 2) total quantities of metals and arsenic in water of Bor and Krivelj Rivers at points after they received all major and minor wastewater effluents in the study area (R1 and R2, respectively); 3) mobility of metals and arsenic downstream from junction of Bor and Krivelj Rivers, that is throughout Bela River (R4, R5, and R6) and Timok River (R8, R9, and R10); and 4) concentrations of metals and arsenic in two AMD-unaffected rivers (Ravna River, R3 and Timok River before the confluence with Bela River, R7). River water and river bed sediment samples were collected on the same date and at the same sampling points (R1–R10; Fig. 6.1, Table 6.1).

Table 6.1 Description of sampling points and dates of sampling

Symbol	Description	Date
	Wastewater samples	
E1	AMD from the overburden and flotation tailing pond "RTH" in Bor	11.08.2015.
E2	Municipal wastewater from Bor Town	11.08.2015.
E3	Metallurgical wastewater from metallurgical facilities in Bor	11.08.2015.
E4	AMD from the underground mine Bor	05.08.2015.
E5	AMD from Saraka stream (near the open pit Veliki Krivelj)	01.09.2015.
	River water (RW) and river bed sediment (RS) samples	
R1	Bor River before junction with Krivelj River	11.08.2015.
R2	Krivelj River before junction with Bor river	11.08.2015.
R3	Ravna River before junction with Bela River	11.08.2015.
R4	Bela River before Rgotina gorge	11.08.2015.
R5	Bela River in Rgotina village	12.08.2015.
R6	Bela River in Vražogrnac village	12.08.2015.
R7	Timok River before confluence with Bela River	12.08.2015.
R8	Timok River near Čokonjar village (after the confluence with Bela River)	19.08.2015.
R9	Timok River near Brusnik village (middle reach)	27.10.2015.
R10	Timok River near Veljkovo village (lower reach)	27.10.2015.

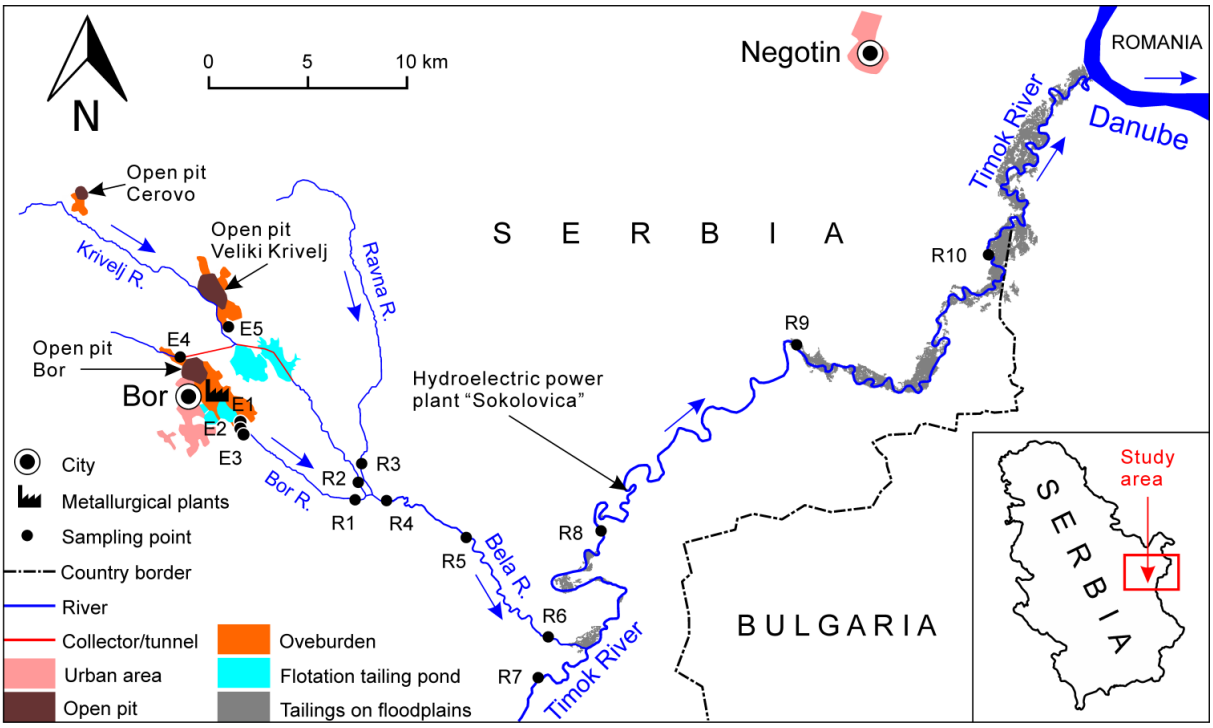

Fig. 6.1 Map of the study area and locations of sampling points. Distributions of urban area, open pits, flotation tailing ponds, and tailings on floodplains were extracted from Landsat satellite imagery. River system was extracted from ASTER Digital Elevation Map.

Wastewater from the overburden (E1), municipal wastewater (E2) and metallurgical wastewater (E3) were released into Bor River at its source, and water of Bor River was therefore composed of wastewater, since the natural river water from the upper reach of Bor River was redirected through the tunnel into Krivelj River. Wastewater from the underground mine Bor (E4) also flowed into Krivelj River through the abovementioned tunnel. In addition, wastewater from Saraka Stream (E5) flowed into Krivelj River (Fig. 6.1). There were other important sources of AMD such as wastewater from Robule Lake (wastewater from the overburden), which flowed into Bor River (Stevanović et al., 2013; Stanković et al., 2017; Jeremić et al., 2016; Radić et al., 2014), and wastewater from the bottom of Veliki Krivelj open pit, which was pumped out into Krivelj River (Šerbula et al., 2016). These other sources were not characterized in this study due to technical reasons.

The main recipients of wastewaters in Bor mining area were Bor River (R1) and Krivelj River (R2). These two rivers merge and form Bela River (R4, R5, and R6), which flows into Timok River (R7, R8, R9, and R10). The water of Timok River flows into Danube River. In one section, Krivelj River flows through the tunnel and collector beneath the flotation tailing ponds. Ravna River (R4), a tributary of Bela River, was not been affected by mining activity. Also Timok River, before the confluence with Bela River (R7), was not

affected by mining activity but the water was greatly contaminated by untreated municipal wastewater from the town of Zaječar.

6.2. Mobility of metals and arsenic in river water

6.2.1. Variations of discharge, pH, and Eh

Results of field measurements of discharge, pH, and Eh are shown in Table 6.2. Discharge of effluents ranged from 1.4 m^3 min^{-1} at underground mine wastewater (E4) to 15.1 m^3 min^{-1} at municipal wastewater (E2). In the studied area the lowest discharge was measured in Ravna River (6.6 m^3 min^{-1}) whereas the highest in Timok River (218 m^3 min^{-1}).

Table 6.2 Field parameters and concentrations of anions and major cations in filtered water samples

Unit	discharge m^3 min^{-1}	pH	Eh mV	Na mg L^{-1}	K mg L^{-1}	Mg mg L^{-1}	Ca mg L^{-1}	Cl^- mg L^{-1}	SO_4^{2-} mg L^{-1}	HCO_3^{-a} mg L^{-1}
LOD	–	–	–	0.005	0.03	0.002	0.7	0.03	0.03	–
Accuracy	–	–	–	6.1%	0.0%	8.0%	9.3%	1.7%	4.0%	–
Wastewater samples										
E1	1.5	5.28	600	137	6.1	305	494	76.6	3430	–
E2	15.1	8.56	687	51.7	8.2	21.8	211	31.5	700	–
E3	7.1	2.61	896	52.8	7.0	226	327	16.8	4550	–
E4	1.4	2.79	910	87.7	2.8	219	415	13.0	5240	–
E5	2.5	4.43	722	23.6	2.0	174	153	5.47	2510	–
River water samples										
RW1	35.0	4.17	697	54.5	8.6	83.4	291	32.3	1510	–
RW2	33.7	4.49	707	98.2	12.5	79.3	477	41.1	2060	–
RW3	6.6	8.41	636	8.4	3.5	10.4	76.4	5.5	42.2	249.9
RW4	43.4	4.45	687	71.1	10.5	78.0	343	33.1	1590	–
RW5	55.6	4.66	688	57.8	7.9	71.4	298	29.4	1360	–
RW6	44.1	4.46	815	54.5	7.7	62.4	276	30.8	1430	–
RW7	174	7.29	420	20.0	2.9	12.2	73.9	17.9	46.7	254.0
RW8	218	7.22	541	30.1	4.8	25.6	118	20.3	348	100.4
RW9	218	7.90	647	8.9	2.1	11.0	94.2	7.9	118	206.9
RW10	218	8.02	615	7.8	2.2	9.9	95.6	6.6	111	213.2

[a]Concentrations of bicarbonate ions were estimated by charge balance calculations.

A diagram showing upstream-to-downstream variations of pH values is presented in Fig. 6.3. Wastewaters at E1, E3, E4, and E5 had acidic pH values (Table 6.2), whereas the municipal wastewater from Bor Town (E2) had an alkaline pH value (pH = 8.6). The lowest pH value was measured in metallurgical wastewater (E3; pH = 2.6). Water of Bor River (RW1) and water of Krivelj River (RW2) were acidic (pH = 4.2 and pH = 4.5, respectively). Although the waters of Ravna River (RW3) were alkaline (pH = 8.4) they were not able to neutralize the acidic water of Bela River (RW4, RW5, and RW6; Table 6.2) due to relative low discharge. Thus, the pH value of Bela River was still acidic (pH = 4.5–4.7) after the confluence with Ravna River. The largest increase of the pH value from upstream to

downstream was found at the confluence of Bela River and Timok River where the acidic water of Bela River (RW4, RW5, and RW6) was neutralized by alkaline water of Timok River (RW7; pH = 7.3). After the confluence with Bela River, the water of Timok River (RW8, RW9, and RW10) continuosly increased the pH value (pH = 7.5–8.0; Table 6.2, Fig. 6.3) (Đorđievski et al., 2018).

River water and wastewater had a relatively oxidizing environment (541–910 mV), except for water of Timok River at P7, which had a relatively reducing environment (420 mV).

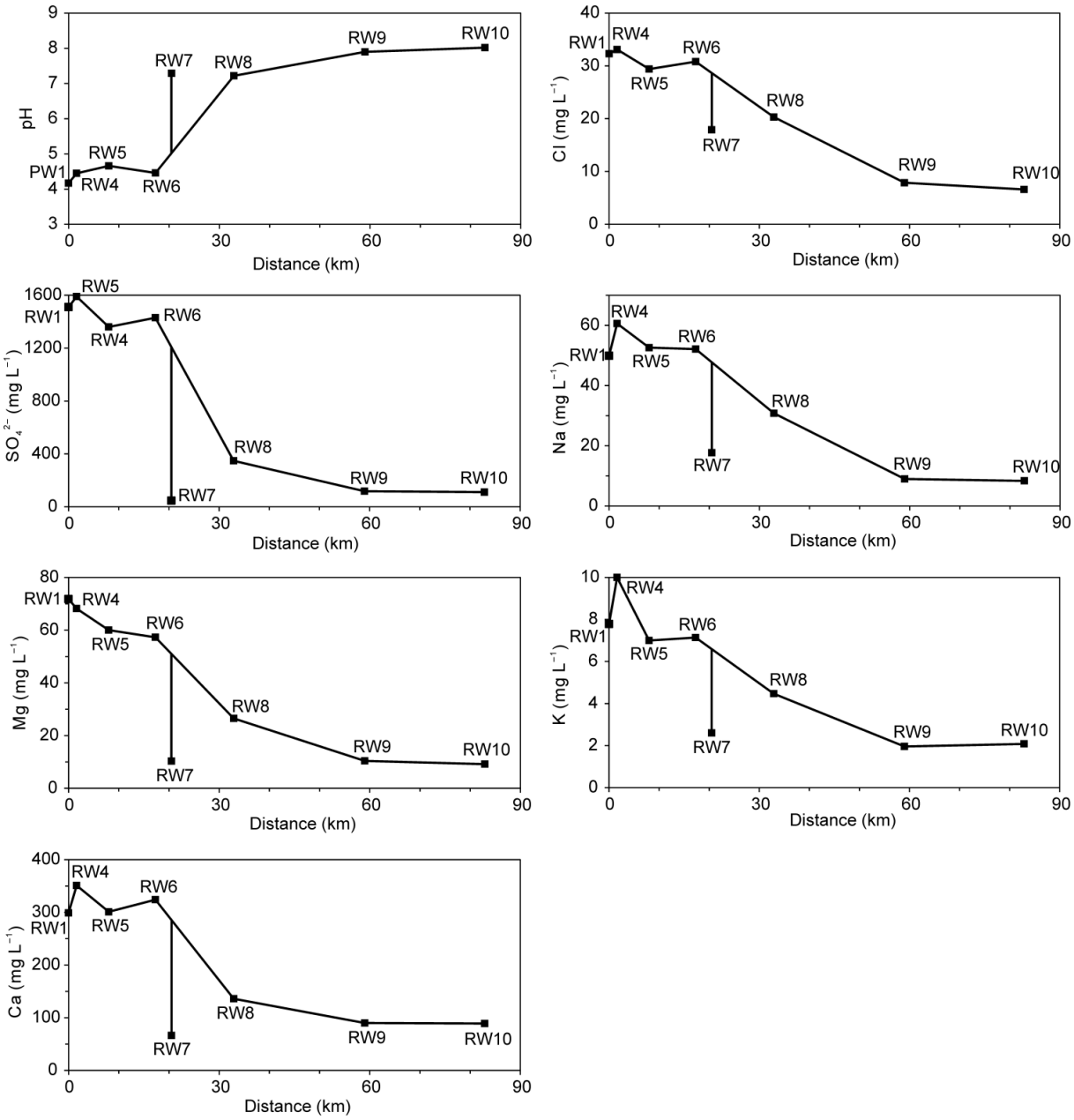

Fig. 6.3 Upstream-to-downstream variations of pH value in river water and concentrations of chlorides, sulfates, Na, Mg, K, and Ca

6.2.2. Concentrations of major anions and cations

Wastewaters having the largest concentrations of chlorides and sulfates were wastewater from the overburden (E1, 77 mg L^{-1} of chlorides) and underground mine wastewater (E4, 5240 mg L^{-1} of sulfates), respectively. The difference between concentrations of chlorides in wastewater, wastewater-bearing river water and natural river water was not large compared to the difference in concentrations of sulfates (Table 6.2 and Fig. 6.3). In fact, even if the concentration of chlorides in contaminated water of Bela River (RW4) was 6-times larger than the concentration of chlorides in natural river water of Ravna River (RW3), the concentration of sulfates in water of Bela River (RW4) was 38-times larger than the concentration of sulfates in water of Ravna River (RW3). As a consequence, concentrations of sulfates in AMD-bearing river water decreased more rapidly from upstream to downstream than did the concentrations of chlorides (Fig. 6.3). At the confluence of Bela River and Timok River (RW6 to RW8), concentrations of chlorides and sulfates were decreased by 1.5 and 4.1 times, respectively (Đorđievski et al., 2018).

Concentrations of major cations (Na, K, Mg, and Ca) and anions (chloride and sulfate) are shown in Table 6.2. Generally, the concentrations of major cations in river water decreased from Bor copper mines to the Danube River (Fig. 6.3). The wastewater with the highest concentration of major cations was AMD coming from the overburden (E1). The concentrations of major cations in water of Krivelj River (RW2) were higher than those in water of Bor River (RW1). Lower concentrations of major cations were found in rivers that did not have an impact of AMD (RW3 and RW7) and also in the middle and lower reaches of Timok River (RW9 and RW10).

6.2.3. Bicarbonate buffering system in river water

Charge balance calculations indicated a deficiency of negative charge in alkaline waters of Ravna River (P3) and Timok River (RW7, RW8, RW9, and RW10). River water at sampling points with acidic pH values did not have deficiency of negative charge (charge balance error for these points ranged from 5% to 14%). Bicarbonate is the main constituent of natural alkaline water (pH = 7.0–8.3) and it was not determined in this study. Thus, a deficiency of negative charge is assumed to originate from the lack of bicarbonate data. Concentrations of bicarbonate ions were calculated using charge balance and are presented in Table 6.2. Concentrations of bicarbonate ions in AMD-unaffected water of Ravna River (RW3) and Timok River (RW7) were similar (250 mg L^{-1} and 254 mg L^{-1}, respectively).

However, after the confluence with Bela River, the concentration of bicarbonate ions in water of Timok River (RW8) decreased to 100 mg L^{-1} due to reaction with acidic wastewater from Bela River. In the lower reach of Timok River (RW9 and RW10), the concentrations of bicarbonate ions increased to 207 mg L^{-1} and 213 mg L^{-1}, respectively. Despite a decrease in the concentrations of bicarbonate ions in water of Timok River from RW7 to RW8 (from 254 to 100 mg L^{-1}), the pH values remained relatively constant at these points (7.29 and 7.22, respectively). This finding is reasonable since bicarbonate ion is an amphiprotic substance (acting both as a proton donor and a proton acceptor), thus buffering the pH value of river water (Đorđievski et al., 2018).

The concentration of bicarbonate ions as world average and in areas dominated by igneous rocks are 58.4 mg L^{-1} and 92.0 mg L^{-1}, respectively (Oyarzún et al., 2013). These values are lower than the concentrations of bicarbonate ions in Ravna River (RW3, 250 mg L^{-1}) and Timok River (RW7, 254 mg L^{-1}). Concentrations of Ca ions as world average and in areas dominated by igneous rocks are 15.0 mg L^{-1} and 58.2 mg L^{-1}, respectively (Oyarzún et al., 2013). These values are also lower than the concentrations of Ca ions in in water of Ravna River (RW3; 76.4 mg L^{-1}) and Timok River (RW7; 73.9 mg L^{-1}, respectively). These differences in concentrations are thought to be caused by dissolution of limestone by groundwater in the catchment of Timok River, as well as by dissolution of calcite that was present in river bed sediments of Ravna River (RS3) and Timok River (RS7). Thus, the high bicarbonate concentrations in natural river water enhanced the processes of natural attenuation by neutralizing acidic wastewater from Bor copper mines and by buffering the pH value at the confluence of Bela River and Timok River. The bicarbonate buffering system in river water was one of the factors that controlled chemical precipitation of metals and arsenic and their temporary immobilization in sediments of Timok River after the confluence with Bela River (RS8) (Đorđievski et al., 2018).

6.2.4. Concentrations of dissolved and particulate forms of metals and arsenic

Concentrations of metals and arsenic in unfiltered and filtered water samples are shown in Table 6.3. Diagrams showing concentrations of dissolved and particulate forms of metals and arsenic in wastewaters and some river waters are presented in Fig. 6.4. Total concentrations of metals and arsenic (sum of the concentrations of dissolved and particulate forms) in AMD-bearing water of Bor River (RW1), Krivelj River (RW2), and Bela River (RW4, RW5, and RW6) were up to 4 orders of magnitude larger than those in natural river water of Ravna

River (RW3) and Timok River (RW7). Total concentrations of Al, Mn, Fe and Cu in water of Bor River (RW1) and Krivelj River (RW2) were similar. However, total concentrations of Ni, Zn, As and Cd were 4–6-times higher and total concentration of Pb was 46-times higher in water of Bor River (RW1) than in Krivelj River (RW2). As expected, total concentrations of metals and arsenic in river water decreased from the Bor mining area to the Timok River. The largest decrease in total concentrations of metals and arsenic was observed at the confluence of Bela River and Timok River (from RW6 to RW8). At that point, total concentrations of Al, Fe, Cu, As, and Pb decreased more drastically (106, 68, 43, 52, and 91 times, respectively) than the total concentrations of Mn, Ni Zn, and Cd (3, 6, 12, and 9 times, respectively).

Table 6.3 Concentrations of metals and arsenic in unfiltered and filtered water samples

		Al	Mn	Fe	Ni	Cu	Zn	As	Cd	Pb
Unit		µg L^{-1}	µg L^{-1}	µg L^{-1}	µg L^{-1}	µg L^{-1}	µg L^{-1}	µg L^{-1}	µg L^{-1}	µg L^{-1}
LOD		4	0.2	100	0.6	0.4	1	0.03	0.02	0.02
Accuracy		9.2%	8.0%	2.0%	4.8%	2.2%	12.4%	2.9%	11.3%	9.3%
Wastewater samples										
E1	UnF	22100	33200	197000	173	10500	5210	123	16.0	1.6
	F	3260	32900	191000	190	7690	5660	94.4	16.0	0.36
E2	UnF	1940	1880	47800	9.1	2552	712	55.9	1.1	30.7
	F	38.9	1590	<100	5.7	<0.4	5.1	1.8	0.04	<0.02
E3	UnF	90100	24200	561000	2240	110000	18900	7350	127	158
	F	98800	23900	581000	2590	109000	18900	7170	145	165
E4	UnF	223000	23300	572000	404	127000	4340	840	32.2	8.5
	F	194000	23600	569000	453	133000	5670	743	34.7	8.5
E5	UnF	76000	22500	38500	276	127000	1790	5.1	17.3	0.15
	F	60000	13200	22700	213	124000	2010	2.7	15.6	1.4
River water samples										
RW1	UnF	17100	7770	79800	392	26300	2500	352	21.9	54.9
	F	16000	6650	26400	420	24200	3190	17.7	22.2	20.4
RW2	UnF	32600	7460	46100	93.7	31500	714	60.2	5.9	1.2
	F	29200	5880	12200	107	30500	998	1.3	6.4	0.45
RW3	UnF	46.2	7.24	<100	<0.6	2.6	2.5	2.8	<0.02	0.17
	F	<4	<0.2	<100	<0.6	<0.4	<1	1.5	<0.02	<0.02
RW4	UnF	32400	8190	302000	265	39900	3160	1830	18.1	218
	F	14900	6020	19300	280	24200	3014	28.6	15.1	9.4
RW5	UnF	14300	5040	48900	215	21000	1680	395	13.7	62.8
	F	10600	5530	11200	234	18900	1838	8.3	13.5	8.9
RW6	UnF	12700	5010	45400	223	23100	1540	373	12.7	43.1
	F	7550	4620	240	219	17200	2020	2.4	14.3	7.8
RW7	UnF	41.0	38.3	<100	<0.6	4.5	3.6	2.3	<0.02	0.26
	F	53.6	34.9	<100	<0.6	3.8	10.7	2.4	<0.02	1.2
RW8	UnF	120	1490	670	37.1	535	127	7.2	1.4	0.47
	F	50.4	1100	<100	31.5	114	87.5	2.9	2.5	0.77
RW9	UnF	221	296	500	15.7	228	36.6	5.0	1.2	0.32
	F	46.2	298	<100	15.8	117	41.9	1.6	1.1	0.08
RW10	UnF	292	128	430	7.7	125	20.0	6.2	0.39	0.50
	F	53.6	111	<100	7.4	49.7	15.5	3.5	0.30	0.09

UnF Unfiltered water sample, F Filtered water sample

In wastewater from the overburden (E1), Mn, Fe, Ni, Zn, and Cd were present in dissolved form, Cu and As were dominantly present in dissolved form (73% and 77% dissolved form, respectively), and Al and Pb were dominantly present in particulate form (85% and 78% particulate form, respectively). Metals and arsenic in municipal wastewater (E2) were dominantly present in particulate form except for Mn and Ni, which were mainly present in dissolved form (84% and 62% dissolved form, respectively). Metals and arsenic in highly acidic metallurgical wastewater (E3) were present in dissolved form. A similar condition was found in AMD from the underground mine Bor (E4), where all metals were present in dissolved form except for Al and As which were in small portions present in particulate form (13% and 11% particulate form, respectively). Metals and arsenic from wastewater of Saraka Stream (E5) were present mainly in dissolved form.

Distributions of dissolved and particulate forms of metals in water of Bor River (RW1) and Krivelj River (RW2) before their junction were similar (Fig. 6.4). In both rivers, Ni, Zn, and Cd were present in dissolved form, less than 20% of Al, Mn, and Cu were present in particulate form, and Fe, As, and Pb were dominantly present in particulate form (about 70%, 95% and 60% particulate form, respectively). In water of Bela River (RW4, RW5, and RW6), Fe, As and Pb were transported mainly in particulate form, while Al and Cu were transported in both forms with a relatively small prevalence of dissolved form (Fig. 6.4). In Timok River (RW8, RW9, and RW10), Fe was transported in particulate form, Al and Cu were transported in both forms with a larger amount of particulate form, and As and Pb were also transported in both forms but with a larger amount of dissolved form. From the wastewater effluents toward Danube River, Mn, Ni, Zn, and Cd were transported mainly in dissolved form. However, in water of Timok River after the confluence with Bela River (RW8), percentages of particulate forms of Mn, Ni, and Zn increased up to 20–40%, and then the abundances of particulate forms of these elements decreased in water from the lower reach of Timok River (RW9 and RW10) (Fig. 6.5) (Đorđievski et al., 2018).

Metals in water of Ravna River (RW3) were present in particulate form except for As, of which 60% was present in dissolved form (Fig. 6.4). Metals and arsenic in water of Timok River (RW7) were mainly present in dissolved form, although total concentrations of these metals and arsenic were low.

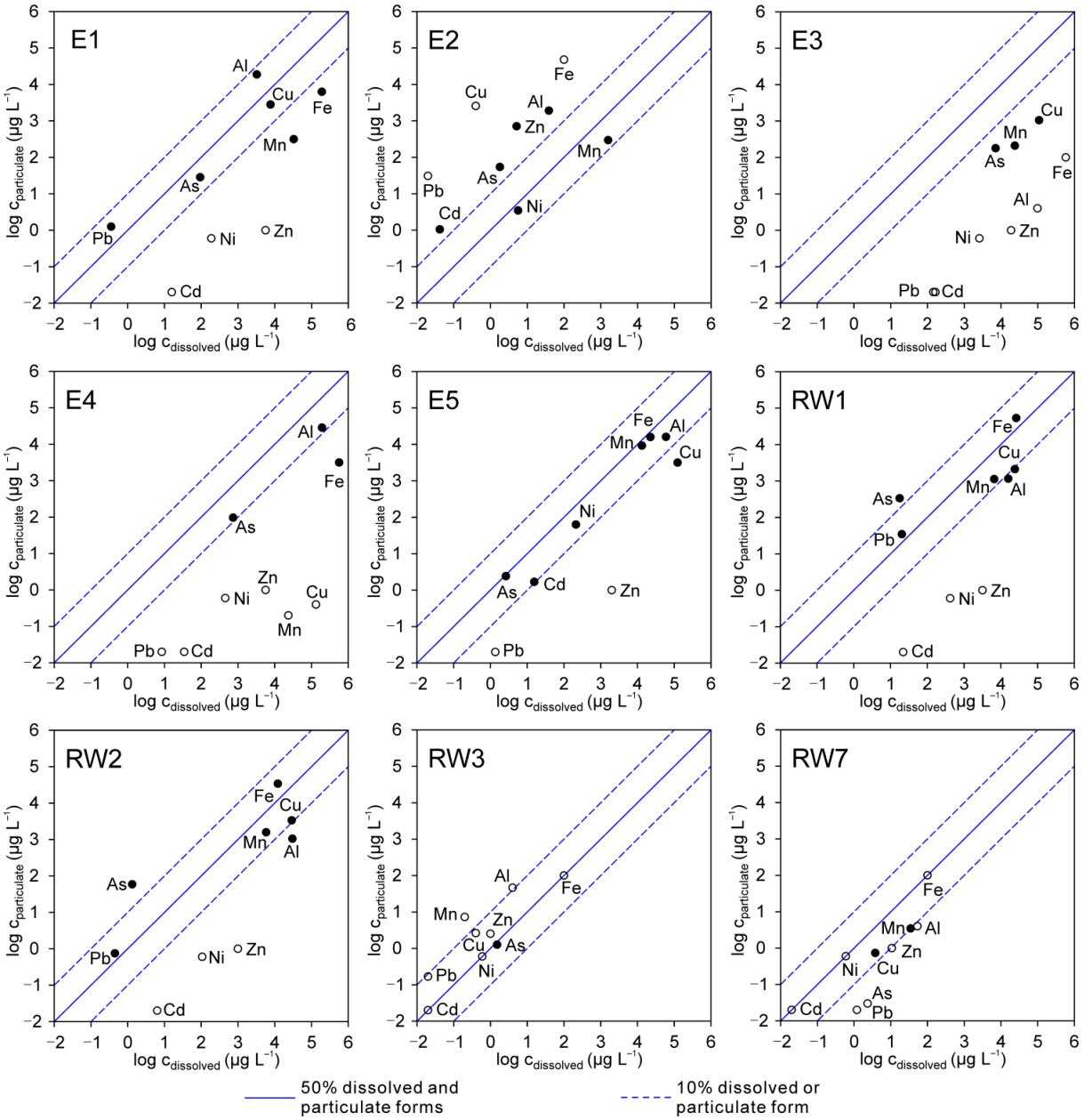

Fig. 6.4 Diagrams showing distributions of concentrations of dissolved ($c_{dissolved}$) and particulate ($c_{particulate}$) forms of metals and arsenic in wastewater effluents (E1–E5), and river water of Bor River (RW1), Krivelj River (RW2), Ravna River (RW3) and Timok River (RW7). Open circles indicate concentrations of dissolved and/or particulate forms that were below the limit of detection (If an open circle is on the 50% line, both forms were below the limit of detection)

6.2.5. Fluxes of metals and arsenic in wastewater and river water

Flux of metals and arsenic at a given sampling point was calculated by multiplying the total concentration of metals in water and discharge (Fig. 6.5). Metallurgical wastewater (E3) had the largest environmental impact since it was releasing the largest quantity of metals into Bor River: 4 kg min^{-1} of Fe, 0.8 kg min^{-1} of Cu, 0.2 kg min^{-1} of Mn, 0.1 kg min^{-1} of Zn, and 52 g

min^{-1} of As. The loss of copper through metallurgical wastewater was about 400 t per year, and this quantity was larger than the total loss of copper from the other effluents (E1, E2, E4, and E5, about 300 t per year all together). In previous studies, it was shown that larger quantities of copper were released into Bor River through metallurgical wastewater: approximately 500 t year^{-1} (Gardić et al., 2015), 150–1400 t year^{-1} (Stevanović et al., 2013) and 525 t year^{-1} (Ishiyama et al., 2012). The reported values show a wide range due to variations of quality and quantity in metallurgical wastewater that was being released from metallurgical facilities. Through water of Bela River (RW6), Timok River received approximately 1000 t of Fe, 500 t of Cu, 100 t of Mn, 35 t of Zn, and 8 t of As per year.

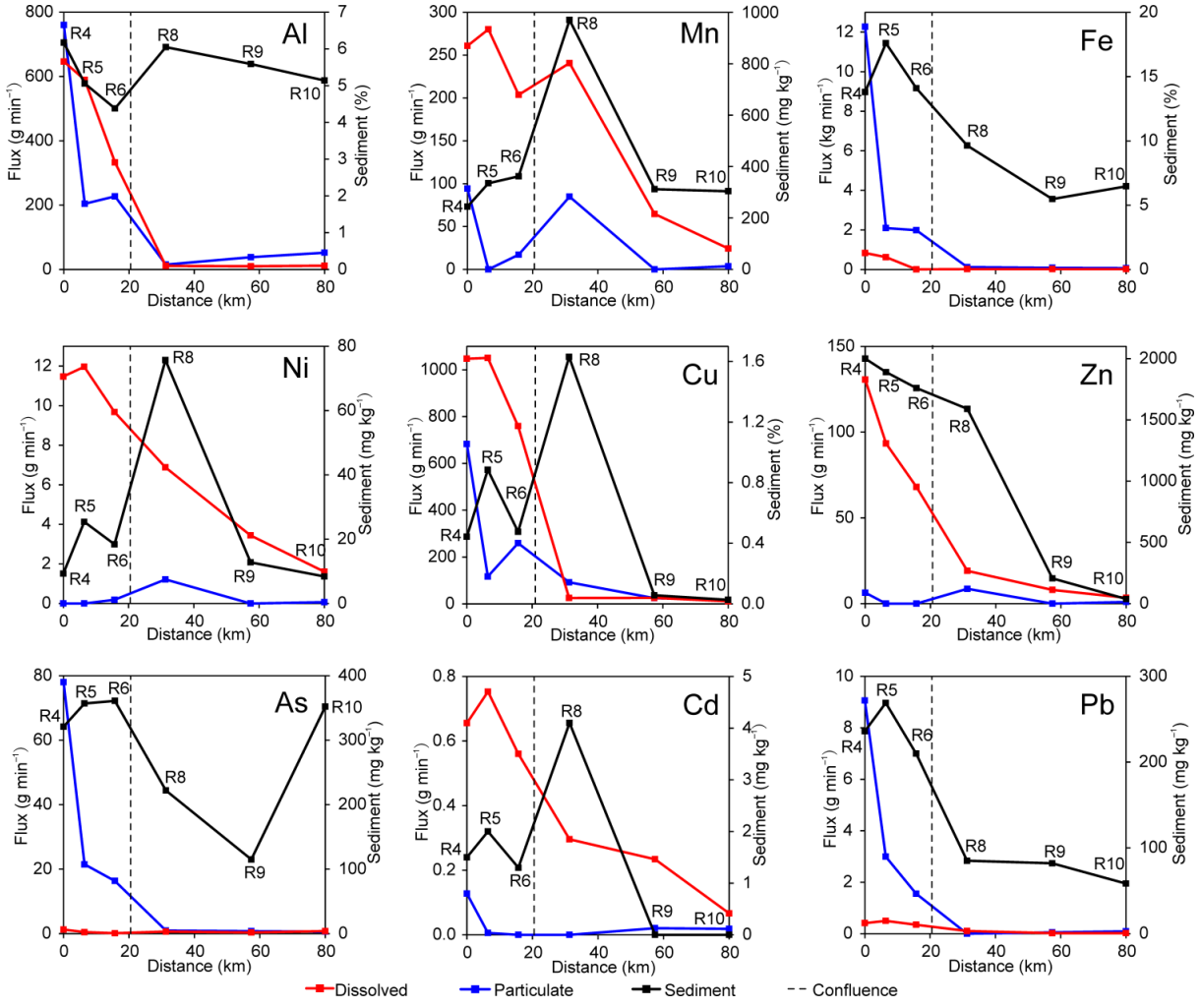

Fig. 6.5 Fluxes of dissolved and particulate forms and sediment concentrations of metals and arsenic at sampling points along Bela River (R4–R6) and Timok River (R8–R10)

Fluxes of dissolved and particulate forms, and sediment concentrations of metals and arsenic from upstream to downstream are shown in Fig. 6.5. If the concentrations of metals

decreased from upstream to downstream due to dilution, the flux of the metals would not change. However, if the decrease in concentrations of metals was due to precipitation on the river bed, then the flux of the metals would decrease. As a general tendency, decreases in fluxes of Al, Fe, Cu, As, and Pb were more drastic than those of other metals, suggesting that precipitation was the main cause of the decrease in concentrations of these metals in river water. However, the decreases in fluxes of Mn, Ni, Zn, and Cd were not intense. This suggests that dilution played an important role in the decrease in concentrations of these metals in river water. Specifically, the ratio of total fluxes of Al, Fe, Cu, As, and Pb in water of Bela River (RW6) and Timok River (RW8), that is RW6/RW8, ranged from 9 to 21 (large change – precipitation predominant), and the same ratio for Mn, Ni, Zn and Cd ranged from 0.7 to 2.5 (small change – dilution predominant). Although concentrations of Mn, Ni, and Cd in river water were decreased mainly by dilution, their concentrations in sediment and the fluxes of particulate forms of Mn and Ni increased simultaneously after the confluence of Bela River and Timok River (R8; Fig. 6.5). This finding suggests that some portion of the particulate forms of Mn, Ni, and Cd precipitated on the river bed sediment of Timok River (RS8) (Đorđievski et al., 2018).

6.3. Seasonal variation of mobility of metals and arsenic in river water

6.3.1. Seasonal changes of pH, Eh and electrical conductivity values

In addition to the results of field survey from August 2015, the results from field surveys from September 2016, February 2017, and August 2017 were presented in this chapter. Comparisons of field parameters and concentrations of metals and arsenic between these four seasons were presented. Locations of sampling points in abovementioned field surveys were same as locations of sampling points in Fig. 6.1.

Results of the field measurements from from September 2016, February 2017, and August 2017 are shown in Table 6.4. Discharge of rivers was not measured in February 2017 due to cold weather and increased discharge of rivers. Measurement of discharge of Timok River was also not possible for RW7 in September 2016 and for RW8 and RW9 in August 2017.

Table 6.4 Discharge (Q), pH, oxidation-reduction potential (Eh) and electrical conductivity (EC) values of river water in Bor mining area from September 2016, February 2017, and August 2017

	September 2016				February 2017				August 2017			
	Q	pH	Eh	EC	Q	pH	Eh	EC	Q	pH	Eh	EC
RW1	0.54	2.92	673	2873	n.d.	2.06	616	6858	0.25	6.30	328	1538
RW2	0.36	4.98	471	2269	n.d.	4.75	474	1929	0.19	6.30	478	2816
RW3	0.20	8.12	340	522	n.d.	7.33	348	348	0.015	7.68	423	492
RW4	1.25	3.28	650	2335	n.d.	2.98	632	2554	0.68	6.40	353	1746
RW5	0.97	3.34	649	2130	n.d.	3.09	634	2202	0.55	2.05	655	6314
RW6	0.92	2.99	694	2690	n.d.	3.32	624	1996	0.57	3.41	601	2766
RW7	n.d.	7.65	299	545	n.d.	7.35	340	507	3.38	7.46	2	564
RW8	2.84	6.64	444	838	n.d.	7.25	413	579	n.d.	7.43	409	668
RW9	8.78	7.68	346	820	n.d.	7.43	423	578	n.d.	7.55	453	910
RW10	7.44	7.80	337	855	n.d.	7.40	439	579	3.76	7.69	422	972

Q discharge (m^3 s^{-1})
Eh oxidation-reduction potential (mV)
EC electrical conductivity (µS cm^{-1})

Variation of pH values of Bor River (RW1) and Krivelj River (RW2) from August 2011 (Ishiyama et al., 2012), August 2015, September 2016, February 2017, and August 2017 are shown in Fig. 6.6 a. The pH value of Bor River in these seasons ranged from 2.06 to 6.30 and pH value of Krivelj River ranged from 6.70 to 4.49. Based on the data in Fig. 6.6 a, there was no clear trend in change of pH value of Bor and Krivelj Rivers.

Comparison of variations of pH value from upstream-to-downstream in August 2015, September 2016, February 2017 and August 2017 is shown in Fig. 6.6 b. Large difference in pH value of two subsequent water samples from Bela River in August 2017 (RW4 and RW5) is thought to be due to inconstant quantity and quality of metallurgical wastewater that was released from metallurgical facilities in Bor. The wave of river water containing large quantity of acidic metallurgical wastewater reached RW5 at the moment of sampling. This caused lower pH value of water of Bela River at RW5. Electrical conductivity also increased from RW4 to RW5 in August 2017 (from 1746 µs cm^{-1} to 6314 µs cm^{-1}).

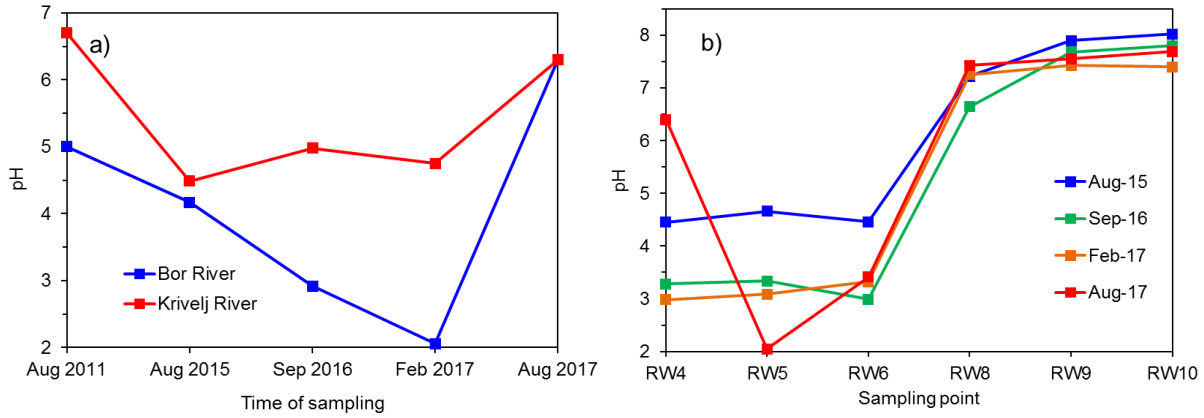

Fig. 6.6 Diagrams showing variations of pH values. **a** Variations of pH values of Bor and Krivelj Rivers in 5 different seasons. **b** Variations of pH values from upstream-to-downstream in 4 different seasons

6.3.2. Seasonal variation of concentrations of particulate, colloidal and dissolved forms of metals and arsenic in river water

Concentrations of metals and arsenic in unfiltered, filtered (<0.2 μm) and ultrafiltered (<6 nm) river water samples from Bor mining area in September 2016 are shown in Table 6.5. The highest concentrations of metals and arsenic were found in water of Bor River (RW1), Krivelj River (RW2), and Bela River (RW4, RW5, and RW6). The lowest concentrations of metals and arsenic were found in natural river water of Ravna River (RW3) and Timok River before confluence with Bela River (RW7).

Table 6.5 Concentrations of metals and arsenic in unfiltered, filtered (<0.2 μm) and ultrafiltered (<3000 Da) river water samples from Bor mining area in September 2016

		Al	Mn	Fe	Ni	Cu	Zn	As	Cd	Pb
	Unit	μg L^{-1}	μg L^{-1}	μg L^{-1}	μg L^{-1}	μg L^{-1}	μg L^{-1}	μg L^{-1}	μg L^{-1}	μg L^{-1}
	LOD	1	0.05		0.05	0.2	1	0.1	0.005	0.1
RW1	UnF	39500	7480	188000	1280	61900	5090	3940	197	176
	F	39000	7430	174000	1270	61000	5005	2191	193	146
	UltraF	33800	6420	171000	1100	52800	4360	1830	167	129
RW2	UnF	25800	7900	14300	102	21300	799	4.4	5.8	9.3
	F	4370	7950	3830	103	20400	801	0.7	6.1	0.7
	UltraF	4102	7670	3740	100	19600	780	0.7	5.5	1.6
RW3	UnF	67	4.7	<0.2	2.5	2.0	<1	2.8	<0.005	0.2
	F	8	2.8	<0.2	2.4	1.6	<1	2.8	<0.005	0.1
	UltraF	4	2.6	<0.2	2.3	1.0	<1	2.5	<0.005	0.1
RW4	UnF	31800	6830	73600	694	40000	2970	1330	106	81
	F	31300	6840	51000	692	39700	2958	222	105	69
	UltraF	30900	6770	49900	695	39500	2930	171	104	72
RW5	UnF	25900	6070	68000	626	35000	2640	1550	100	77
	F	25400	5990	23600	635	34900	2652	137	99	59
	UltraF	25100	5940	25400	627	34600	2640	136	97	59
RW6	UnF	49100	6210	198000	886	54700	5960	2800	311	93
	F	48300	6130	191000	876	54000	5862	1750	308	87
	UltraF	47600	6040	187000	870	53400	5790	1470	306	88
RW7	UnF	33	34	<0.2	2.5	1.9	1.9	2.8	<0.005	0.2
	F	21	34	<0.2	2.3	2.8	1.5	2.5	<0.005	0.2
	UltraF	16	33	<0.2	2.3	0.8	1.5	2.3	<0.005	0.2
RW8	UnF	95	943	569	159	1440	646	11.0	30	0.6
	F	9	943	<0.2	159	1260	641	8.6	30	0.2
	UltraF	7	948	<0.2	159	1220	640	8.4	30	0.2
RW9	UnF	56	759	283	89	532	384	5.7	17	0.3
	F	25	761	<0.2	89	405	375	3.2	17	0.2
	UltraF	21	751	<0.2	87	360	368	2.6	17	0.2
RW10	UnF	47	374	415	54	235	218	4.4	10	0.3
	F	19	372	<0.2	54	140	201	2.4	9.2	0.2
	UltraF	17	367	<0.2	53	101	194	1.9	8.8	0.1

UnF – unfiltered; F – filtered; UltraF - ultrafiltered

Variations of percentage of particulate, colloidal and dissolved forms of metals and arsenic from uspstream-to-downstream in September 2016 are shown in Fig. 6.7. In Bela River (RW4, RW5, and RW6) and Timok River after the confluence with Bela River (RW8,

RW9, and RW10), Mn, Ni, Zn, and Cd were present in dissolved form. Al and Cu were present in dissolved form in Bela River (RW4, RW5, and RW6), and the form of these metals changed to particulate form in Timok River after the confluence of Bela River (RW8, RW9, and RW10). Fe was present in particulate and dissolved form in Bela River (RW8, RW9, and RW10). However, in Timok River after the confluence of Bela River (RW8, RW9, and RW10), Fe was present only in particulate form. As and Pb were present in both forms from upstream-to-downstream. Colloidal form of metals and arsenic was not abundant in river water from September 2016. The highest percentages of colloidal form were found in RW10 for Pb (33%), Cu (17%), and As (11%).

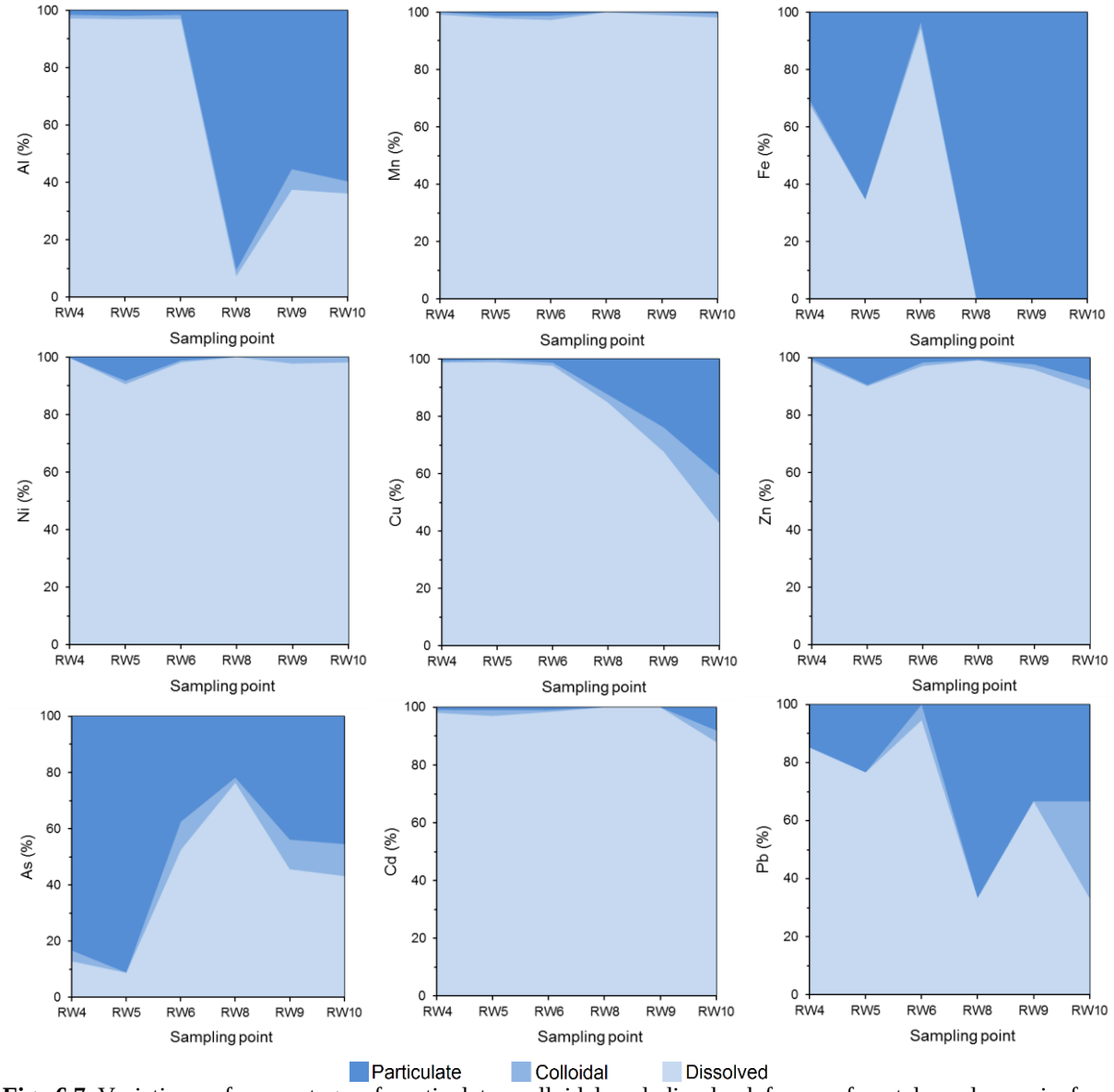

Fig. 6.7 Variations of percentage of particulate, colloidal and dissolved forms of metals and arsenic from uspstream-to-downstream in September 2016

Concentrations of metals and arsenic in unfiltered, filtered (<0.2 μm) and ultrafiltered (<6 nm) river water samples from Bor mining area in February 2016 are shown in Table 6.6. The highest concentrations of metals and arsenic in February 2017 were found in water of Bor River (RW1), Krivelj River (RW2), and Bela River (RW4, RW5, and RW6). The lowest concentrations of metals and arsenic were found in natural river water of Ravna River (RW3) and Timok River before confluence with Bela River (RW7).

Table 6.6 Concentrations of metals and arsenic river water from Bor mining area in February 2017

		Al	Mn	Fe	Ni	Cu	Zn	As	Cd	Pb
	Unit	μg L^{-1}	μg L^{-1}	μg L^{-1}	μg L^{-1}	μg L^{-1}	μg L^{-1}	μg L^{-1}	μg L^{-1}	μg L^{-1}
	LOD	1	0.05		0.05	0.2	1	0.1	0.01	0.1
RW1	UnF	46700	8200	324000	2182	116000	11500	13000	372	1265
	F	44900	8290	224000	2202	110000	10300	12400	375	949
	UltraF	44900	8230	229000	2186	110000	10200	12500	372	945
RW2	UnF	38800	6560	47000	153	23400	1850	73	30	3.8
	F	23500	6220	22800	145	21400	1741	3.0	29	2.6
	UltraF	19800	5710	22300	132	18900	1283	4.4	25	1.7
RW3	UnF	82	9.0	<0.2	2.1	1.4	<1	1.8	<0.01	0.2
	F	3	4.4	<0.2	2.1	1.1	<1	1.8	<0.01	0.1
	UltraF	2	4.4	<0.2	2.0	0.9	<1	1.8	<0.01	0.1
RW4	UnF	24400	4250	82100	627	37400	2960	2997	98	379
	F	23600	4330	61100	642	36200	2790	1990	101	295
	UltraF	22800	4210	62600	622	35000	2660	1910	98	289
RW5	UnF	23600	4180	74900	544	33300	2820	2494	91	336
	F	22500	4180	61800	546	32200	2560	1290	91	271
	UltraF	22200	4100	60300	538	31700	2530	1260	90	268
RW6	UnF	20800	3890	68800	494	30400	2610	2154	86	335
	F	19700	3850	55700	488	29000	2610	1050	86	269
	UltraF	19100	3740	53000	475	28200	2260	1020	83	261.5
RW7	UnF	186	26	<0.2	2.4	1.4	<1	1.0	<0.01	0.3
	F	18	19	<0.2	2.2	1.0	<1	1.1	<0.01	0.1
	UltraF	n.a.	n.a.	<0.2	n.a.	n.a.	n.a.	n.a.	n.a.	n.a.
RW8	UnF	1030	223	4150	27	1295	128	102	3.8	15
	F	25	212	<0.2	26	203	72	23	2.9	0.2
	UltraF	14	89	<0.2	11	75	27	8.9	1.1	0.1
RW9	UnF	114	203	470	21	236	64	25	2.5	1.2
	F	24	205	<0.2	22	153	59	20	2.4	0.1
	UltraF	22	203	<0.2	21	142	57	19	2.3	0.1
RW10	UnF	172	212	703	22	274	73	24	2.7	1.5
	F	24	207	<0.2	22	144	64	15	2.5	0.1
	UltraF	23	208	<0.2	22	133	62	15	2.4	0.1

UnF – unfiltered; F – filtered; UltraF - ultrafiltered

Variations of percentage of particulate, colloidal and dissolved forms of metals and arsenic in river water from uspstream-to-downstream in February 2017 are shown in Fig. 6.8. Distributions of particulate and dissolved forms of metals and arsenic in river water from upstream-to-downstream were similar as that in September 2016. However, larger percentage of colloidal form of metals and arsenic were found in February 2017. The largest percentages of colloidal form were found in water of Timok River after the confluence with Bela River

(RW8) for Mn (55%), Ni (56%), Cd (47%) and Zn (35%). As a general tendency, quantity of colloidal form of metals and arsenic was small compared to the quatities of particulate and dissolved forms in both seasons (September 2016 and February 2017).

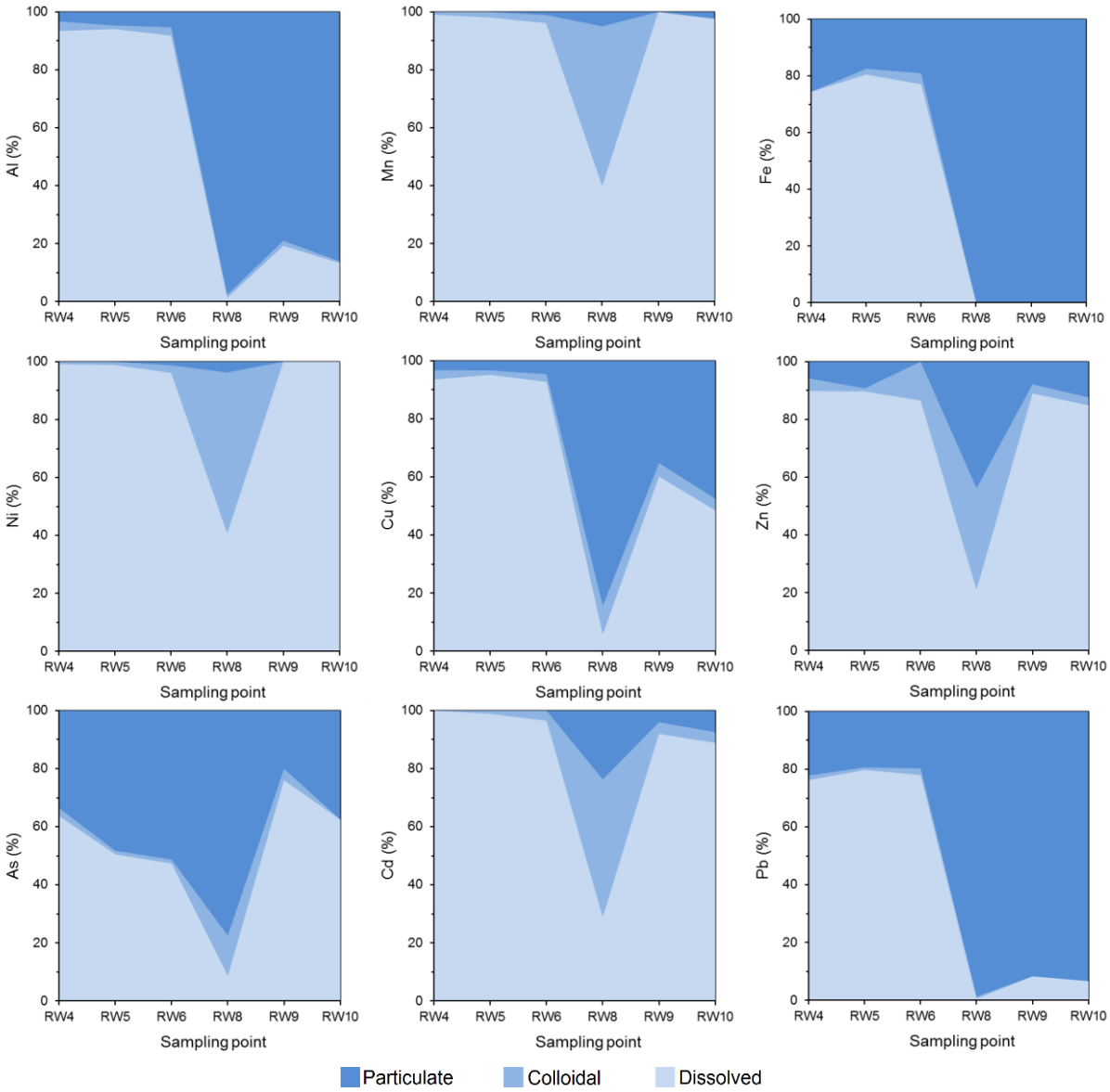

Fig. 6.8 Variations of percentage of particulate, colloidal and dissolved forms of metals and arsenic from uspstream-to-downstream in February 2017

Variation of total concentrations of metals and arsenic in water of Bor and Krivelj Rivers in August 2015, September 2016, and February 2017 is shown in Fig. 6.9. Total concentrations of Al, Mn, Cu, Fe, Cu, and Zn in Bor and Krivelj Rivers were not greatly different. However, total concentrations of Ni, As, Cd, and Pb were generally higher in Bor River than in Krivelj River in all three seasons. Concentrations of metals and arsenic in water

of Bor River increased from August 2015 through September 2016 to February 2017. This tendency was not evident in water of Kriverlj River.

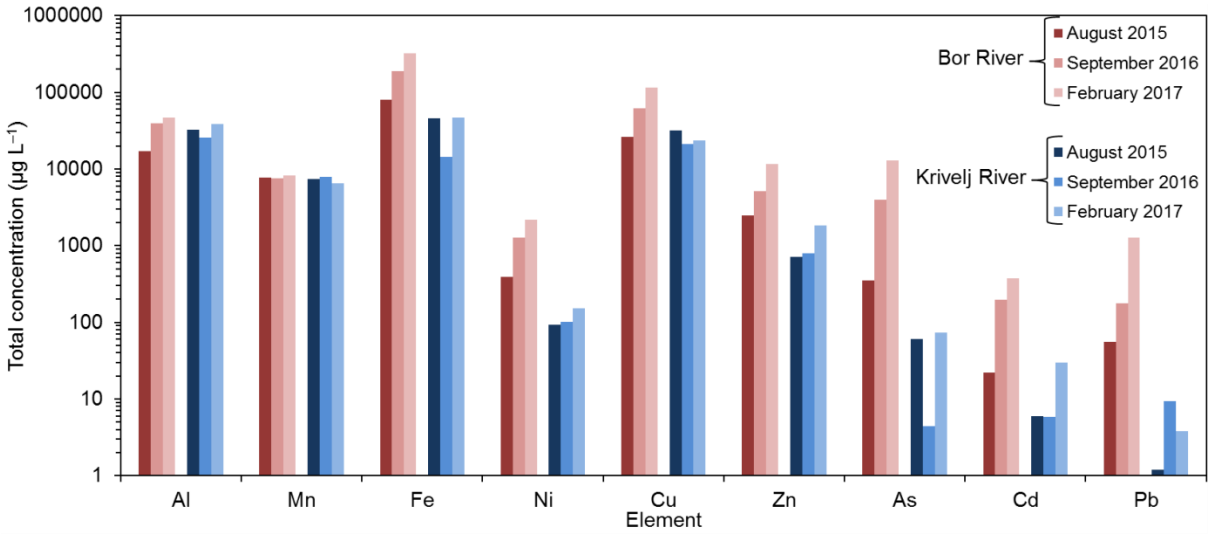

Fig. 6.9 Variation of total concentrations of metals and arsenic in water of Bor and Krivelj Rivers in 3 seasons

Variation of total concentrations of metals and arsenic from upstream-to-downstream in September 2016 and February 2017 is shown in Fig. 6.10. Generally, total concentrations of metals and arsenic decreased from upstream-to-downstream in both seasons, except that concentrations increased in water of Bela River from RW5 to RW6 in September 2016. This increase is thought to be due to the large quantity of metal-rich metallurgical wastewater that was released into the Bor River, and transported downstream to Bela River. This wave of wastewater reached RW6 at the moment of sampling. In both seasons, the largest decrease in concentrations of metals and arsenic were from RW6 to RW8. In February 2017, large decrease in concentrations was also from RW8 to RW9.

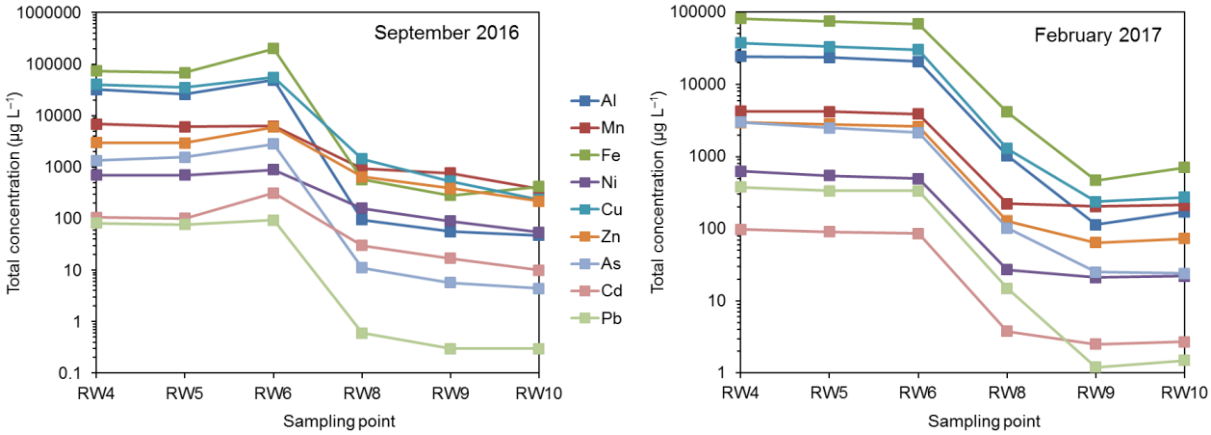

Fig. 6.10 Variation of total concentrations of metals and arsenic from upstream-to-downstream in September 2016 and February 2017

6.3.3. Temporal immobilization of metals and acidity in efflorescent sulfate salts

Photographs of locations from which samples of efflorescent sulfate salts were collected are shown in Fig. 6.11. Samples ES1, ES2 and ES3 were taken from the banks of Bor River, 500 m downstream from the dicharge of municipal wastewater and metallurgical wasterwater (near the points E1, E2 and E3 in Fig. 6.1). Sample ES4 was taken from the banks of Robule Lake (location of Robule Lake is shown in Fig. 2.3). Sample ES5 was taken near the exit of the collector of Saraka Stream (near point E5 in Fig. 6.1).

XRD patterns obtained by measurements of efflorescent sulfate salts from Bor mining area are shown in Appendix 7. Results of the identification of minerals are shown in Table 6.7. In sample ES1 following minerals were identified: epsomite ($MgSO_4 \cdot 7H_2O$) and melanterite ($FeSO_4 \cdot 7H_2O$). In sample ES2 following minerals were identified: epsomite ($MgSO_4 \cdot 7H_2O$), melanterite ($FeSO_4 \cdot 7H_2O$), chalcanthite ($CuSO_4 \cdot 5H_2O$) and Gypsum ($CaSO_4 \cdot 2H_2O$). In sample ES3 following minerals are identified: melanterite ($FeSO_4 \cdot 7H_2O$) and hexahydrite ($MgSO_4 \cdot 6H_2O$). In samples ES4 following minerals were identified: epsomite ($MgSO_4 \cdot 7H_2O$), halotrichite ($FeAl_2(SO_4)_4 \cdot 22H_2O$) and hexahydrite ($MgSO_4 \cdot 6H_2O$). In sample ES5 following minerals were identified: epsomite ($MgSO_4 \cdot 7H_2O$), melanterite ($FeSO_4 \cdot 7H_2O$) and halotrichite ($FeAl_2(SO_4)_4 \cdot 22H_2O$).

Fig. 6.11 Photographs of locations from which samples of efflorescent sulfate salts were collected. **a** Sample ES1 (near Bor River) **b** Samples ES2 and ES3 (near Bor River). **c** Sample ES4 (near Robule Lake). **d** Sample ES5 (near Saraka Stream)

Table 6.7 Results of qualitative XRD analysis of efflorescent sulfate salt samples

		Sample name				
Mineral name	Chemical formula	ES1	ES2	ES3	ES4	ES5
Epsomite	$MgSO_4 \cdot 7H_2O$	+	+		+	+
Melanterite	$FeSO_4 \cdot 7H_2O$	+	+	+		+
Chalcanthite	$CuSO_4 \cdot 5H_2O$		+			
Halotrichite	$FeAl_2(SO_4)_4 \cdot 22H_2O$				+	+
Gypsum	$CaSO_4 \cdot 2H_2O$		+			
Hexahydrite	$MgSO_4 \cdot 6H_2O$			+	+	

+ Mineral was identified in the sample

Minerals that were identified in samples of efflorescent sulfate salts from Bor mining area are hydrated sulfate salts of magnesium, calcium, iron, aluminum and copper. Divalent metals were present in all identified minerals, except in halotrichite where iron was divalent, and aluminum was trivalent. Chalcanthite belongs to triclinic crystal system, melanterite, halotrichite, gypsum and hexahydrite belong to monoclinic crystal system, and epsomite belongs to orthorhombic crystal system.

Divalent metals that constitute efflorescent sulfate salts may be replaced by other divalent metals, thus forming solid solutions. Mg in epsomite makes complete solid solution with Zn and Ni (Jambor et al., 2000). Respective endmember minerals are goslarite ($ZnSO_4 \cdot 7H_2O$) and morenosite ($NiSO_4 \cdot 7H_2O$). All three minerals (epsomite, goslarite and morenosite) belong to epsomite group. There is a possibility that Mg in epsomite from Bor mining area was replaced with Zn or Ni because concentrations of Zn and Ni in wastewater from Bor mining area were high (Table 6.3). However, it is not possible to determine the exact content of these metals using XRD method because minerals from epsomite group have same crystal structure, and therefore they also have same positions of peaks in XRD pattern. Fe in melanterite ($FeSO_4 \cdot 7H_2O$) could be also replaced by bivalent metals, but in the limited amount. For example, in Fe-Zn series, maximal fraction of zinc in melanterite is $(Fe_{0.45}Zn_{0.55})SO_4 \cdot 7H_2O$, and in Fe-Mg series, maximal fraction of magnesium in melanterite is $(Fe_{0.47}Mg_{0.53})SO_4 \cdot 7H_2O$ (Jambor et al., 2000). Other minerals that were identified in samples from Bor mining area may also include different bivalent metals.

Color of efflorescent minerals may vary depending on the content of some cations in crystal structure. Fig. 6.11 b shows the photograph of samples ES2 i ES3. Salts of blue color (ES2) and white-yellowish color (ES3) are present on the same location. Paragenesis of these minerals depends on humidity, temperature and pH value of the surrounding environment (Jambor et al., 2000). Blue color of sample ES2 originates from chalcanthite ($CuSO_4 \cdot 5H_2O$) that was identified in this sample. Blue color may originate from other minerals that contain Cu^{2+} ions in crystal structure, and green color may originate from divalent (ferrous) iron.

In the dry and warm period of year, efflorescent salts were crystalized on the banks of Bor River and near the sources of wastewater. In that way, metals and acidity were transferred from the solution into the solid phase. After the rainfall, these salts hydrolyze in rainwater, and acidity and heavy metals were returned into the Bor River. For example, hydrolysis of iron(II)-sulfate and formation of hydrogen ions (H^+) could be shown by following reversible reaction:

$$FeSO_{4(s)} + 2H_2O_{(l)} \leftrightarrow Fe(OH)_{2(s)} + SO_4^{2-}{}_{(aq)} + 2H^+{}_{(aq)}$$

Seasonal variation of concentrations of metals and arsenic in river water downstream from Bor copper mines was also influenced by formation of efflorescent sulfate salts. Due to dissolution of efflorescent sulfate salts, peaks in concentrations of metals in river water occur immidiately after the rainfal, then concentration of metals decrease to the level that is lower than the level before rainfall (Nordsrom, 2011). There is a possibility that this fhenomenon was also present in Bor mining area because efflorescent sulfate salts are formed in summer season.

6.4. Mobility of metals and arsenic in river bed sediments

6.4.1. Mineralogical characteristics of river bed sediments

Results of the qualitative XRD analysis of powdered sediment samples are shown in Table 6.8. The following minerals were identified in those sediment samples (RS1–RS10): Silicate minerals (quartz, plagioclase, and amphibole), clay minerals (illite, kaolinite, chlorite, and pyrophyllite), Fe-rich minerals (fayalite, magnetite, and pyrite), sulfate minerals (jarosite, alunite, and gypsum) and carbonate minerals (calcite).

Quartz was present in all river bed sediment samples. Plagioclase was present in all samples except RS1 and RS4. Amphibole was present in all samples except RS4. Illite was present in all samples except RS1. Chlorite was present in all samples except RS1, RS4, and RS10. Kaolinite was identified in RS1, RS4, and RS10. Pyrophyllite was identified in RS2, RS4, RS5, and RS6. Fayalite, magnetite, and pyrite were identified in river bed sediments of Bor River (RS1) and Bela River (RS4, RS5, and RS6). Pyrite was also identified in river bed sediments of Krivelj River (RS2) and Timok River after the confluence with Bela River (RS8). Gypsum was identified in river bed sediment of Timok River after the confluence with Bela River (RS8). Secondary sulfate minerals (jarosite and alunite) were identified in sediment samples from the lowermost sampling points of Timok River (RS9 and RS10). Calcite was identified in river bed sediments of Ravna River (RS3) and Timok River (RS7 and RS8).

Table 6.8 Results of the qualitative XRD analysis of powdered sediment samples

		RS1	RS2	RS3	RS4	RS5	RS6	RS7	RS8	RS9	RS10
Silicate minerals	Quartz	+	+	+	+	+	+	+	+	+	+
	Plagioclase		+	+		+	+	+	+	+	+
	Amphibole	+	+	+		+	+	+	+	+	+
Clay minerals	Illite		+	+	+	+	+	+	+	+	+
	Kaolinite	+			+						+
	Chlorite		+	+		+	+	+	+	+	
	Pyrophyllite		+		+	+	+				
Fe-rich minerals	Fayalite	+			+	+	+				
	Magnetite	+			+	+	+				
	Pyrite	+	+		+	+	+		+		
Sulfate minerals	Jarosite									+	+
	Alunite									+	+
	Gypsum								+		
Carbonate minerals	Calcite			+				+	+		

+ Mineral was identified in the sample

6.4.2. Concentrations of metals and arsenic in river bed sediments

Concentrations of metals and arsenic in river bed sediments are shown in Table 6.9. Variations in the concentrations of metals and arsenic in sediments from upstream to downstream are shown in Fig. 6.5. Concentrations of metals in sediments of AMD-bearing rivers were much higher than those in AMD-unaffected sediment of Ravna River (RS3). Concentrations of Cu in contaminated sediments were up to 300-times higher, concentrations of As and Zn were up to 50-times higher, and concentrations of Cd and Pb were up to 20-times higher than those in sediment RS3. Concentrations of Ni, Al, Mn and Fe in AMD-affected sediments were not greatly different from concentrations in AMD-unaffected sediment of Ravna River (RS3). The highest concentrations of metals and arsenic were found in sediments of Bor River (RS1) and in Timok River after the confluence with Bela River (RS8). According to these comparisons, river bed sediments that were affected by AMD-bearing river water were greatly polluted with metals and arsenic.

6.4.3. Fluvial transport of river bed sediments

In addition to pyrite-rich copper ores from the underground mine Bor, the mineral processing plant in Bor was processing old copper slag since 2001 in order to recover copper (Stanojlović and Sokolović, 2014). Fayalite and magnetite were major constituents (60% and 30%, respectively) of copper slag that was formed the copper smelter in Bor (Stanojlović and

Sokolović, 2014). These Fe-rich minerals (fayalite, magnetite, and pyrite) were identified in river bed sediments of Bor River (RS1) as a result of releases of flotation tailings from the mineral processing plant in Bor since 2001. Fine-grained particles containing Fe-rich minerals were mechanically transported by river water from Bor River (RS1) throughout Bela River (RS4, RS5, and RS6). River bed sediments from Bor River (RS1) and Bela River (RS4, RS5, and RS6) had about 10- and 5-times higher contents of total Fe, respectively, than the river bed sediment of Ravna River (RS3) in which Fe-rich minerals were not identified (Tables 6.4 and 6.5). Pyrite was also present in river bed sediment of Timok River after the confluence with Bela River (RS8), but not in river bed sediment at the point upstream from the confluence (RS7). This finding confirms that flotation tailings were transported throughout Timok River toward Danube River. Pyrite was not detected by XRD analysis in sediments from the lower reach of Timok River (RS9 and RS10); however, there is a possibility that small quantity of pyrite was present due to fluvial transport to downstream. Secondary sulfate minerals (jarosite and alunite) that were determined in sediment samples from the lower reach of Timok River (RS9 and RS10) are thought to be formed by the process of weathering of pyrite. Another evidence of pyrite weathering is acidic pH value of soils on floodplains of Timok River (Nikolic et al. 2016).

Table 6.9 Concentrations of metals and arsenic in river bed sediment samples

	Al	Mn	Fe	Ni	Cu	Zn	As	Cd	Pb
Unit	mg kg^{-1}	mg kg^{-1}	mg kg^{-1}	mg kg^{-1}	mg kg^{-1}	mg kg^{-1}	mg kg^{-1}	mg kg^{-1}	mg kg^{-1}
LOD	100	1	100	0.5	0.2	0.5	0.5	0.1	0.5
Accuracy	24.3%	7.8%	3.3%	8.9%	11.7%	6.2%	1.1%	34.9%	8.4%
RS1	29300	329	306000	27.4	14100	3470	673	3.2	497
RS2	83000	317	53800	9.5	3230	139	20.7	0.2	12
RS3	48300	701	30000	25.8	55.6	69	11.7	0.2	18.8
RS4	61700	244	138000	9.3	4440	2000	321	1.5	236
RS5	50600	335	176000	25.4	8850	1890	357	2	269
RS6	43800	362	141000	18.4	4760	1760	361	1.3	210
RS7	60200	1310	64000	29	78.6	113	10.6	0.1	22.2
RS8	60500	970	96400	75.7	16300	1590	222	4.1	85
RS9	55900	312	54800	12.8	567	206	115	< 0.1	82
RS10	51400	304	64700	8.4	264	37.4	352	< 0.1	58.4

Based on previous considerations, two processes contributed to increased concentration of metals and arsenic in river bed sediments: 1) chemical precipitation of metals and arsenic from river water to the river bed and 2) release of flotation tailings into the river water and their fluvial transport toward Danube River. On the other hand, another process caused lower concentrations of Mn in river bed sediments that were in contact with acidic river water (Table 6.4). The concentrations of Mn in AMD-affected sediments of Bor, Krivelj,

and Bela Rivers (RS1, RS2, RS4, RS5, and RS6; 244–362 mg kg^{-1}) were lower than those of AMD-unaffected sediments of Ravna River (RS3, 701 mg kg^{-1}) and Timok River (RS7, 1310 mg kg^{-1}). This fact suggests that concentration of Mn in river bed sediment depends on the pH value of river water. Van Ha et al. (2011) also found that a low pH value of river water facilitates dissolution of Mn from river bed sediments.

Metals for which total fluxes decreased more drastically (Al, Fe, Cu, As, and Pb) were also dominantly present in particulate form in river water. As the speed of river water decreases in the summer season, sedimentation of particulate forms of metals and arsenic becomes favorable. The presence of man-made lake downstream from the confluence of Bela River and Timok River additionally decreases the speed of river water. Concentration of copper in river bed sediment after the confluence of Bela River and Timok River (RS8; 1.6% of Cu) was much higher than the copper grade in the currently active open pit Veliki Krivelj (0.3% of Cu). This result indicates that the man-made lake on Timok River plays an important role in controlling transport of particulate forms of metals and arsenic. However, during the periods of high discharge of rivers, especially in snowmelt season, there is a possibility that particulate forms of metals and arsenic were transported downstream toward the Danube River. This possibility is supported by the fact that flotation tailings (coarser material than chemically precipitated metals) were transported to Danube River since 1950s in spite of the presence of the dam on Timok River (Paunović, 2010; Bogdanović et al., 2014). High temporal resolution monitoring of discharges and metal concentrations in river water is necessary (Elbaz-Poulichet et al., 2017) for accurate assessment of metals fluxes from Bor copper mines to Danube River during the periods of high discharge.

Ochreous muds were precipitated on the river bed and near the banks of Timok River after the confluence with Bela River (Fig. 6.12 b). The XRD-pattern of this sample is shown in Fig. 6.12 a. Sharp peaks were not present on the XRD pattern of ochreous precipitates. This finding indicates that ochreous precipitates were consisted mainly of amorphous materials. However, some peaks on XRD pattern indicate the presence of mineral schwertmannite.

Processes of natural attenuation from Bor mining area toward Danube River were occurring both in river water and river bed sediments: neutralization of acidic river water by bicarbonate-rich natural river water, dilution and precipitation of metals and arsenic, and transport of precipitated metals and flotation tailings to downstream during the periods of high discharge. Remediation of river bed and floodplain sediments in large area around Timok River may require significant financial investments. On the other hand, the concept of

"monitored natural attenuation" (MNA) advocates long-term monitoring of natural reduction in concentrations of contaminants without applying cleanup procedures. However, application of MNA also requires removal of the sources of contamination and a complete understanding of the site-specific conditions (Wilkin, 2008). MNA could be a possible remediation option for areas downstream from Bor copper mines since concentrations of metals and arsenic were reduced by natural processes in this area.

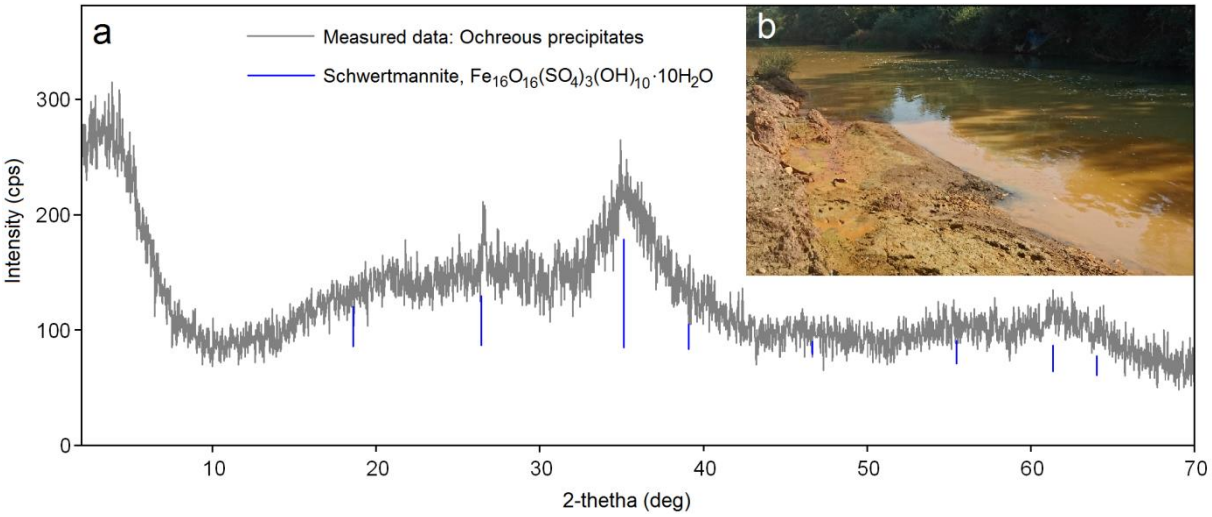

Fig. 6.12 Ochreous precipitates from the confluence of Bela River and Timok River. **a** XRD pattern. **b** Photograph of the sampling point.

7. Conclusions

Geochemical maps, histograms and cumulative probability (CP) diagrams were created for 9 elements in river water and river bed sediments from eastern Serbia. Variations of background and threshold concentrations were determined from histograms and CP diagrams. Spatial distribution of elements was determined from geochemical maps. Grouping of data points on histograms, CP diagrams and geochemical maps indicated patterns that were considered in detail. Minimum, median, mean, maximum, mean–2σ and mean+2σ values for 9 elements were calculated, and threshold values that separate background and anomalous concentrations were obtained from the brakes of slope on CP diagrams.

Concentration of Mn was decreased in river bed sediments that were in contact with acidic river water because of dissolution caused by acidic pH value. Higher concentrations of Ni were found in an area that consists of ultramafic rocks. High concentrations of Cu, Zn, As, Cd and Pb were found in river bed sediments downstream from Bor and Majdanpek copper

mines; however, those concentrations were higher downstream from Bor copper mines. There were no anomalous values of Al in river bed sediment. Higher concentrations of Fe were found in the region of Timok Magmatic Complex that consists of upper Cretaceous andesitic rocks. Concentration of Fe was also high in river bed sediments of Bor and Bela Rivers due to presence of Fe-rich minerals (pyrite, fayalite, magnetite) that originated from flotation tailings.

Water of rivers downstream from Bor copper mines was acidic. Geochemical maps of total and dissolved concentrations of metals and arsenic in river water showed that rivers downstream from Bor and Majdanpek copper mines were contaminated. Higher concentrations of metals and arsenic were more frequently found in water of rivers downstream from Bor copper mines. Metallurgical facilities in Bor had the largest impact on Bor River by discharging about 400 t of Cu per year through highly acidic wastewater (pH = 2.6). The highest measured concentrations of Cu in river water and sediments were 40 mg/L and 1.6%, respectively. Dissolution of calcite from limestone bedrock and a high concentration of bicarbonate ions in natural river water (about 250 mg/L) enhanced the neutralization of acidic river water and subsequent precipitation of metals and arsenic on the river bed. Decreases in the concentrations of Al, Fe, Cu, As and Pb in river water were mainly due to precipitation on the river bed. On the other hand, dilution played an important role in the decreases in concentrations of Mn, Ni, Zn and Cd.

Instead of remediation of contaminated river bed sediments downstream from Bor mining area, natural attenuation of metals and arsenic should be monitored. However, in order to enhance the processes of natural attenuation, removal of sources of contaminanation is necessary.

References

Alagić, S. Č., Tošić, S. B., Dimitrijević, M. D., Antonijević, M. M., Nujkić, M. M. (2015) Assessment of the quality of polluted areas based on the content of heavy metals in different organs of the grapevine (Vitis vinifera) cv Tamjanika. Environ. Sci. Pollut. Res., 22, 7155–7175.

Armstong, R., Koželj, D., Herrington, R. (2005) The Majdanpek Cu-Au Porphyry Deposit of Eastern Serbia: A Review. In: Porter T. M. (ed.), Super Porphyry Copper & Gold Deposits: A Global Perspective; PGC Publishing, Adelaide, v. 2, 453–466.

Bararunyeretse, P., Yao, J., Dai, Y., Bigawa, S., Guo, Z., Zhu, M. (2017) Toxic effect of two kinds of mineral collectors on soil microbial richness and activity: analysis by microcalorimetry, microbial count, and enzyme activity assay. Environ. Sci. Pollut. Res. 24, 1565–1577.

Birke, M., Rauch, U., Stummeyer, J. (2015) How robust are geochemical patterns? A comparison of low and high sample density geochemical mapping in Germany. J. Geochem. Explor., 154, 105–128.

Blowes, D. W., Ptacek, C. J., Jambor, J. L., Weisener, C. G. (2003) The Geochemistry of Acid Mine Drainage. In Environmental Geochemistry; Lollar, B.S., Ed.; Elsevier-Pergamon: Oxford, UK, pp. 149–204.

Bogdanović, D., Obradović, L., Miletić, S. (2014) Selection of the optimum method of rehabilitation the degraded areas around the Bor river downstream from the flotation tailing dump Bor. Mining & Metallurgy Engineering Bor, 4, 137–156.

Bogdanović, G., Trumić, M., Trumić, M., Anti,ć D. V. (2011) Mining waste management – Genesis and possibility of processing. Recycling and sustainable development 4, 37–43 (in Serbian, English abstract).

Brankov, J., Milijašević, D., Milanović, A. (2012) The assessment of the surface water quality using the water pollution index: a case study of the Timok River (the Danube River Basin), Serbia. Arch Environ Prot 38(1), 49–61.

Buccianti, A. (2015). The FOREGS repository: Modelling variability in stream water on a continental scale revising classical diagrams from CoDA (compositional data analysis) perspective. Journal of Geochemical Exploration, 154, 94–104.

Casiot, C., Egal, M., Elbaz-Poulichet, F., Bruneel, O., Bancon-Montigny, C., Cordier, M.-A., Gomez, E., Aliaume, C. (2009) Hydrological and geochemical control of metals and

arsenic in a Mediterranean river contaminated by acid mine drainage (the Amous River, France); preliminary assessment of impacts on fish (Leuciscus cephalus). Appl. Geochem., 24, 787–799.

Consani, S., Carbone, C., Dinelli, E., Balić-Žunić, T., Cutroneo, L., Capello, M., Salviulo, G., Lucchetti, G. (2017) Metal transport and remobilisation in a basin affected by acid mine drainage: the role of ochreous amorphous precipitates. Environ. Sci. Pollut. Res., 24, 15735–15747.

De Vos, V., Tarvainen, T. (Chief-editors), Salminen, R., Reeder, S., De Vivo, B., Demetriades, A., Pirc, S., Batista, M.J., Marsina, K., Ottesen, R.T., O'Connor, P.J., Bidovec, M., Lima, A., Siewers, U., Smith, B., Taylor, H., Shaw, R., Salpeteur, I., Gregorauskiene, V., Halamic, J., Slaninka, I., Lax, K., Gravesen, P., Birke, M., Breward, N., Ander, E.L., Jordan, G., Duris, M., Klein, P., Locutura, J., Bel-lan, A., Pasieczna, A., Lis, J., Mazreku, A., Gilucis, A., Heitzmann, P., Klaver, G., Petersell, V. (2006) Geochemical Atlas of Europe, Part 2: Interpretation of Geochemical Maps, Additional Tables, Figures, Maps and Related Publications. Geological Survey of Finland, Espoo, 618 pp., http://weppi.gtk.fi/publ/foregsatlas/part2.php.

Đorđievski S., Petrović J., Krstić V., Stevanović Z., Marković R., Jonović R., Avramović L. (2016) Comparative XRD and XRF analysis of selected mine waste samples from Oštreljski Planir dump (Bor, Serbia). Recycling and sustainable development, 9, 21–27 (in Serbian, English abstract).

Đorđievski, S., Sovrlić Z., Urošević T., Petrović J., Krstić V. (2017) Preventing decomposition of 2-mercaptobenzothiazole during gas chromatography analysis using programmable temperature vaporization injection. J. Serb. Chem. Soc., 82(10), 1147–1153.

Đorđievski, S., Ishiyama, D., Ogawa, Y. and Stevanović, Z. (2018): Mobility and natural attenuation of metals and arsenic in acidic waters of the drainage system of Timok River from Bor copper mines (Serbia) to Danube River. Environ. Sci. Pollution Res., v. 25, 25005–25019.

Đurović, P., Živković, N. (2013) Morphological and hydrological characteristics of the Serbian border zone towards Bulgaria. Bulletin of the Serbian Geographical Society, 93(4), 51–82.

Elbaz-Poulichet, F., Resongles, E., Bancon-Montigny, C., Delpoux, S., Freydier, R., Casiot, C. (2017) The environmental legacy of historic Pb-Zn-Ag-Au mining in river basins of

the southern edge of the Massif Central (France). Environ. Sci. Pollut. Res., 24, 20725–20735.

España, J. S., Pamo, E. L., Santofimia, E., Aduvire, O., Reyes, J., Barettino D. (2005) Acid mine drainage in the Iberian Pyrite Belt (Odiel river watershed, Huelva, SW Spain): geochemistry, mineralogy and environmental implications. Appl. Geochem., 20, 1320–1356.

Filimon, M. N., Nica, D. V., Ostafe, V., Bordean, D. M., Borozan, A. B., Vlad, D. C., Popescu, R. (2013) Use of enzymatic tools for biomonitoring inorganic pollution in aquatic sediments: a case study (Bor, Serbia). Chem. Cent. J., 7:59.

Filimon, M. N., Popescu, R., Horhat, F. G., Voia, O. S. (2016) Environmental impact of mining activity in Bor area as indicated by the distribution of heavy metals and bacterial population dynamics in sediment. Knowl. Manag. Aquat. Ecosyst., 417:30.

Förstner, U. (2004) Sediment dynamics and pollutants mobility in rivers: an interdisciplinary approach. Lakes and reservoirs: Research and Management, 9, 25–40.

Gardić, V. R., Petrović, J. V., Đurđevac-Ignjatoviić L. V., Kolaković S. R., Vujović S. R. (2015) Impact assessment of mine drainage water and municipal wastewater on the surface water near the city of Bor. Hem. Ind., 69(2), 165–174 (in Serbian, English abstract)

Grimalt, J. O., Ferrer, M., Macpherson, E. (1999) The mine tailing accident in Aznalcollar. Sci. Total Environ., 242, 3–11.

Hissner, F., Daus, B., Mattusch, J., Heinig, K. (1999) Determination of flotation reagents used in tin-mining by capillary electrophoresis. J. Chromatogr. A, 853, 497–502.

Ishiyama, D., Kawaraya, H., Sato, H., Obradović, L., Blagojević, B., Petrovic, J., Gardic, V., Stevanovic, Z., Shibayama, A., Masuda, N., Takasaki, Y. (2012) Geochemical Characteristics of Mine Drainage Water and River Water in the Bor Mining Area, Serbia: Results of Study in 2011. Scientific and Technical Reports of Graduate School of Engineering and Resource Science, Akita University, 33, 41–49.

Jambor, J. L., Nordstrom, D. K., Alpers, C. N. (2000) Metal-sulfate Salts from Sulfide Mineral Oxidation. Reviews in Mineralogy and Geochemistry, 40(1), 303–350.

Jelenković, R., Milovanović, D., Koželj, D., Banješević, M. (2016) The Mineral Resources of the Bor Metallogenic Zone: A Review. Geol Croat, 69(1), 143–155.

Jeremic, S., Beškoski, V. P., Djokic, L., Vasiljević, B., Vrvić, M. M., Avdalović, J., Gojgić Cvijović, G., Beškoski, L. S., Nikodinovic-Runic, J. (2016) Interactions of the metal

tolerant heterotrophic microorganisms and iron oxidizing autotrophic bacteria from sulphidic mine environment during bioleaching experiments. J. Environ. Manag., 172, 151–161.

Jia, Y., Demopoulos, G. P. (2008) Coprecipitation of arsenate with iron(III) in aqueous sulfate media: effect of time, lime as base and co-ions on arsenic retention. Water. Res., 42, 661–668.

Korać, M., Kamberović, Ž. (2007) Characterization of wastewater streams from Bor site. Metalurgija, 13(1), 41–51.

Kossoff, D., Dubbin, W. E., Alfredsson, M., Edwards, S. J., Macklin, M. G., Hudson-Edwards, K. A. (2014). Mine tailings dams: characteristics, failure, environmental impacts, and remediation. Applied Geochemistry, 51, 229–245.

Koželj, D. I. (2002) Epithermal Gold Mineralization in the Bor Metallogenic Zone – Morphogenetic types, structural-texture varieties and potentiality. Institut za Bakar Bor, Bor (in Serbian, English summary).

Lekovski, R., Mikić, M., Kržanović, D. (2013) Impact of the flotation tailing dumps on the living environment of Bor and protective measures. Mining & Metallurgy Engineering Bor, 2, 97–116.

Markovic, R., Gardic V., Obradovic, L., Djordjievski, S., Stevanovic, Z., Stevanovic, J. Gvozdenovic, M. (2015) The Application of a Natural Zeolite for Acid Mine Drainage Purification. Materials Transactions, 56(12), 2053–2057.

Matschullat, J., Ottenstein, R., Reimann, C. (2000) Geochemical background - can we calculate it? Environ. Geol., 39, 990–1000.

Mikić, M., Kržanović, D., Jovanović, M., Maksimović, M. (2015) Review of the open pit South mining district – Majdanpek: Impact on the environment and protective measures. Mining & Metallurgy Engineering Bor, 3, 1–16.

Milijašević, D., Milanović, A., Brankov, J., Radovanović, M. (2011) Water quality assessment of the Borska Reka River using the WPI (Water Pollution Index) method. Arch. Biol. Sci. Belgrade, 63(3), 819–824.

Milošković, A., Dojčinović, B., Kovačević, S., Radojković, N., Radenković, M., Milošević, Đ., Simić, V. (2016) Spatial monitoring of heavy metals in the inland waters of Serbia: a multispecies approach based on commercial fish. Environ. Sci. Pollut. Res., 23, 9918–9933.

Mrvić, V., Kostić-Kravljanac, L., Zdravković, M., Koković, N., Perović, V., Čakmak, D., Nikoloski, M. (2011a) Methods for Assessment of Background Limit of Ni and Cr in Soils of Eastern Serbia. Field Veg. Crop Res., 48, 189–194.

Mrvić, V., Kostić-Kravljanac, L., Čakmak, D., Sikirić, B., Brebanović, B., Perović, V., Nikoloski, M. (2011b) Pedogeochemical mapping and background limit of trace elements in soils of Branicevo Province (Serbia). Journal of Geochemical Exploration, 109, 18–25.

Mrvić, V., Zdravković, M., Sikirić, B., Čakmak, D., Kostić-Kravljanac, Lj. (2009) Content of hazardous and harmful elements. In: Mrvić, V., Antonović, G., Lj, Martinović (Eds.), Fertility Status and Content of Hazardous and Harmful Elements in the Soils of Central Serbia. Institute for Soil Science, Belgrade, 75–145 (in Serbian).

Nikolic, N., Böcker, R., Nikolic, M. (2016) Long-term passive restoration following fluvial deposition of sulphidic copper tailings: nature filters out the solutions. Environ. Sci. Pollut. Res., 23, 13672–13680.

Nordstrom, D. K. (2011) Hydrogeochemical processes governing the origin, transport and fate of major and trace elements from mine wastes and mineralized rock to surface waters. Appl. Geochem., 26, 1777–1791.

Nystrand, M. I., Österholm, P., Nyberg, M. E., Gustafsson, J. P. (2012) Metal speciation in rivers affected by enhanced soil erosion and acidity. Appl Geochem 27, 906–916.

Ogawa, Y., Ishiyama, D., Shikazono, N., Iwane, K., Kajiwara, M., Tsuchiya, N. (2012) The role of hydrous ferric oxide precipitation in the fractionation of arsenic, gallium, and indium during the neutralization of acidic hot spring water by river water in the Tama River watershed, Japan. Geochim Cosmochim Acta, 86, 367–383.

Oyarzún, J., Carvajal, M. J., Maturana, H., Núñez, J., Kretschmer, N., Amezaga, J. M., Rötting, T. S., Strauch, G., Thyne, G., Oyarzún, R. (2013) Hydrochemical and isotopic patterns in a calc-alkaline Cu- and Au-rich arid Andean basin: The Elqui River watershed, North Central Chile. Appl. Geochem., 33, 50–63.

Paunović, P. (2010) Unsuccessful attempt of regulation of Timok in order to prevent destruction of the land from industrial waste from Bor copper mine. In: Proceedings of XVIII International Scientific and Professional Meeting "Ecological Truth" Eco-Ist'10, 1–4 June, Spa Junakovic, Apatin, Serbia, Publisher: Univ. of Belgrade – Technical Faculty in Bor, Serbia, pp 224–251.

Pejović, M., Bajat, B., Gospavić, Z., Saljnikov, E., Kilibarda, M., Čakmak, D. (2017) Layer-specific spatial prediction of As concentration in copper smelter vicinity considering the terrain exposure. J. Geochem. Explor., 179, 25–35.

Plathe, K. L., von der Kammer, F., Hassellöv, M., Moore, J. N., Murayama, M., Hofmann, T., Hochella, M. F. (2013) The role of nanominerals and mineral nanoparticles in the transport of toxic trace metals: Field-flow fractionation and analytical TEM analyses after nanoparticle isolation and density separation. Geochim. Cosmochim. Acta, 102, 213–225.

Prica, M., Dalmacija, B., Dalmacija, M., Agbaba, J., Krčmar, D., Tricković, J., Karlovic, E. (2010) Changes in metal availability during sediment oxidation and the correlation with immobilization potential. Ecotoxicol. Environ. Saf., 73, 1370–1377.

Protić, N., Martinović, L., Milicić, B., Stevanović, D., Mojasević M. (2005) The Status of Soil Surveys in Serbia and Montenegro. In: Soil Resources of Europe, second edition. R. J. A. Jones, B. Houšková, P. Bullock and L. Montanarella (eds). European Soil Bureau Research Report No.9, EUR 20559 EN, 420pp. Office for Official Publications of the European Communities, Luxembourg.

Rabadjieva, D., Tepavitcharova, S., Todorov, T., Dassenakis, M., Paraskevopoulou, V., Petrov, M. (2009) Chemical speciation in mining affected waters: the case study of Asarel-Medet mine. Environ Monit Assess, 159, 353–366.

Radić, S., Vujčić, V., Cvetković, Z., Cvjetko, P., Oreščanin, V. (2014) The efficiency of combined CaO/electrochemical treatment in removal of acid mine drainage induced toxicity and genotoxicity. Sci. Total. Environ., 466–467, 84–89.

Ranđelović, D., Gajić, G., Mutić, J., Pavlović, P., Mihailović, N., Jovanović, S. (2016) Ecological potential of Epilobium dodonaei Vill. for restoration of metalliferous mine wastes. Ecol. Eng., 95, 800–810.

Reimann, C., de Caritat, P. (2017) Establishing geochemical background variation and threshold values for 59 elements in Australian surface soil. Sci. Total Environ., 578, 633–648.

Reimann, C., Fabian, K., Birke, M., Filzmoser, P., Demetriades, A., Négrel, P., Oorts, K., Matschullat, J., de Caritat, P., The GEMAS Project Team. (2017) GEMAS: Establishing geochemical background and threshold for 53 chemical elements in European agricultural soil. Applied Geochemistry, http://dx.doi.org/10.1016/j.apgeochem.2017.01.021

Reimann, C., Filzmoser, P. (2000) Normal and lognormal data distribution in geochemistry: death of a myth. Consequences for the statistical treatment of geochemical and environmental data. Environ. Geol., 39 (9), 1001–1014.

Reimann, C., Filzmoser, P., Garrett, R. (2005) Background and threshold: critical comparison of methods of determination. Sci. Total Environ., 346, 1–16.

Reimann, C., Filzmoser, P., Garrett, R., Dutter, R. (2008) Statistical Data Analysis Explained: Applied Environmental Statistics with R. Wiley, Chichester.

Reimann, C., Garrett, R.G. (2005) Geochemical background - concept and reality. Sci. Total Environ., 350, 12–27.

Rodríguez-Lado, L., Hengl, T., Reuter, H. I. (2008) Heavy metals in European soils: a geostatistical analysis of the FOREGS Geochemical database, Geoderma, 148, 189–199.

Salminen, R. (Chief-Editor), Batista, M.J., Bidovec,M., Demetriades, A., De Vivo, B., De Vos,W., Duris,M., Gilucis, A., Gregorauskiene, V., Halamic, J., Heitzmann, P., Lima, A., Jordan, G., Klaver, G., Klein, P., Lis, J., Locutura, J., Marsina, K., Mazreku, A., O'Connor, P.J., Olsson, S.Å., Ottesen, R.-T., Petersell, V., Plant, J.A., Reeder, S., Salpeteur, I., Sandström,H., Siewers, U., Steenfelt, A., Tarvainen, T., 2005. Geochemical atlas of Europe. Part 1 – Background information, methodology and maps. Geological Survey of Finland, Espoo, Finland, 525 pp., http://weppi.gtk.fi/publ/foregsatlas/index.php.

Šerbula, S., Stanković, V., Živković, D., Kamberović, Ž., Gorgievski, M., Kalinović, T. (2016) Characteristics of Wastewater Streams Within the Bor Copper Mine and Their Influence on Pollution of the Timok River, Serbia. Mine. Water. Environ., 35, 480–485.

Šerbula, S. M., Milosavljević, J. S., Radojević, A. A., Kalinović, J. V., Kalinović, T. S. (2017) Extreme air pollution with contaminants originating from the mining–metallurgical processes. Sci. Total. Environ. 586, 1066–1075.

Stanković, S., Vasiljević, B., Jeremić, S., Cvetković, V., Morić, I. (2017) Evaluation of microbial diversity of the microbial mat from the extremely acidic Lake Robule (Bor, Serbia). Botanica Serbica, 41(1), 17–54.

Stanojlović, R. D., Sokolović, J. M. (2014) A study of the optimal model of the flotation kinetics of copper slag from copper mine Bor. Arch. Min. Sci., 59(3), 821–834.

Stevanović, Z., Dragišić, V. (1998) An example of identifying karst groundwater flow. Environ. Geol., 35(4), 241–244.

Stevanović, Z., Jemcov, I., Milanović, S. (2007) Management of karst aquifers in Serbia for water supply. Environ. Geol., 51(5), 743–748.

Stevanović, Z., Obradović, L., Marković, R., Jonović, R., Avramović, L., Bugarin, M., Stevanović, J. (2013) Mine Waste Water Management in the Bor Municipality in Order to Protect the Bor River Water. In: García Einschlag FS (ed) Waste Water – Treatment Technologies and Recent Analytical Developments, InTech, pp 41–62.

Stevanović, Z. O., Antonijević, M. M., Bogdanović, G. D., Trujić, V. K., Bugarin, M. M. (2011) Influence of the chemical and mineralogical composition on the acidity of an abandoned copper mine in the Bor river valley (eastern Serbia). Chem. Ecol., 27(5), 401–414.

Tang, D., Warnken, K. W., Santschi, P. H. (2001) Organic complexation of copper in surface waters of Galveston Bay. Limnol, Oceanogr., 46, 321–330.

Van Ha, N. T., Takizawa, S., Oguma, K., Van Phuoc, N. (2011) Sources and leaching of manganese and iron in the Saigon River Basin, Vietnam. Wat. Sci. Tech. 63, 2231–2237.

Waeles, M., Tanguy, V., Riso, R. D. (2015) On the control of copper colloidal distribution by humic substances in the Penzé estuary. Chemosphere, 119, 1176–1184.

Wilkin, R. T. (2008) Contaminant attenuation processes at mine sites. Mine. Water. Environ., 27, 251–258.

Apendices

Appendix 1. Map of the study area with labels of the sampling sites

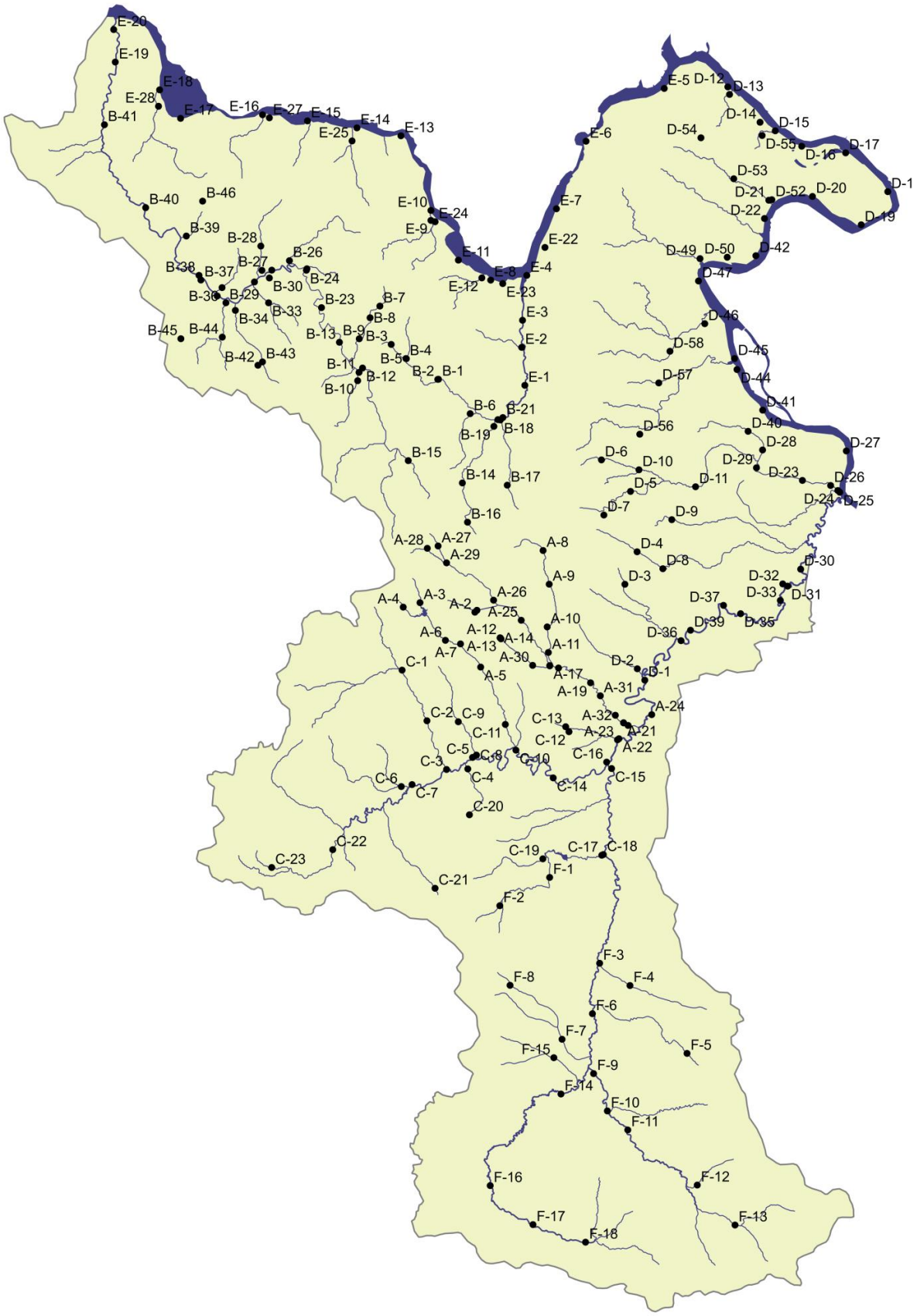

Appendix 2. Coordinates of sampling points, pH and Eh values, discharge, and concentrations of chlorides and sulfates

Sampling point	X	Y	pH	Eh (mV)	Discharge (L min^{-1})	Chloride (mg L^{-1})	Sulfate (mg L^{-1})
A-1 (E4)	44.09366	22.09533	2.79	910	1,394	13.0	5240
A-2	44.09152	22.09210	7.32	676	1,397	8.91	494
A-3	44.10308	22.00631	7.37	456	108	6.14	62.5
A-4	44.09825	21.97992	7.21	579	50	2.84	65.7
A-5	44.02939	22.10000	7.91	658	7,315	5.06	86.4
A-6	44.06014	22.04536	7.91	682	17,341	9.29	83.7
A-7	44.05592	22.06892	8.28	710	1,577	7.5	170
A-8	44.16017	22.20033	8.14	658	752	7.63	44.2
A-9	44.12200	22.20914	8.13	679	1,703	4.65	48.8
A-10	44.07375	22.20503	8.27	567	1,299	3.01	23.2
A-11 (R3)	44.04483	22.20625	8.41	636	6,605	5.5	42.2
A-12 (E1)	44.06222	22.13099	5.28	600	1,490	76.6	3430
A-13 (E2)	44.06210	22.13108	8.56	687	15,141	31.5	700
A-14 (E3)	44.06192	22.13154	2.61	896	7,136	16.8	4550
A-15	44.06103	22.13243	4.05	758	21,738	32.6	1400
A-16 (R1)	44.02966	22.20814	4.17	697	34,951	32.3	1510
A-17 (R2)	44.03004	22.20814	4.49	707	33,746	41.1	2060
A-18 (R4)	44.02717	22.22176	4.45	687	43,361	33.1	1590
A-19 (R5)	44.00987	22.27157	4.66	688	55,584	29.4	1360
A-20	43.96099	22.32920	4.48	746	54,980	30.3	1440
A-21 (R6)	43.96415	22.32218	4.46	815	44,095	30.8	1430
A-21-1	43.96394	22.32223	5.00	656	-	21.1	1070
A-22 (R7)	43.94612	22.31454	7.29	420	-	17.9	46.7
A-23	43.94497	22.31227	7.15	641	4	18.4	114
A-24	43.97276	22.36640	6.87	591	-	19	316
A-25	44.08168	22.16451	6.23	835	36,023	28.7	2360
A-26 (E5)	44.10481	22.12164	4.43	722	2,462	5.47	2510
A-27	44.16692	22.03576	7.96	584	2,675	2.41	485
A-28	44.16441	22.01879	7.73	581	6,314	2.1	196
A-29	44.14771	22.04872	8.79	568	9,894	4.83	254
A-30	44.03053	22.18136	2.91	867	175,507	29.8	2010
A-31	43.99497	22.28653	5.41	644	306,439	18.1	924
A-32	43.97273	22.30953	5.06	655	354,718	18.5	935
B-1	44.35530	22.03972	7.73	589	10,535	4.94	38.1
B-2	44.35523	22.03857	7.84	653	20,411	7.61	74.2
B-3	44.39538	21.96597	7.92	557	615	22.8	57.8
B-4	44.37903	21.98952	7.70	598	14,421	2.19	29.1
B-5	44.37920	21.98885	7.66	600	1,310	12.3	154
B-6	44.31599	22.08884	7.98	572	7,166	28.8	30.3
B-7	44.43887	21.94881	7.65	646	1,272	0.97	28
B-8	44.42577	21.93316	8.07	611	3,584	4.42	26
B-9	44.40217	21.91575	7.25	443	34,234	11.7	1630
B-10	44.35478	21.91250	7.97	610	9,529	2.68	28
B-11	44.36421	21.91478	8.17	571	53,887	4.98	155
B-12	44.36906	21.92039	7.55	578	2,581	22.9	863
B-13	44.39846	21.88445	8.42	576	53,887	9.78	680
B-14	44.23779	22.07513	8.34	552	7,401	5.08	25.1
B-15	44.26380	21.99058	8.28	547	2,466	2.92	51
B-16	44.19336	22.08240	8.19	559	412	6.77	24.4
B-17	44.23459	22.14559	8.29	517	5,651	7.19	33.8
B-18	44.30848	22.13620	8.35	545	4,052	8.22	38
B-19	44.30126	22.12585	8.08	543	539	21.8	53.3
B-20	44.30882	22.13230	7.81	604	13,479	16.0	46.8

B-21	44.31109	22.14014	8.16	568	5,342	12.2	42.9
B-23	44.43782	21.85680	8.25	570	-	11.2	142
B-24	44.48028	21.83355	8.19	544	-	12.5	51
B-25	44.48190	21.83444	8.41	567	59,504	10.7	24.5
B-26	44.49128	21.80701	8.28	559	385,680	3.24	22.4
B-27	44.48077	21.77899	7.99	601	-	3.76	111
B-28	44.50808	21.76205	7.98	560	81,555	3.07	25.4
B-29	44.44435	21.70625	7.94	586	133,317	1.93	18.7
B-30	44.47193	21.77507	7.74	598	33,444	3.66	27.1
B-31	44.48061	21.76343	8.02	554	510,330	3.2	27.8
B-32	44.46762	21.75149	8.03	571	-	4.62	105
B-33	44.44388	21.77348	8.22	567	423,995	15.8	24.3
B-34	44.43565	21.72101	7.91	602	101,415	1.48	20.3
B-35	44.45209	21.69258	7.68	637	-	3.03	135
B-36	44.46153	21.70032	7.95	581	240,833	8.3	31.8
B-37	44.47030	21.66709	8.36	543	82,486	5.21	24
B-38	44.47559	21.66416	7.89	569	-	3.94	153
B-39	44.52016	21.64465	8.22	552	110,533	2.91	14.1
B-40	44.55256	21.58080	7.29	559	-	4.34	151
B-41	44.64663	21.51655	7.90	614	-	4.44	140
B-42	44.37340	21.75580	7.83	618	456,449	1.41	18.2
B-43	44.37714	21.76297	7.79	617	195,228	1.31	20.8
B-44	44.40556	21.70005	8.09	624	758,348	1.7	18.6
B-45	44.40414	21.63478	8.17	568	230,508	1.81	17.2
B-46	44.55946	21.67082	8.22	559	31,431	2.1	15.8
C-1	44.02706	21.97697	8.13	740	10,871	0.91	25.7
C-2	43.96948	22.01491	7.88	681	3,239	5.05	36
C-3	43.91415	22.04458	7.60	643	115	12	32.4
C-4	43.91450	22.07778	7.92	618	61	22	67.6
C-5	43.92739	22.08544	8.38	566	18,169	7.06	24.2
C-6	43.89547	21.97361	8.03	603	247	10.4	57.2
C-7	43.89758	21.99044	7.89	676	15,467	5.98	21.7
C-8	43.93000	22.09156	7.98	662	1,612	2.34	14.4
C-9	43.96792	22.06389	7.46	655	0	28.7	39.4
C-10	43.93497	22.15333	8.07	715	12,140	9.7	45.7
C-11	43.96422	22.13736	8.45	654	24,901	9.99	88.5
C-12	43.95494	22.23666	7.59	368	373	30.4	62.5
C-13	43.96062	22.23164	7.14	329	2	15.9	153
C-14	43.90300	22.21096	8.46	586	54,738	11.8	43
C-15	43.91259	22.30233	8.25	618	119,540	13.8	42.2
C-16	43.91993	22.29483	7.19	268	-	28.2	55
C-17	43.81475	22.28491	7.93	589	6,796	6.67	26.2
C-18	43.81554	22.28737	8.11	597	21,944	15	36.9
C-19	43.81169	22.19297	7.85	601	390	13.9	54.5
C-20	43.86261	22.07940	7.27	512	0	12.2	70
C-21	43.78006	22.02432	8.46	562	1,195	7.46	105
C-22	43.82501	21.86553	7.51	598	1,634,595	15.6	13.9
C-23	43.80555	21.77004	7.76	634	746,337	23.8	11.4
D-1 (R8)	44.01188	22.35650	7.22	541	-	20.3	348
D-2	44.02487	22.34505	8.00	634	190	21.3	53.9
D-3	44.12060	22.32775	8.06	579	1,479	6.64	70.1
D-4	44.15709	22.34774	7.99	645	4,362	6.36	38.7
D-5	44.22545	22.33898	8.53	621	4,965	4.27	33.9
D-6	44.26160	22.29410	8.46	645	2,128	2.6	19.5
D-7	44.19923	22.29655	8.22	633	4,512	1.92	17.4
D-8	44.13748	22.38767	7.97	632	7,710	17.6	47.5
D-9	44.19271	22.40301	8.15	630	961	28.8	69.1
D-10	44.24971	22.35279	7.99	608	5,723	3.37	26.5
D-11	44.22946	22.44121	8.39	562	7,214	8.51	53.1
D-12	44.68069	22.50340	8.17	578	-	19.6	27.7

D-13	44.67211	22.50587	8.44	524	281	2.03	53.4
D-14	44.64001	22.55333	8.45	528	469	9.2	79.1
D-15	44.63004	22.57711	8.06	508	1,737	334	36.6
D-16	44.61201	22.61844	8.31	531	-	19.5	27.7
D-17	44.60353	22.68761	8.72	552	-	19.4	27.7
D-18	44.55869	22.75288	8.23	539	-	19.6	27.5
D-19	44.52186	22.70985	8.41	491	-	19.5	27.5
D-20	44.55504	22.63378	8.38	517	1,693	12.3	31.3
D-21	44.55172	22.56478	8.32	506	8,703	12.5	41.7
D-22	44.53118	22.55742	8.32	513	-	19.5	27.9
D-23	44.23438	22.60913	7.81	610	291,307	4.98	38.4
D-24	44.22218	22.66443	7.35	645	-	21.3	130
D-25	44.22018	22.66736	7.69	603	-	11.1	74.5
D-26	44.22802	22.65326	7.64	624	192,558	5.3	37.2
D-27	44.26669	22.67900	7.75	644	-	21.7	32.3
D-28	44.26965	22.54745	7.89	626	14,908	13.7	74.1
D-29	44.24964	22.53737	7.76	644	199,919	4.98	35.9
D-30 (R10)	44.13409	22.6037	8.02	615	-	6.58	111
D-31	44.11525	22.58274	8.10	617	-	6.49	92.6
D-32	44.11787	22.57516	8.36	592	1,752	9.81	69.2
D-33	44.09921	22.57089	8.08	616	-	6.78	98.5
D-35	44.08511	22.50825	7.50	644	-	6.51	112
D-36	44.05580	22.41422	7.91	676	-	7.72	110
D-37 (R9)	44.09485	22.48170	7.90	647	-	7.86	118
D-39	44.0674	22.42936	7.88	629	-	8.04	110
D-40	44.29104	22.52526	8.01	611	11,725	12.8	65.9
D-41	44.31465	22.54885	8.55	586	-	15.8	22.9
D-42	44.48932	22.54273	7.98	624	-	14.8	22.6
D-44	44.36110	22.50965	7.42	561	228,999	10.1	41.7
D-45	44.37352	22.50596	7.89	525	-	15.8	22.7
D-46	44.41357	22.46022	7.81	599	355,301	6.94	51.8
D-47	44.46196	22.45153	7.70	577	10,369	4.94	47.2
D-49	44.48717	22.45456	7.93	563	134,947	13.8	22.8
D-50	44.48820	22.49753	7.41	544	50,450	246	52.6
D-52	44.55225	22.56958	7.73	556	80,786	10.5	32.6
D-53	44.57674	22.51006	8.01	541	111,200	5.46	32.1
D-54	44.62371	22.45941	7.77	621	101,794	2.74	12.7
D-55	44.62502	22.55618	8.10	539	126,563	6.29	29.1
D-56	44.2899	22.35496	7.24	441	121,281	18.1	95.1
D-57	44.34753	22.38622	7.65	556	341,341	10.1	68.2
D-58	44.38309	22.40465	7.96	580	183,341	4.34	36.8
E-1	44.34716	22.17544	8.23	539	16,730	11.3	43.6
E-2	44.39012	22.17132	7.97	568	2,474	8.91	72.3
E-3	44.42073	22.17326	8.00	570	18,123	10.9	44.6
E-4	44.47138	22.18097	7.91	540	-	19.8	28.3
E-5	44.68020	22.40277	8.28	553	-	20.2	28.2
E-6	44.62201	22.27776	7.94	552	-	19.6	28.2
E-7	44.54620	22.22934	7.98	527	-	19.6	28.1
E-8	44.46661	22.12396	8.08	530	54	14.2	99.9
E-9	44.53498	22.03097	9.01	515	7,277	5.31	49.3
E-10	44.54626	22.03114	8.37	556	-	19.8	27.4
E-11	44.48968	22.07343	8.32	532	-	20.5	29.6
E-12	44.46926	22.11008	8.80	531	4,022	5.98	57.8
E-13	44.63106	21.98523	7.75	690	-	16.5	22.8
E-14	44.6406	21.91579	7.42	698	-	15.5	23.9
E-15	44.64907	21.83763	7.19	659	-	15.9	24
E-16	44.65650	21.76678	7.73	663	-	15	22.8
E-17	44.65321	21.63703	7.53	675	-	15.2	23.5
E-18	44.68564	21.60421	7.75	639	-	15.3	24.8
E-19	44.71740	21.53432	7.45	631	-	7.83	265

E-20	44.75411	21.53215	7.62	598	-	8.09	257
E-22	44.50268	22.21030	8.05	600	874,054	4.51	50
E-23	44.46251	22.14290	8.37	562	21,884	9.17	82.7
E-24	44.53341	22.03751	8.91	529	152,224	5.01	37.5
E-25	44.62588	21.90786	8.18	570	182,833	2.83	28.8
E-27	44.65298	21.77747	8.46	537	164,645	3.44	26.9
E-28	44.66708	21.60227	8.16	600	71,393	13.6	25.9
F-1	43.79058	22.20314	8.15	537	450,066	2.77	19.4
F-2	43.75940	22.12489	8.2	563	185,420	5.18	32.2
F-3	43.69269	22.27897	8.07	561	-	12.7	25.4
F-4	43.66698	22.32564	8.46	531	329,384	3.59	30.9
F-5	43.58923	22.41258	8.24	541	507,248	1.21	13.1
F-6	43.63583	22.26653	8.08	555	1,837,829	8.64	24.2
F-7	43.60740	22.21877	8.22	556	6,849	9.4	43.4
F-8	43.66925	22.13908	8.45	560	265,412	5.78	49.7
F-9	43.56810	22.26692	8.00	654	2,683,800	3.6	15.6
F-10	43.52565	22.28742	8.19	537	1,474,199	3.17	15.1
F-11	43.50377	22.31866	8.66	544	2,834,956	4.51	13.7
F-12	43.44020	22.42497	8.27	539	516,905	1.34	15
F-13	43.39428	22.48235	7.71	534	2,165,549	2.37	7.28
F-14	43.54556	22.21582	8.17	537	4,277,101	11.3	19.2
F-15	43.58673	22.20558	8.08	539	591,652	23.2	113
F-16	43.44315	22.10409	7.90	602	2,121,997	20.1	27.1
F-17	43.39839	22.16953	8.07	658	1,588,918	5.92	16.1
F-18	43.37766	22.25052	7.98	658	1,334,686	4.93	16.5

Appendix 3. Concentrations of elements in river bed sediments

Sampling Site	Al %	Mn mg kg^{-1}	Fe %	Ni mg kg^{-1}	Cu mg kg^{-1}	Zn mg kg^{-1}	As mg kg^{-1}	Cd mg kg^{-1}	Pb mg kg^{-1}
A-1	6.78	294	13.3	7	810	132	368	0.3	47.7
A-2	7.37	1880	12.2	16.4	1330	300	68.2	0.9	72
A-3	7.08	1810	6.39	11.3	337	125	34.3	0.8	35.8
A-4	7.16	1150	6.6	10.4	217	150	28.3	1	63.9
A-5	5.95	1510	12.9	25.1	261	202	14.5	0.8	45.2
A-6	4.79	2500	23.5	36.8	265	337	29.9	0.8	136
A-7	5.89	2200	15.2	28.9	386	275	40.5	2.2	71.9
A-8	6.53	890	4.26	45.2	67.7	71.7	13.7	0.1	13.5
A-9	6.48	1110	4.69	47.9	77.7	90.2	25.5	0.3	20.8
A-10	4.35	898	4.04	18.5	124	89.5	5.9	0.2	23.2
A-11 (RS3)	4.83	701	3	25.8	55.6	69	11.7	0.2	18.8
A-12	4.82	278	15.3	10.4	2010	2270	347	1.2	237
A-13	2.58	307	30.2	14.2	8590	4080	361	1.8	442
A-15	3.2	258	29.8	15.4	11100	3570	611	4	434
A-16 (RS1)	2.93	329	30.6	27.4	14100	3470	673	3.2	497
A-17 (RS2)	8.3	317	5.38	9.5	3230	139	20.7	0.2	12
A-18 (RS4)	6.17	244	13.8	9.3	4440	2000	321	1.5	236
A-19 (RS5)	5.06	335	17.6	25.4	8850	1890	357	2	269
A-20	6.81	244	14.3	47.3	12800	1290	1600	3.8	158
A-21 (RS6)	4.38	362	14.1	18.4	4760	1760	361	1.3	210
A-21-1	5.45	346	15.3	21.9	6430	1720	446	1.9	318
A-22 (RS7)	6.02	1310	6.4	29	78.6	113	10.6	0.1	22.2
A-23	6.11	1410	6.14	25.1	63.9	106	9.5	0.2	24.7
A-24	7.79	818	12.2	60.6	26400	2700	809	12.6	129
A-25	7.21	252	6.5	9.1	1300	38.5	27.4	0.1	7.8
A-26	7.28	274	4.58	4.6	1080	35.1	5.5	0.05	8.7
A-27	5.06	594	13.1	18	4420	652	75.9	2.8	114
A-28	7.24	2580	7.89	16.7	214	194	20.2	0.8	62.8
A-29	4.64	2920	27.3	31.2	1210	409	12.6	0.8	30
A-30	4.69	261	20.3	32.2	9420	3190	561	2	719
A-31	6.03	288	13.7	27.4	6980	1720	502	1.7	449
A-32	5.08	306	15.1	18.9	5090	1620	452	1.4	261
B-3	5.75	3220	4.73	29.6	311	346	25.9	0.9	29.8
B-4	6.48	1460	4.66	31	32.8	81.7	12.8	0.3	16.2
B-5	5.8	6810	7.97	54.3	1960	1220	80.4	4.1	105
B-6	6.6	940	6.03	22.4	41.9	79	7.5	0.05	24.8
B-7	5.66	1680	4.54	26.4	15.6	76.6	4.4	0.2	10
B-8	6.41	1360	5.32	32.6	484	252	60.9	25.3	307
B-9	6.32	1240	5.55	32.2	1460	1140	69.4	4.7	127
B-10	5.82	1130	6.33	23.2	37.5	93.1	12.1	0.1	16
B-11	6.05	1700	8.88	26.1	620	232	37.4	0.7	24.9
B-12	4.79	1540	12.1	33.1	1650	2900	159	12.2	54.2
B-13	5.81	1880	6.85	54.8	2570	1710	60.1	6.7	164
B-14	6.03	874	8.97	13.4	15.6	41.5	6.2	0.05	24.4
B-15	4.8	1860	13.7	15.8	65.6	153	2.6	0.1	15.4
B-16	5.92	861	3.91	27.1	25.3	54.8	15.5	0.2	14
B-17	6.38	1060	3.9	45.5	35.7	69.6	10.8	0.1	18.4
B-18	6.47	1070	5.42	90.6	201	137	55.7	0.2	27
B-19	6.95	946	3.95	19.9	21.7	46.6	5.3	0.05	20.7
B-20	6.52	1370	4.7	30.8	68.2	87.9	12.4	0.2	17.6
B-21	6.6	990	3.92	40.9	73.5	84.4	13.2	0.2	27.9
B-23	8.15	5320	5.81	52.8	1950	1950	69.2	8.7	268
B-24	6.55	2540	5.08	43.2	703	596	32.3	2.9	66.9
B-25	6.58	1850	5.63	63.7	91	101	29.2	0.6	30.2
B-26	7.21	1180	5.75	39.7	24.5	71.3	21.5	0.3	16

B-27	6.32	1800	4.95	33.2	705	511	37.8	1.9	48.5
B-28	6.48	854	4.37	20.2	20.4	54.6	13.9	0.2	15.1
B-29	7.25	1130	2.67	21	16.9	46.4	29	0.2	27.5
B-30	6.64	1030	4.16	36.1	38.9	76.7	32.3	0.4	15.9
B-31	6.52	832	4.39	27.9	27.4	59.2	17.8	0.2	27.6
B-32	5.47	1540	5	31.2	1260	625	50.3	2.2	59
B-33	6.9	776	3.91	26.5	18.4	51.1	17.8	0.2	15.1
B-34	7.16	685	2.75	16.1	216	63.4	19.4	0.3	30.6
B-35	6.65	1250	3.93	30.3	653	335	26.7	1.6	49.1
B-36	6.36	1290	3.36	25.9	26.2	56.1	13.7	0.4	21.3
B-37	5.87	791	1.78	15.3	15.2	148	13.1	0.7	66.6
B-38	6.4	1280	4.32	27.6	900	565	31.3	2.3	55.2
B-39	3.87	822	2.84	10.9	11.7	40.3	7.7	0.2	17.6
B-42	7.86	472	1.69	7.4	3.1	20.9	6	0.05	18.1
B-43	7.53	959	3.34	28.4	24.1	53.8	5	0.3	18.2
B-44	7.75	476	1.92	12	5	15.3	5.4	0.05	18.9
B-45	5.32	623	2.47	40.8	7.9	40.6	12.1	0.2	19.7
B-46	3.74	700	2.37	11.5	9	31	6.5	0.5	13.5
C-1	5.73	1290	11.3	41.6	61.8	170	12.5	0.3	26.4
C-2	6.19	1220	5.96	26.3	98.8	118	13.8	0.4	30.7
C-3	5.75	1620	16.5	40.9	70.6	187	13	0.2	21.9
C-4	5.01	1660	11	36	58.5	132	10	0.2	24.4
C-5	6.14	1220	6.31	22.9	181	101	9.5	0.1	19.9
C-6	5.18	1520	3.44	45.3	77.4	111	14	0.5	28.5
C-8	5.19	2170	22.8	41.7	90	258	6	0.2	33.8
C-9	4.62	2050	21.1	44.6	82.2	194	8.3	0.2	18.8
C-10	5.77	1690	10.9	29.8	127	147	12.6	0.2	26.6
C-11	4.51	2280	19.1	43.3	113	239	10.8	0.5	38.2
C-12	6.36	1160	6.55	17.6	120	103	10.5	0.05	18.2
C-13	5.94	1990	10.9	13.7	49.8	120	10	0.05	17.1
C-14	6	946	5.47	16.8	65.1	98	6.8	0.1	19.2
C-15	5.7	1150	5.04	30.4	34.2	68.7	11.7	0.05	47.9
C-16	6.06	719	4.06	27.2	171	100	14.2	0.1	61.2
C-17	4.72	1700	14.1	30.7	39	171	7.2	0.1	17.4
C-18	5.38	1680	7.52	33.8	26.7	70.6	13.2	0.05	15.5
C-19	5.72	1230	9.98	28.3	54.6	124	8.3	0.3	21.2
C-20	5.83	1820	10.6	30.1	81.4	171	38.5	0.2	38.1
C-21	5.41	1170	3.65	18.3	56.1	80.4	10.9	0.2	24.1
C-22	2.8	452	1.22	10.8	18	92.5	6.7	0.2	10.1
C-23	4.49	206	1.78	17.5	28	40	11.6	0.2	24.8
D-1 (RS8)	6.05	970	9.64	75.7	16300	1590	222	4.1	85
D-2	5.61	1230	3.97	37.8	50.2	90.8	18.3	0.1	22.8
D-3	6.53	796	3.21	120	48.7	54.1	5.1	0.2	17.8
D-4	7.16	897	3.81	201	43.8	77.8	18.6	0.1	20
D-5	6.77	854	3.89	110	99.7	97.4	9.6	0.2	19.3
D-6	3.22	766	1.4	30.2	18.3	34.4	3.8	0.3	9.2
D-7	7.6	1080	5.15	138	79.6	96.7	10.7	0.1	19.1
D-8	7.51	1420	4.62	154	36.1	116	10.1	0.1	31.2
D-9	6.12	1200	4.36	619	42.1	69.8	5.9	0.2	11.8
D-10	5.04	714	1.79	28.2	22.8	61.2	4.9	0.1	17.7
D-13	4.25	428	2.15	40.5	28.1	53.7	5.6	0.05	12
D-14	6.91	1500	4.15	33.5	22.7	81.5	2.1	0.1	19.4
D-15	5.97	684	2.6	33.1	21.5	52.7	8.3	0.05	17.4
D-17	5.27	3030	8.83	35.3	46.5	70.9	3.9	0.4	16.6
D-18	4.25	1660	5.08	26.7	44.1	66.1	5.5	0.1	11.9
D-19	4	1470	5.09	28	54.3	115	7.4	0.2	200
D-20	5.3	1220	3.06	48.3	22.1	58.4	15.4	0.1	20.7
D-21	5.15	1770	2.89	36.3	23.2	105	6.8	0.05	15.2
D-22	4.33	1650	4.42	32.4	15.8	74.8	3.4	0.1	13.5
D-23	5.27	637	2.52	60.5	50.8	71	6.7	0.1	19.2

D-24	6.17	732	3.25	36.6	26.5	50.8	9.5	0.2	17.5
D-25	5.61	1210	3.72	62.6	63.5	117	11.6	0.3	29.2
D-26	5.92	953	3.22	71.8	58.1	89.7	11.5	0.2	21.2
D-27	4.61	1510	3.82	38	59.4	79.3	7	0.4	22
D-28	5.84	443	2.88	47.8	42.6	91.8	8.2	1.4	25.5
D-30 (RS10)	5.14	304	6.47	8.4	264	37.4	352	0.05	58.4
D-31	5.88	69	0.93	4.8	75.5	12.1	34.3	0.05	57.7
D-32	4.01	1050	3.08	26.3	37.9	57.9	11.4	0.1	22.9
D-35	5.56	947	6.51	48	1590	412	112	0.9	68.4
D-36	4.7	1640	9.83	46.9	2700	653	180	1.5	79.4
D-37 (RS9)	5.59	312	5.48	12.8	567	206	115	0.05	82
D-40	5.83	1030	3.36	59.8	49.8	115	9.6	0.2	48.3
D-41	5.61	2700	6.93	37.5	11.4	66	6.2	0.4	17.1
D-42	4.77	2070	5.76	42.4	31.2	92.2	10	0.3	22.6
D-44	4.74	777	1.83	24.5	160	40.4	2.6	0.05	16.6
D-45	6.03	1030	2.94	38.1	13.1	80.6	6.4	0.3	22.6
D-46	4.51	769	1.79	22.5	14.4	48.5	5.5	0.2	16.4
D-47	6.68	1700	4.18	27.8	32.4	66.5	9.5	0.2	19.7
D-48	6.23	1070	3.23	37	24.3	71.6	7.7	0.3	22.1
D-49	2.53	561	1.61	16.8	15.3	28.9	6.8	0.05	8
D-50	3.37	853	1.66	18	19.2	39.6	6.8	0.05	11.4
D-51	6.74	830	3.79	29.5	20.5	57.1	2.9	0.1	17.6
D-52	5.84	796	2.87	40.6	23.7	49.2	8	0.2	17.4
D-53	5.75	749	2.7	45.4	28.8	54.6	8.5	0.2	16.9
D-54	6.54	1680	3.38	177	29.8	68.1	5.3	0.05	24.6
D-55	7.26	651	2.83	36.2	21.5	53.3	5.9	0.1	18.2
D-56	5.24	434	2.34	22.4	37.2	222	8.3	0.2	22.7
D-57	5.53	761	2.59	34.5	54.7	303	9.8	0.3	33.9
D-58	4.89	666	2.39	20	23.5	49.4	9.4	0.1	14.5
E-1	6.29	1260	5.24	46.8	124	92.4	10.8	0.2	16.2
E-2	6.31	786	3.35	29	34.5	75.3	11.8	0.1	17.3
E-3	6.14	1200	4.42	50.5	56.7	77.9	9.6	0.2	18.5
E-5	4.87	1030	2.74	10.9	17.2	36.6	8.2	0.1	19.9
E-7	9.39	589	4.25	52	49.3	134	20.1	0.1	39.6
E-8	6.25	2670	4.73	41.2	21.1	60.2	16.5	0.1	12.5
E-9	6.4	1210	4.55	51.1	60.5	83.7	9.5	0.2	13.1
E-12	6.25	1470	5.01	51.3	70.8	106	20.7	0.2	15.6
E-13	3.99	378	2.47	17.6	15.5	54.7	12.9	0.1	20.2
E-14	6.36	1270	7.03	59.8	51.1	116	15.8	0.3	25.4
E-15	7.15	1170	5.44	46.1	23.9	134	11.3	0.3	27.5
E-19	6.58	986	4.39	34	299	257	17.4	1	38.5
E-22	8.06	696	4.17	46.8	36.1	109	10.8	0.05	23.8
E-23	6.19	3040	11.9	107	24.7	115	14.6	0.05	16.7
E-24	6.67	1540	6.32	56.1	30.5	80.4	9.8	0.2	21.2
E-25	7.72	1810	5.14	102	47.8	82	29.7	0.3	18.1
E-26	7.13	1620	6.49	37	32.2	77.5	16.8	0.5	17.9
E-27	7.4	1560	2.65	11.2	11.1	57.8	6	0.2	50.4
E-28	5.38	963	2.84	32.4	19.5	66.6	8.4	0.2	20.2
F-1	5.66	1040	7.68	17.3	36.1	82.3	5.9	0.1	15.5
F-2	6.68	1110	5.46	19.5	67	86.2	5.9	0.2	21
F-3	6.28	812	3.68	35.8	22.5	44.7	10.2	0.2	14.9
F-4	6.25	375	2.2	17	17.9	47.3	8.3	0.05	22.9
F-5	6.49	2400	13.1	41.3	27.6	119	10.8	0.05	22.6
F-6	5.79	1200	4.39	35	21.9	54.9	12.4	0.05	18.6
F-7	4.81	681	3.75	26.8	20.5	53.7	10.3	0.1	19.7
F-8	6.38	1070	4.89	39.2	48.2	76.5	17.8	0.3	26.3
F-9	6	1170	5.57	32.8	22.1	52.4	14.1	0.1	17.4
F-10	6.41	958	4.7	36.4	26.6	49.3	16.7	0.05	16.5
F-11	5.71	775	3.89	27	18.1	59.2	14.4	0.1	20
F-12	7.5	1140	5.45	41.1	27	71.2	25.9	0.2	28.5

F-13	7.54	1220	3.89	32.2	24.6	57.6	15.1	0.2	24.1
F-14	4	703	2.68	18.1	18.4	57.7	7.9	0.5	14
F-15	5.36	666	2.38	23.3	30.4	44.6	14.6	1.7	22.5
F-16	4.09	496	1.55	15.3	15.2	28.9	6.3	0.3	14.2
F-17	3.69	582	2.23	12.7	10.7	27.8	7.8	0.05	14.3
F-18	4.25	550	2.19	14.3	12.9	32.2	9.6	0.05	15.1

Appendix 4. Concentrations of elements in unfiltered water samples

Sampling Site	Al µg L^{-1}	Mn µg L^{-1}	Fe µg L^{-1}	Ni µg L^{-1}	Cu µg L^{-1}	Zn µg L^{-1}	As µg L^{-1}	Cd µg L^{-1}	Pb µg L^{-1}
A-1 (E4)	223000	23300	572000	404	127000	4340	840	32.2	8.5
A-2	433	716	780	0.9	89.3	29.6	7.7	0.23	2
A-3	19	590	2110	0.2	3.7	2.5	2.1	0.02	0.16
A-4	9	53	60	0.2	4.4	1.7	4.9	0.01	0.19
A-5	229	43.7	220	0.2	17.4	3.5	5.4	0.03	0.93
A-6	192	23.7	180	0.2	12.8	5.5	6.2	0.03	0.71
A-7	284	42.6	320	0.2	19.8	7	14	0.06	2
A-8	97	5.1	120	0.2	3.5	1.3	2.6	0.005	0.18
A-9	50	4.6	70	0.2	2.2	1.1	2.5	0.005	0.12
A-10	207	6.9	170	0.2	3.5	1.9	0.8	0.005	0.29
A-11 (RW3)	46	7.2	60	0.2	2.6	2.5	2.8	0.005	0.17
A-12 (E1)	22100	33200	197000	173	10500	5210	123	16	1.6
A-13 (E2)	1940	1880	47800	9.1	2550	712	55.9	1.1	30.7
A-14 (E3)	90100	24200	561000	2240	110000	18900	7350	127	158
A-15	33100	8090	819000	466	69300	14700	2910	33.9	473
A-16 (RW1)	17100	7770	79800	392	26300	2500	353	21.9	54.9
A-17 (RW2)	32600	7460	46100	93.7	31500	714	60.2	5.9	1.2
A-18 (RW4)	32400	8190	302000	265	39900	3160	1830	18.1	218
A-19	14300	5040	48900	215	21000	1680	395	13.7	62.8
A-20	16000	5250	48000	261	5250	1770	528	14.9	50.6
A-21 (RW6)	12700	5010	45400	224	23100	1540	373	12.7	43.1
A-21-1	22800	4320	67000	286	21000	2120	690	53.9	177
A-22 (RW7)	41	38.3	60	0.4	4.5	3.6	2.3	0.005	0.26
A-23	7	0.4	10	0.2	3.3	1.7	0.25	0.005	0.06
A-24	432	1330	540	30.7	615	164	5.4	1.7	0.3
A-25	47600	10200	102000	187	38900	1630	104	12.9	2.8
A-26 (E5)	76000	22500	38500	276	127000	1790	5.1	17.3	0.15
A-27	211	731	460	1.6	221	24.4	0.54	0.7	0.29
A-28	475	29.4	480	0.2	12.6	4.5	1.6	0.15	0.27
A-29	246	120	380	1.1	281	48.2	1.6	0.5	0.17
A-30	66600	8190	260000	1190	52500	6970	2920	224	313
A-31	19300	4680	47300	293	15600	1640	573	25.5	64.9
A-32	18300	4190	50900	365	19700	1640	715	32.8	81.9
B-1	543	41.3	1090	63	7.5	39.1	2.5	0.3	0.47
B-2	441	58.5	920	62.3	10.1	41.9	2.7	0.11	0.44
B-3	242	146	610	0.6	1.9	4.5	4.4	0.01	0.25
B-4	446	51.8	740	0.8	2.9	3	2.4	0.005	0.47
B-5	35	56.2	80	0.6	8.9	13.8	0.91	0.07	0.03
B-6	769	43.1	970	0.8	1.9	4.2	1.2	0.005	1.1
B-7	256	130	600	3.5	1.8	3.5	1.4	0.01	0.21
B-8	1310	185	2610	5.7	24.3	16.1	7.7	0.11	10.3
B-9	1290	15900	9410	125	354	2370	5	13.2	10.8
B-10	533	59	810	3.9	4.2	5.6	2.3	0.03	1.2
B-11	365	56.3	380	3.5	8.5	7.5	1.8	0.05	0.41
B-12	77	436	190	3.6	6	12.2	5.6	0.05	0.26
B-13	946	3710	3630	39.1	126	496	4.1	3.8	28.6
B-14	191	17.1	220	0.2	1.9	7.1	1.4	0.005	0.17
B-15	355	18.4	220	0.2	3.4	2.8	1.1	0.02	0.34
B-16	423	32.4	500	0.7	2.1	9.7	2.1	0.02	0.53
B-17	328	29.6	370	1.1	3.3	4.3	3.2	0.01	0.54
B-18	30	8.9	40	0.8	2.8	2.2	5.1	0.005	0.14
B-19	44	14.8	60	0.2	1.6	1.7	1.4	0.005	0.08
B-20	59	18.6	60	0.2	10.5	3.3	3.4	0.04	0.11
B-21	36	15.8	60	0.4	2.6	2.3	4.2	0.005	0.17
B-23	5020	773	7830	10.6	278	205	12.7	1.1	26.6

B-24	1750	186	2470	3.7	70.4	49.2	3.9	0.24	5.6
B-25	988	41.9	1070	2.2	10.6	4.3	1.7	0.02	0.63
B-26	1510	70.4	2010	2.6	5.9	5.3	3	0.03	1
B-27	4260	531	6730	7.9	218	172	10.4	0.8	20.5
B-28	2070	87.8	2800	2.8	5.9	6.6	2.3	0.03	1.2
B-29	660	41.3	760	0.8	2.5	4.1	1.9	0.01	0.71
B-30	3090	279	4440	5.1	12.7	13.9	9.7	0.08	2.2
B-31	772	39.1	970	1.2	3.4	2.6	2	0.01	0.88
B-32	3540	426	5800	6.6	163	140	10.5	0.63	20.4
B-33	396	24.7	500	0.5	3.8	2.3	1.5	0.01	0.38
B-34	485	41.6	590	0.5	2.4	1.6	0.7	0.01	0.56
B-35	1220	313	1830	4.7	74.7	69.3	3.3	0.4	6.3
B-36	350	65.3	490	1.2	2.6	1.9	1.9	0.01	0.35
B-37	427	43.6	420	1.4	3	7.7	3	0.04	1.7
B-38	1300	307	1850	4.6	78.6	69.5	3.2	0.41	7.5
B-39	83	32.4	200	0.2	1.2	2.4	1.2	0.005	0.27
B-40	973	188	1460	4	53.6	54.7	3	0.33	5
B-41	1100	153	1640	3.6	52.6	50.4	3.2	0.26	4.8
B-42	658	64.7	740	0.5	2.3	3.7	0.57	0.02	0.9
B-43	402	38.5	510	0.4	2.1	2.1	0.74	0.01	0.66
B-44	768	48.7	890	1.1	2.8	2.1	2	0.01	0.74
B-45	330	32.9	390	1.8	1.7	3.3	1.5	0.01	0.54
B-46	243	40.7	360	0.4	1.8	2.4	1.2	0.005	0.33
C-1	34	5.5	50	0.2	1.7	1.1	1.1	0.005	0.33
C-2	170	19.1	160	0.2	2	1.5	1.8	0.005	0.14
C-3	9	10.3	20	0.2	1.3	1.1	0.74	0.005	0.05
C-4	175	19.7	170	0.2	2	1.2	1.8	0.005	0.13
C-5	71	10.9	70	0.2	2	1.6	1	0.005	0.17
C-6	66	10.3	80	0.5	2.3	2.4	0.89	0.005	0.18
C-7	40	15.9	50	0.2	1.6	1.5	0.75	0.005	0.14
C-8	117	3.2	110	0.2	1.2	1.3	0.91	0.005	0.32
C-9	24	547	90	0.4	1.4	1.2	2	0.005	0.08
C-10	44	17.4	40	0.2	2.6	1.1	2.8	0.005	0.07
C-11	161	15.5	160	0.2	8.5	3	6.5	0.02	0.46
C-12	6	1.7	30	0.2	0.9	1.3	0.63	0.005	0.005
C-13	67	945	510	1.2	2	1.4	2.3	0.005	0.19
C-14	8	12.9	10	0.2	2.6	1.1	3	0.005	0.13
C-15	60	14.5	40	0.2	31.6	0.95	2.1	0.005	0.17
C-16	101	36.9	140	0.6	11.8	21.7	3.4	0.01	0.91
C-17	13	7	20	0.2	3	3.5	0.67	0.005	0.16
C-18	53	14.9	70	0.2	2.4	3.4	2.1	0.005	0.16
C-19	240	38.7	300	0.4	2.8	3.2	1	0.005	0.25
C-20	48	1390	360	2.3	2.6	14.2	3.4	0.005	0.16
C-21	130	16.8	150	0.2	3.3	5.9	1.4	0.005	0.43
C-22	20	9.3	50	0.2	2.3	4.7	1.1	0.005	0.12
C-23	37	5.5	50	0.3	2.6	4.2	2.1	0.01	0.37
D-1 (RW8)	120	1490	670	37.1	536	127	7.2	1.4	0.47
D-2	102	105	150	1.8	5.1	6.2	2.8	0.02	0.17
D-3	150	22.9	250	6.2	4.2	3.5	2.3	0.005	0.26
D-4	41	9.3	40	3	2.5	20.2	4.6	0.005	0.03
D-5	22	4.9	20	1.8	2.4	2.4	1.7	0.005	0.005
D-6	26	2.2	20	0.2	0.9	1.8	0.23	0.005	0.005
D-7	186	23.3	150	2.8	3.8	1.7	1.2	0.06	0.16
D-8	72	28.6	90	3.4	2.6	1.6	4.1	0.005	0.03
D-9	103	16.7	90	9.9	1.7	10.7	0.7	0.005	0.06
D-10	25	3.4	20	0.2	1.5	4.7	0.4	0.005	0.005
D-11	8	7.2	10	0.9	1.3	0.95	0.8	0.005	0.005
D-12	49	10.9	70	0.9	2.6	2.5	2.1	0.005	0.27
D-13	7	1.1	10	0.2	3.2	2.8	0.18	0.005	0.14
D-14	23	2	40	0.6	0.8	1.3	0.15	0.005	0.08

D-15	93	340	280	0.4	1.9	2.1	0.85	0.005	0.18
D-16	42	10	60	0.9	2.9	3.2	2.2	0.005	0.46
D-17	89	11.4	130	1.1	3.3	2.8	2.3	0.005	0.33
D-18	46	9.1	50	0.9	2.6	4.2	2.3	0.005	0.18
D-19	40	8	40	0.8	2.3	12.4	2.3	0.005	0.14
D-20	2080	144	2720	7.4	4.5	106	2	0.02	3
D-21	119	98.5	130	0.6	39.8	69	1.1	0.005	0.18
D-22	141	10.8	70	0.9	40.7	3	2.3	0.005	0.25
D-23	729	25.2	740	4.3	46.5	6.2	1.1	0.005	0.76
D-24	727	221	890	2.7	45.8	8.3	1.5	0.05	0.81
D-25	473	51.8	450	2.2	9	3.5	0.85	0.005	0.36
D-26	425	10.8	340	2.6	40.3	4	0.83	0.04	0.42
D-27	3170	251	4310	11.3	10.4	28.2	3.7	0.33	6.4
D-28	186	10.7	210	1.1	8.9	2.7	1.2	0.005	0.2
D-29	312	11.4	250	2.4	41.3	3	0.81	0.005	0.3
D-30 (RW10)	292	128	430	7.7	125	20	6.2	0.39	0.5
D-31	383	164	580	6.7	159	22.2	7	0.47	0.79
D-32	345	16.5	320	0.8	10.7	2.5	1.3	0.005	0.35
D-33	392	205	660	7.7	185	23.9	7.3	0.4	0.68
D-35	175	237	280	16.1	158	31.7	5.3	0.92	0.28
D-36	413	321	760	8.2	265	29.9	4.2	0.63	0.34
D-37 (RW9)	221	296	500	15.8	228	36.6	5	1.2	0.32
D-39	239	298	590	8	226	27.9	3.5	0.59	0.2
D-40	63	85.6	170	0.8	9.5	2.9	1.1	0.005	0.13
D-41	165	44	300	2.1	2.6	2.9	1.8	0.005	0.47
D-42	393	47.6	660	3	10.7	6.5	1.7	0.03	1.5
D-44	38	31.3	80	0.7	4.2	6.9	0.93	0.04	0.06
D-45	56	40.3	80	0.7	1.6	2.2	1.8	0.02	0.13
D-46	62	19.3	110	0.3	2.4	2.9	0.76	0.01	0.09
D-47	11	0.9	10	0.2	0.8	0.74	0.26	0.005	0.005
D-49	12	3.5	20	0.2	1.1	2.2	0.57	0.005	0.03
D-50	12	16.3	20	2.3	2.2	10.5	0.68	0.02	0.02
D-52	24	71.1	90	1.5	1.7	9	0.96	0.01	0.01
D-53	27	4	40	0.9	3.2	10.6	0.88	0.005	0.03
D-54	44	78.2	150	2.4	4.5	10.3	0.6	0.03	0.12
D-55	30	17.3	60	0.8	1.6	10.2	0.65	0.005	0.005
D-56	23	95.7	80	0.9	1.2	4	0.64	0.01	0.01
D-57	11	21	30	0.3	5.8	4.5	0.64	0.01	0.13
D-58	13	5	70	0.7	1.4	10	0.51	0.005	0.05
E-1	45	15	60	0.3	3.8	3.4	3.6	0.005	0.17
E-2	132	11.6	130	0.4	8	5.8	2.7	0.005	0.17
E-3	56	6.9	40	0.8	4.9	4.5	1.9	0.005	0.11
E-4	43	8.4	50	0.8	2.8	3.7	2.3	0.005	0.17
E-5	57	10.4	70	0.8	2.5	2.2	2.3	0.005	0.22
E-6	65	9.2	70	1.1	3.8	3.2	2.4	0.005	0.26
E-7	69	11.9	110	1.1	3.8	6.8	2.3	0.005	0.3
E-8	81	314	390	3.4	6.9	5.5	3.3	0.005	0.16
E-9	16	6	20	0.2	3.3	2.8	2.1	0.005	0.09
E-10	126	16	190	1.5	5.4	6.2	2.4	0.02	0.63
E-11	146	17.6	170	1.7	7.8	8.2	2.4	0.01	0.61
E-12	32	21.3	40	0.4	3.5	1.7	5.1	0.005	0.09
E-13	224	14.4	290	2.5	13.8	11.6	1.6	0.02	0.97
E-14	161	21.7	250	1.8	11.1	4.4	1.6	0.01	0.68
E-15	177	39.7	280	2	10.7	5.1	1.8	0.03	0.81
E-16	198	16.5	290	2.1	11.9	5.3	1.6	0.02	0.8
E-17	155	11	220	2.1	11.7	4.3	1.5	0.01	0.6
E-18	154	16.8	220	2	10.6	3.8	1.6	0.01	0.58
E-19	900	140	1910	4	60.9	68	3.1	0.34	9
E-20	1390	155	2370	4.6	71.4	79.8	3.8	0.39	12.8
E-22	39	10.5	60	0.2	0.8	2.9	0.39	0.005	0.005

E-23	187	234	350	3.3	2	3.6	9.4	0.01	0.09
E-24	9	8.2	20	0.9	2.2	9.5	2.5	0.005	0.005
E-25	86	60	280	0.5	0.8	3.6	6.2	0.005	0.005
E-27	161	48.1	420	0.2	1.2	0.74	0.68	0.005	0.08
E-28	47	32.1	150	0.6	1.5	0.53	2.4	0.01	0.01
F-1	114	7.2	110	0.2	1.7	1.8	0.66	0.005	0.16
F-2	716	27.2	540	0.8	3.2	2.6	1	0.01	0.43
F-3	110	33.8	130	0.8	3.7	10.4	2.3	0.01	0.2
F-4	106	7.8	110	0.2	9.5	1.1	0.56	0.005	0.16
F-5	105	4.7	90	0.2	1.8	2.3	0.74	0.005	0.11
F-6	71	31.2	90	0.3	2.1	3.6	1.8	0.01	0.16
F-7	170	30.5	160	0.9	2.1	2.1	2	0.01	0.17
F-8	550	63.3	630	2	3.8	2.5	2.6	0.01	0.53
F-9	75	14.7	90	0.2	1.3	1.9	1.9	0.005	0.08
F-10	64	11.7	70	0.2	2.8	1.7	2.1	0.005	0.13
F-11	63	9.8	80	0.2	1.1	1.7	1.2	0.005	0.17
F-12	144	10.9	180	0.4	2.1	3.4	2.5	0.005	0.55
F-13	183	12.8	200	0.2	0.9	1.8	1.1	0.005	0.13
F-14	76	17	80	0.2	1.4	5.1	1.3	0.005	0.13
F-15	2650	145	2560	3.9	8.4	9.6	3.4	0.03	2.2
F-16	662	111	1080	2.4	8.4	26.9	1.9	0.03	1.6
F-17	165	32.7	180	0.3	1.5	2.9	1.3	0.005	0.16
F-18	355	49.8	330	0.5	1.6	2.7	1.1	0.005	0.2

Appendix 5. Concentrations of elements in filtered water samples

Sampling Site	Al µg L^{-1}	Mn µg L^{-1}	Fe µg L^{-1}	Ni µg L^{-1}	Cu µg L^{-1}	Zn µg L^{-1}	As µg L^{-1}	Cd µg L^{-1}	Pb µg L^{-1}
A-1 (E4)	194000	23600	569000	453	133000	5670	743	34.7	8.5
A-2	6	644	30	2.5	28	20.3	4.7	0.08	0.21
A-3	2	570	1070	2.1	0.2	0.5	0.49	0.01	0.57
A-4	2	47.6	30	2.4	0.2	0.5	3.7	0.01	0.17
A-5	2	10.6	10	0.6	4.1	0.5	3.8	0.01	0.22
A-6	2	7.5	10	0.3	0.2	0.5	4.5	0.01	0.01
A-7	2	6.4	10	0.8	1.6	0.5	12.5	0.01	0.05
A-8	2	0.1	10	0.3	0.2	0.5	1.2	0.01	0.19
A-9	2	0.1	10	0.3	0.2	0.5	1.3	0.01	0.15
A-10	2	0.1	10	0.3	0.2	0.5	0.03	0.01	0.01
A-11 (RW3)	2	0.1	10	0.3	0.2	0.5	1.5	0.01	0.01
A-12 (E1)	3260	32900	191000	190	7690	5660	94.4	16	0.36
A-13 (E2)	39	1590	10	5.7	0.2	5.1	1.8	0.04	0.01
A-14 (E3)	98800	23900	581000	2590	109000	18900	7170	145	165
A-15	17000	5830	24800	470	22100	3280	19.8	23.5	12
A-16 (RW1)	16000	6650	26400	420	24200	3190	17.7	22.2	20.4
A-17 (RW2)	29200	5880	12200	107	30500	999	1.3	6.4	0.45
A-18 (RW4)	14900	6020	19300	280	24200	3010	28.6	15.1	9.4
A-19	10600	5530	11200	234	18900	1840	8.3	13.5	8.9
A-20	12900	5280	2660	289	23100	1760	1.5	15	7.8
A-21 (RW6)	7550	4620	240	219	17200	2020	2.4	14.3	7.8
A-21-1	13700	4540	40200	298	21000	1930	86.3	54.5	73.4
A-22 (RW7)	54	34.9	50	1.6	3.8	10.7	2.4	0.05	1.2
A-23	11	0.5	50	11.3	15.4	9.2	0.16	0.05	1.6
A-24	49	1230	650	219	249	261	2.9	1.9	0.93
A-25	44400	6870	27700	181	29800	1860	3.1	14.8	11
A-26 (E5)	60000	13200	22700	213	124000	2010	2.7	15.6	1.4
A-27	55	716	50	1.6	86.6	36.3	0.36	0.77	0.86
A-28	68	14.1	50	3.6	5.7	69.4	1	0.05	1.1
A-29	68	125	50	3.5	173	57.6	1.5	0.79	4.5
A-30	65500	7940	219000	1180	52500	6130	1740	219	224
A-31	2030	5070	23700	302	13900	1460	25.6	25.8	5
A-32	5330	4770	28700	379	18000	1680	36	32.2	15.4
B-1	48	49.2	260	310	15.4	209	2.6	0.05	2
B-2	11	8.6	50	1.6	4.9	8.1	2.1	0.05	1.6
B-3	11	119	350	59.1	6.9	48.9	3.4	0.16	1.1
B-4	24	41	300	54.6	6.8	42.8	2.1	0.12	1.6
B-5	11	35.7	50	1.6	9.6	20.6	1.2	0.13	16.9
B-6	54	5.4	50	1.6	2.7	7.4	0.78	0.05	0.85
B-7	41	121	130	5.9	1.1	6.4	1.1	0.05	0.85
B-8	42	46.5	50	4	5.5	8.3	4	0.05	3.8
B-9	55	12000	320	117	23.4	1880	0.34	10.5	2.8
B-10	38	20.4	50	4.2	1.1	13.5	1.5	0.05	0.67
B-11	62	21.2	50	3.5	5.1	10.6	1.4	0.05	4.7
B-12	29	447	50	3.4	1.1	14.5	4.4	0.05	0.38
B-13	55	3580	50	33.6	13.3	202	1	2.5	0.53
B-14	40	4.2	50	1.6	1.1	19	1.2	0.05	0.65
B-15	81	4.7	50	1.6	2.3	25.9	0.93	0.05	0.29
B-16	39	13.1	50	1.6	2.7	32.1	1.9	0.05	0.38
B-17	40	7.9	50	1.6	3.2	11.2	3.3	0.05	0.79
B-18	30	7.4	50	1.6	3.5	6.6	5.4	0.05	1
B-19	33	11.7	50	1.6	3.4	8	1.6	0.05	1.2
B-20	29	16.2	50	1.6	4.1	8.2	3.4	0.05	0.87
B-21	32	12.3	50	1.6	2.7	2.6	4.1	0.05	1
B-23	217	522	170	6.2	32.4	27.9	1.4	0.35	0.91

B-24	101	102	80	1.8	12.6	9.1	1.3	0.09	0.35
B-25	109	5.9	120	1.1	6.9	9.2	1.4	0.02	0.46
B-26	286	6	120	0.7	5.1	5.9	2	0.02	0.63
B-27	174	249	120	2.9	17.9	15.6	1.4	0.2	0.55
B-28	60	11.2	70	0.6	3.2	1.8	1.3	0.005	0.24
B-29	46	9.1	60	0.9	2.1	0.3	1.4	0.005	0.08
B-30	21	8	30	0.4	2.9	1.9	6.1	0.005	0.2
B-31	18	6.6	20	0.5	3.4	2.2	1.8	0.005	0.19
B-32	138	208	90	2.6	17.2	14.6	1.5	0.19	0.47
B-33	20	3.4	20	0.3	2.6	2	1.4	0.01	0.22
B-34	25	10.2	40	0.2	2.9	2.5	0.62	0.005	0.18
B-35	75	232	40	4	12.5	15.2	1.2	0.22	0.49
B-36	15	41	60	2	2.4	0.5	1.7	0.01	0.16
B-37	20	19.2	40	0.6	2.6	3.2	3.3	0.02	0.24
B-38	53	211	30	3.8	11	15	1.2	0.19	0.32
B-39	9	24.3	40	0.4	2.5	2.1	1.1	0.01	0.14
B-40	55	88.4	30	3.5	9.2	12.6	1.1	0.12	0.38
B-41	53	32.9	30	2.7	9.2	9.2	1.2	0.11	0.22
B-42	49	5.5	60	0.2	1.5	2.4	0.46	0.005	0.19
B-43	22	3.5	30	0.2	1.5	0.6	0.54	0.005	0.05
B-44	67	10.3	110	4.4	5.5	26.4	1.6	0.005	0.63
B-45	12	15.9	20	0.9	1.3	2	1.1	0.005	0.18
B-46	13	23.3	30	0.5	1.9	2.2	1.1	0.005	0.15
C-1	30	3	50	1.6	1.1	7	0.99	0.05	1.4
C-2	35	9	50	1.6	3.4	24.4	1.1	0.05	0.64
C-3	28	7.2	50	1.6	1.1	10	0.72	0.05	0.87
C-4	51	10.4	50	1.6	3.8	12	1.7	0.05	0.44
C-5	45	7.2	50	1.6	1.1	7	0.9	0.05	9.3
C-6	30	3.5	50	1.6	2.1	7.6	0.84	0.05	1
C-7	40	10	50	1.6	2.1	7.4	0.67	0.05	2.2
C-8	39	1.2	50	1.6	1.1	22.8	0.89	0.05	0.83
C-9	60	521	130	1.6	2.5	15.9	1.9	0.05	9.7
C-10	38	11	50	1.6	2.7	12.4	2.6	0.05	1.6
C-11	39	4.5	50	1.6	5.6	2.6	6.2	0.05	0.45
C-12	30	3.5	50	1.6	1.1	5.4	0.81	0.05	1.5
C-13	30	889	250	1.6	1.1	9.8	2	0.18	1.2
C-14	33	8.4	50	1.6	2.3	5.8	2.7	0.11	1.1
C-15	64	25.9	3540	1.6	4.6	17.2	2.3	0.05	8.2
C-16	49	31.1	50	1.6	7.7	12.8	3.4	0.05	1.1
C-17	50	6.3	50	1.6	4.7	32.8	0.72	0.05	2.7
C-18	83	6.9	50	1.6	3.9	8.4	2	0.05	0.82
C-19	34	21.8	50	1.6	2.1	8.2	0.81	0.05	0.88
C-20	39	1440	50	1.6	1.1	47.5	2.8	0.05	0.75
C-21	21	5	50	1.6	2.3	2.6	0.16	0.05	0.65
C-22	8	8.1	40	0.2	2.6	6	1.2	0.005	0.22
C-23	11	4.9	30	1.4	2	6	2.2	0.01	0.24
D-1 (RW8)	50	1100	50	31.5	114	87.5	2.9	2.5	0.77
D-2	34	92.1	50	1.6	6.6	2.6	0.95	0.2	0.05
D-3	11	4.1	50	4.9	7.8	2.6	0.8	0.05	0.79
D-4	53	5.1	50	4.2	4.1	23.9	3	0.05	7.2
D-5	32	4.7	50	9	3.8	39.7	1.3	0.27	2.9
D-6	78	2.9	50	3.6	2.3	100	0.84	2.1	2.3
D-7	24	8.6	50	1.6	1.1	17.7	1.1	1.1	0.05
D-8	11	19.6	50	1.6	2.2	2.6	3.9	0.82	0.27
D-9	11	9.5	50	7.9	1.1	45.2	0.59	0.05	0.25
D-10	23	2.1	50	1.6	2.1	73	0.16	0.72	0.34
D-11	11	4.9	50	1.6	1.1	15.6	0.77	0.05	0.05
D-12	22	1.9	50	1.6	3.4	2.6	1.9	1.1	0.12
D-13	25	1.2	50	52.5	46.7	5.7	0.16	0.05	1.1
D-14	44	1.3	50	1.6	1.1	2.6	0.16	1.4	17.4

D-15	11	263	50	1.6	3.9	2.6	0.74	0.05	0.55
D-16	11	3.7	50	1.6	2.2	2.6	2.1	0.05	0.15
D-17	11	2.6	50	1.6	2.5	6.8	2.1	0.45	0.05
D-18	11	4.5	50	1.6	3.3	22.9	2	0.71	0.05
D-19	11	3.7	50	1.6	2.4	36.1	1.9	0.18	0.3
D-20	72	14	50	1.6	34.7	56.5	0.57	0.84	0.13
D-21	71	71.2	50	1.6	35.5	106	0.91	0.33	0.05
D-22	71	4.1	50	1.6	34.5	19.1	2.1	10.4	0.05
D-23	109	4.9	70	2.5	15.9	7.6	0.79	0.05	0.55
D-24	76	107	80	1.7	42.6	7.7	1.1	0.05	0.43
D-25	90	41.9	60	1.9	41.6	5.3	1	0.01	0.17
D-26	122	5.9	70	2	17.3	7.5	0.81	0.01	0.21
D-27	50	14	20	0.8	10.7	2.1	2.2	0.04	0.12
D-28	71	6.2	30	1.1	44.2	7.6	1.1	0.05	0.37
D-29	66	6.9	50	1.8	4.4	3.6	0.77	0.05	0.11
D-30 (RW10)	54	111	10	7.4	49.7	15.5	3.5	0.3	0.09
D-31	62	138	10	6	52.4	15.4	3.5	0.26	0.17
D-32	29	5.3	10	0.4	17.3	9.7	1.2	0.05	0.41
D-33	80	155	10	6.4	54.4	15	3.3	0.29	0.15
D-35	49	243	10	16.6	88.7	32.1	3.1	0.86	0.27
D-36	39	343	20	8.5	98	45.9	1.1	0.51	0.05
D-37 (RW9)	46	298	40	15.8	117	41.9	1.6	1.1	0.08
D-39	51	299	20	8	102	33.3	1	0.54	0.09
D-40	12	82.3	50	0.9	8.8	7.7	0.87	0.005	0.05
D-41	11	24.7	20	1.2	2.6	4.8	1.5	0.005	0.05
D-42	25	5.4	20	1.3	3	6.4	1.3	0.005	0.03
D-44	17	32.8	40	2.1	6	10.5	0.92	0.07	0.23
D-45	12	55.8	20	1.2	2.8	4.3	2.9	0.02	0.09
D-46	9	16.6	20	1.9	3.6	6.2	0.81	0.02	0.39
D-47	8	1.2	10	0.4	2	3.9	0.51	0.01	0.16
D-49	13	3.7	10	0.6	3.7	6.5	0.69	0.02	0.23
D-50	4	16.5	20	5.7	2.1	12.4	0.8	0.02	0.02
D-52	13	60.6	50	1.9	2.3	3.4	1.1	0.01	0.05
D-53	8	2.8	20	1.4	3.6	12.8	0.81	0.005	0.07
D-54	17	62.1	70	0.6	5.4	4.7	0.82	0.02	0.15
D-55	9	13.9	30	1.3	1.9	11.1	0.63	0.005	0.05
D-56	7	95.4	70	1.7	1.2	1.2	0.72	0.01	0.23
D-57	27	23	140	1.9	8.5	9.6	0.81	0.01	0.98
D-58	11	5	20	11.4	1.2	3.6	0.64	0.005	0.05
E-1	11	8.2	50	1.6	5.8	2.6	3	0.13	0.43
E-2	25	1.5	50	1.6	1.1	22.2	0.54	0.05	0.56
E-3	24	5.6	50	1.6	2.5	35.2	2.1	0.05	0.35
E-4	11	1.2	50	1.6	1.1	2.6	2.1	0.05	0.05
E-5	22	1.6	50	1.6	2.3	2.6	1.9	0.16	0.05
E-6	11	1.8	50	1.6	2.6	2.6	2.1	1.4	0.36
E-7	26	2.2	50	1.6	2.7	2.6	2	0.05	0.05
E-8	38	208	50	1.6	5.7	6.7	2.7	0.41	0.21
E-9	11	2.7	50	1.6	3.9	7.8	1.9	0.29	3.5
E-10	11	2	50	1.6	2.9	2.6	1.8	0.05	0.05
E-11	11	3.9	50	1.6	4.4	8.7	2	2.3	0.57
E-12	11	12.6	50	1.6	3.3	16.3	4.5	0.05	0.23
E-13	45	3.4	30	1.6	11.7	5.8	1.5	0.01	0.21
E-14	32	21.3	30	1.6	10.3	4.3	1.6	0.005	0.61
E-15	41	25.6	30	1.3	11.9	2.9	1.6	0.005	0.19
E-16	40	4.8	30	1.4	12	3.3	1.5	0.005	0.28
E-17	38	3.2	30	1.4	10	2.3	1.4	0.005	0.18
E-18	32	8.3	30	1.3	10.7	2.4	1.5	0.005	0.16
E-19	39	59.3	10	2.2	21	15.6	0.81	0.15	1
E-20	20	36.6	20	3.6	7.5	13.9	0.87	0.13	0.09
E-22	3	3.3	10	0.4	0.9	3.6	0.39	0.005	0.005

E-23	4	63.3	40	3.7	2	3.7	8.9	0.01	0.01
E-24	3	6.3	10	0.7	2.3	3.7	2.5	0.005	0.01
E-25	14	32.6	30	0.5	1.2	7.2	5	0.005	0.25
E-27	5	3.7	60	0.3	1.2	0.3	0.65	0.005	0.005
E-28	6	28.8	50	1.8	1.6	2.8	2.3	0.01	0.01
F-1	15	5.3	20	0.3	1.6	2.8	0.64	0.005	0.005
F-2	21	5.4	10	1.5	1.9	2.1	0.95	0.01	0.01
F-3	9	21.7	20	0.7	2.6	10.1	2.2	0.005	0.17
F-4	8	3	10	0.5	2	3.4	0.55	0.005	0.14
F-5	16	2.5	10	0.2	1.5	1.6	0.64	0.005	0.01
F-6	8	25.8	20	1.6	1.4	5.1	1.8	0.01	0.01
F-7	13	19.4	10	1.7	1.7	3	1.9	0.01	0.01
F-8	14	15	30	1.8	2.3	5.6	2.5	0.01	0.01
F-9	20	9.2	30	0.4	1.2	2.1	1.8	0.005	0.005
F-10	18	8.5	30	0.2	1.6	1.2	2	0.005	0.02
F-11	16	6.5	20	0.2	1.3	1.9	1.2	0.005	0.03
F-12	50	5.3	40	0.7	1.7	4.4	2.2	0.005	0.05
F-13	30	4	30	0.2	0.7	4.5	1	0.005	0.02
F-14	9	13.5	20	0.5	1.6	2.6	1.3	0.01	0.05
F-15	33	9.1	40	1.9	3.8	94.8	2.8	0.01	0.14
F-16	17	59.2	120	2.9	4	19	1.3	0.01	0.12
F-17	22	25.4	30	0.7	1.7	2.9	1.2	0.005	0.005
F-18	25	32.2	30	0.6	1.3	2.5	1	0.005	0.005

Appendix 6. XRD patterns of river bed sediments downstream from Bor copper mines

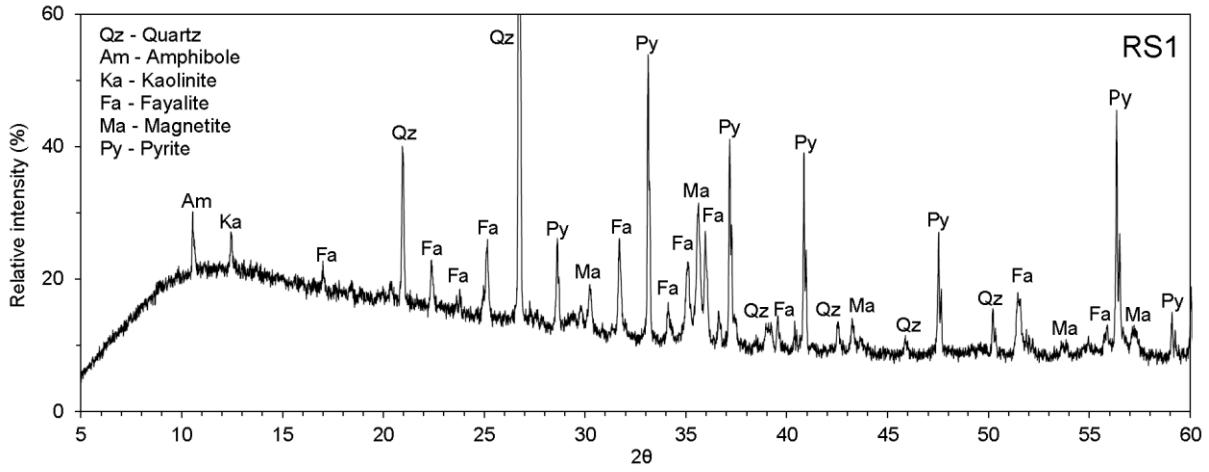

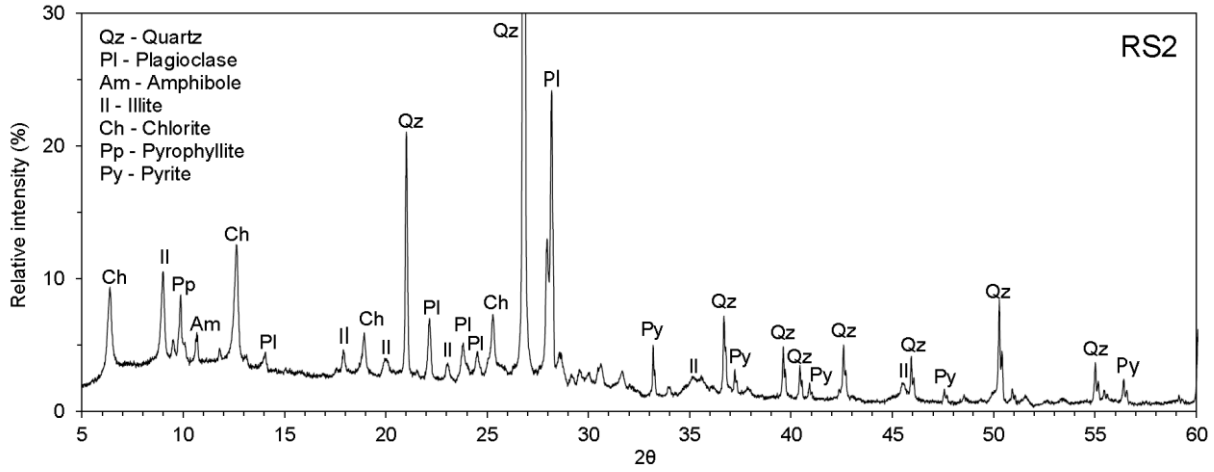

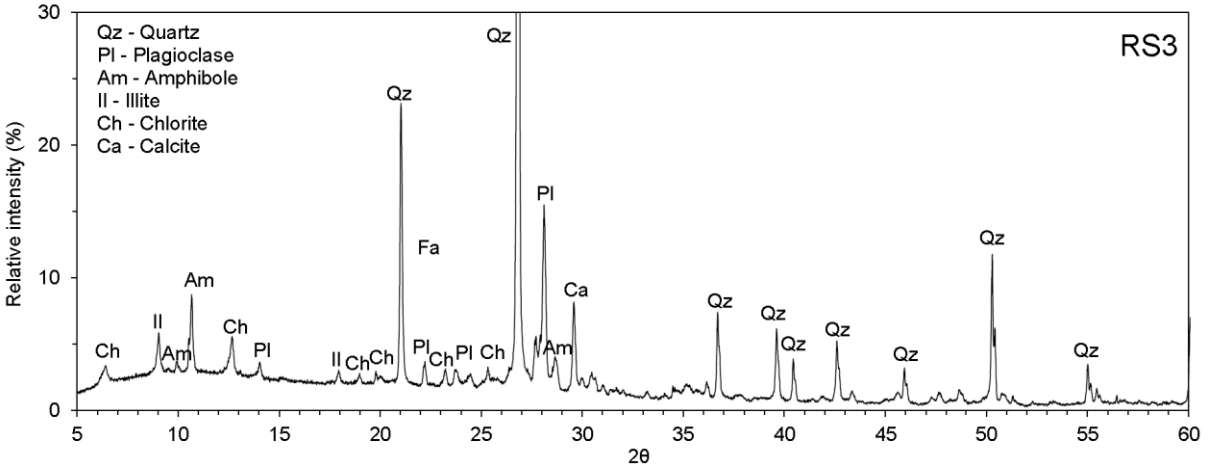

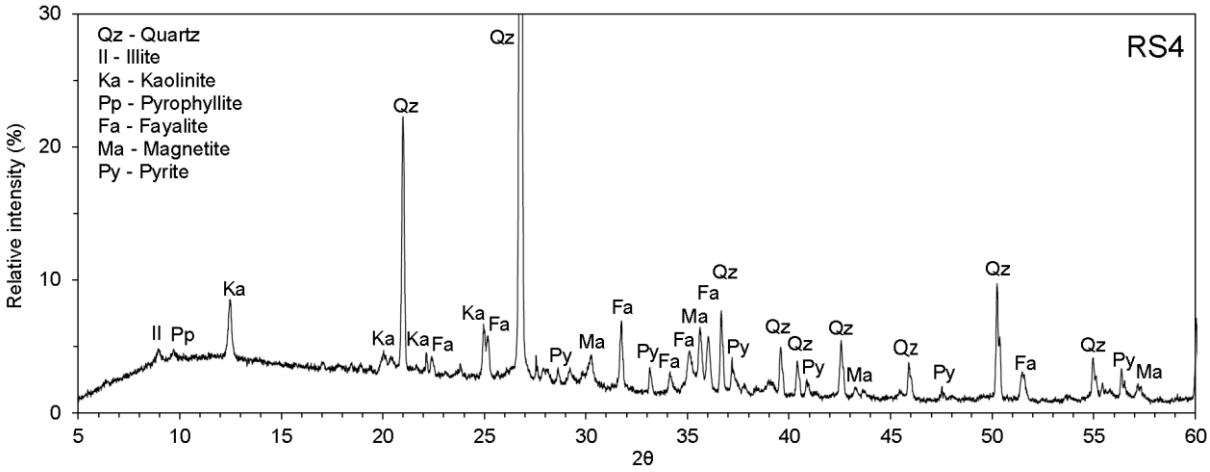
Qz - Quartz
Il - Illite
Ka - Kaolinite
Pp - Pyrophyllite
Fa - Fayalite
Ma - Magnetite
Py - Pyrite
RS4
Relative intensity (%)
2θ

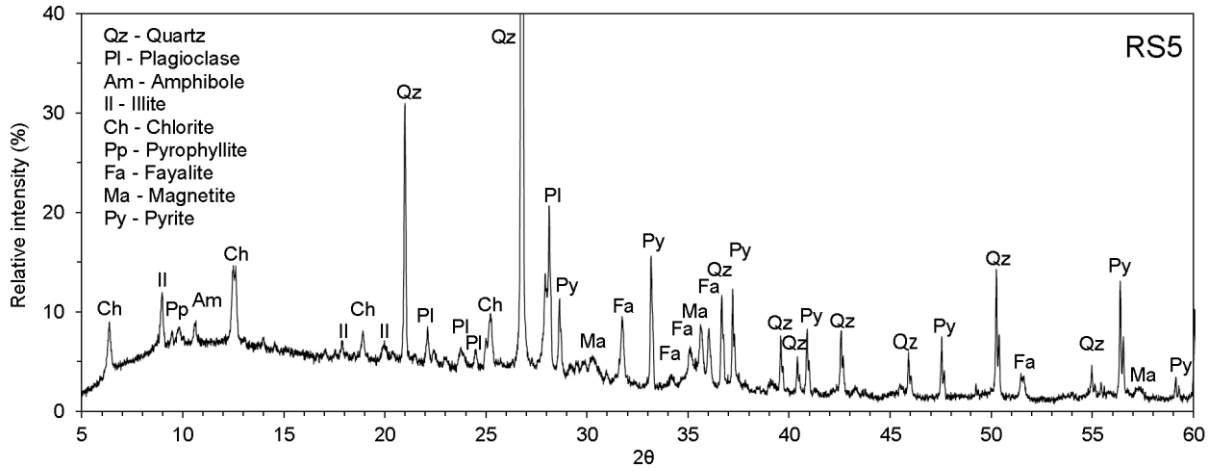
Qz - Quartz
Pl - Plagioclase
Am - Amphibole
Il - Illite
Ch - Chlorite
Pp - Pyrophyllite
Fa - Fayalite
Ma - Magnetite
Py - Pyrite
RS5
Relative intensity (%)
2θ

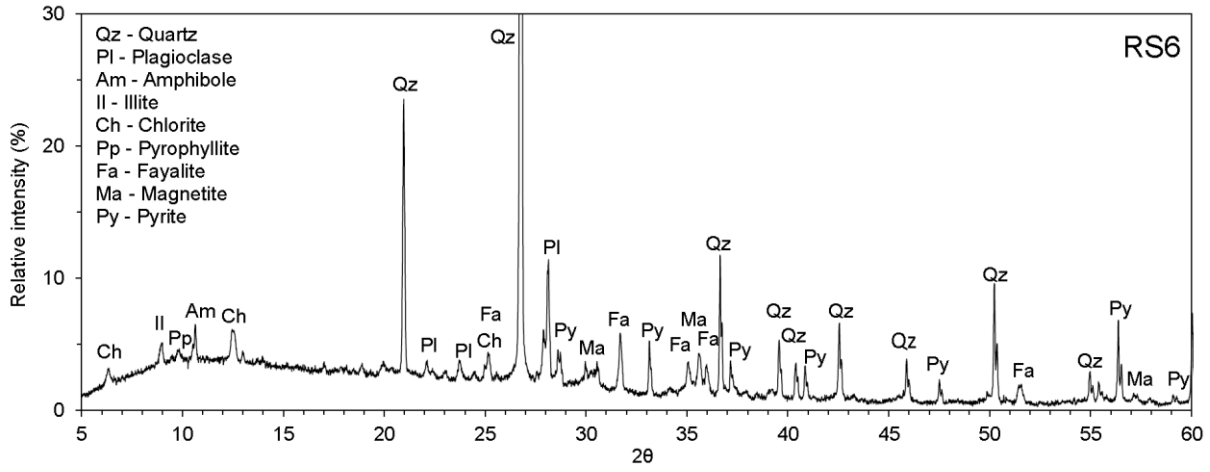
Qz - Quartz
Pl - Plagioclase
Am - Amphibole
Il - Illite
Ch - Chlorite
Pp - Pyrophyllite
Fa - Fayalite
Ma - Magnetite
Py - Pyrite
RS6
Relative intensity (%)
2θ

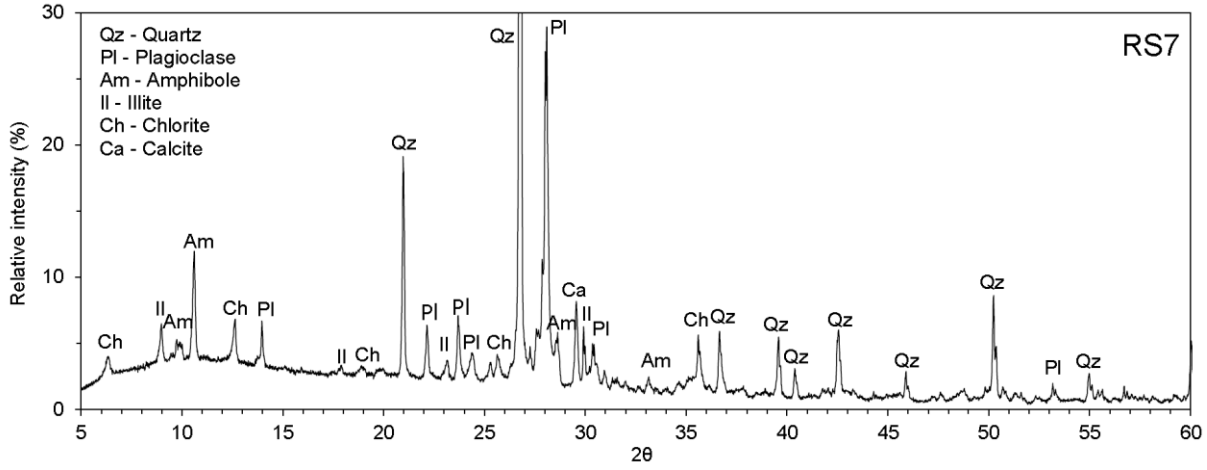
Qz - Quartz
Pl - Plagioclase
Am - Amphibole
Il - Illite
Ch - Chlorite
Ca - Calcite
RS7
Relative intensity (%)
2θ

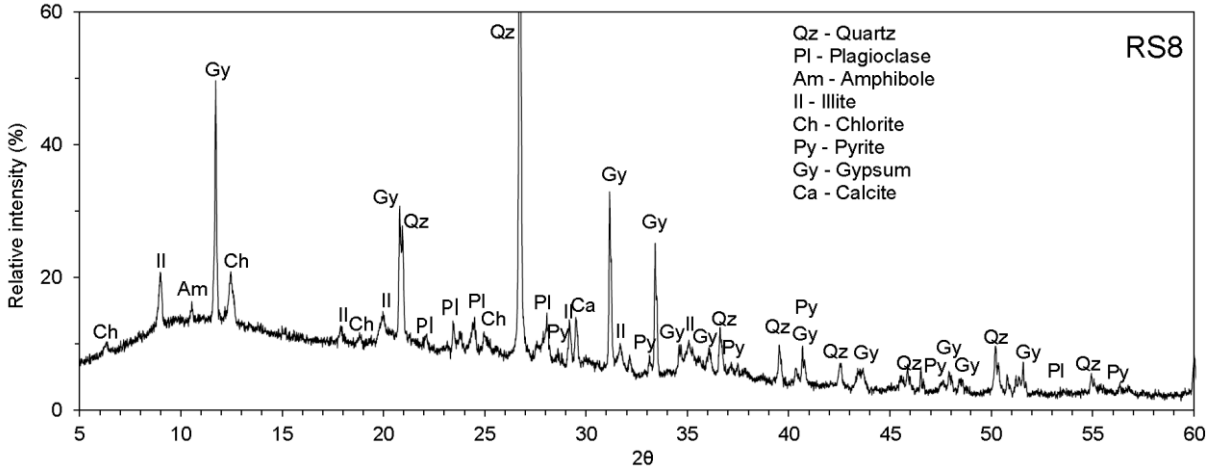
Qz - Quartz
Pl - Plagioclase
Am - Amphibole
Il - Illite
Ch - Chlorite
Py - Pyrite
Gy - Gypsum
Ca - Calcite
RS8
Relative intensity (%)
2θ

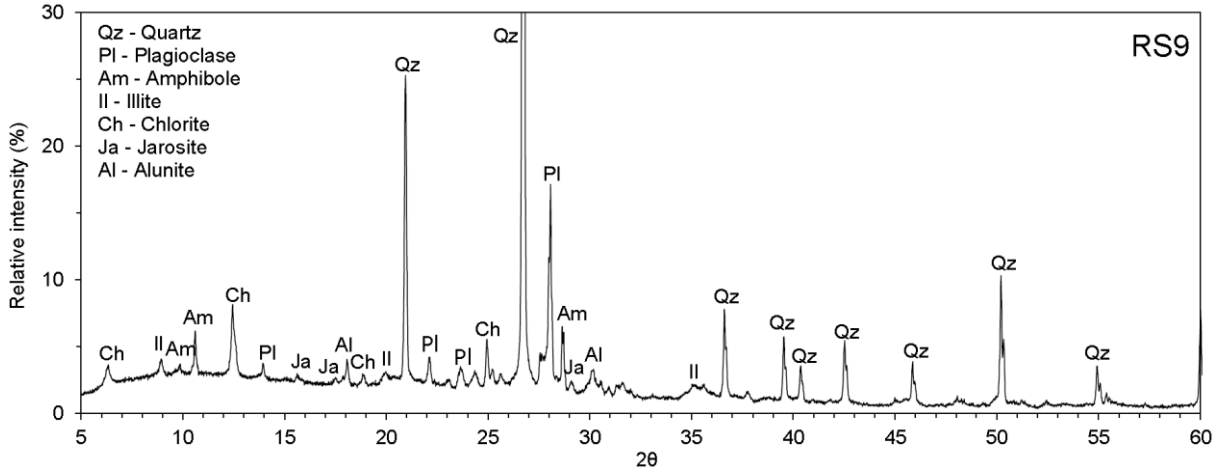
Qz - Quartz
Pl - Plagioclase
Am - Amphibole
Il - Illite
Ch - Chlorite
Ja - Jarosite
Al - Alunite
RS9
Relative intensity (%)
2θ

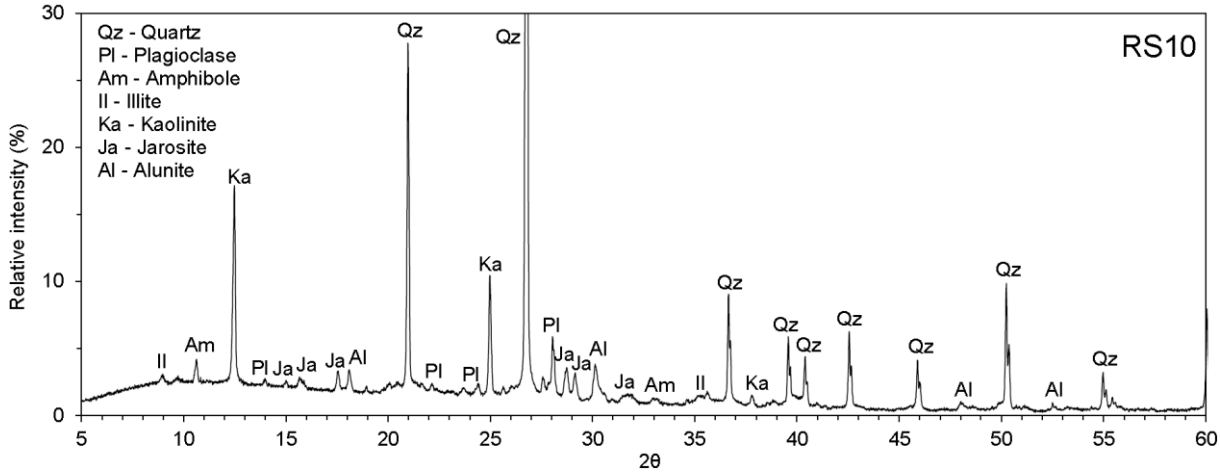
Qz - Quartz
Pl - Plagioclase
Am - Amphibole
Il - Illite
Ka - Kaolinite
Ja - Jarosite
Al - Alunite
RS10
Relative intensity (%)
2θ

Appendix 7. XRD patterns of efflorescent sulfate salts

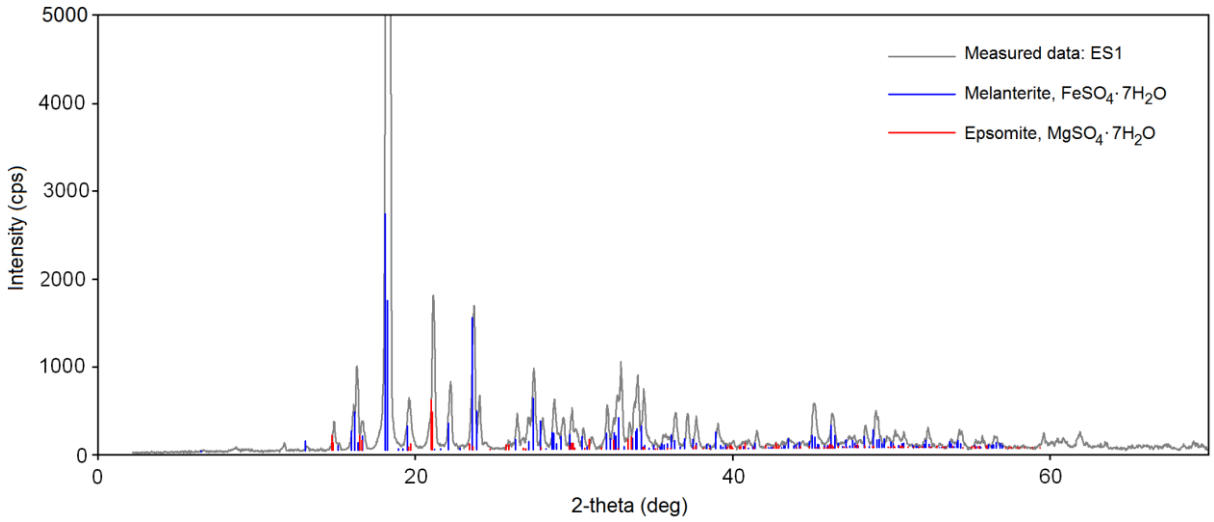

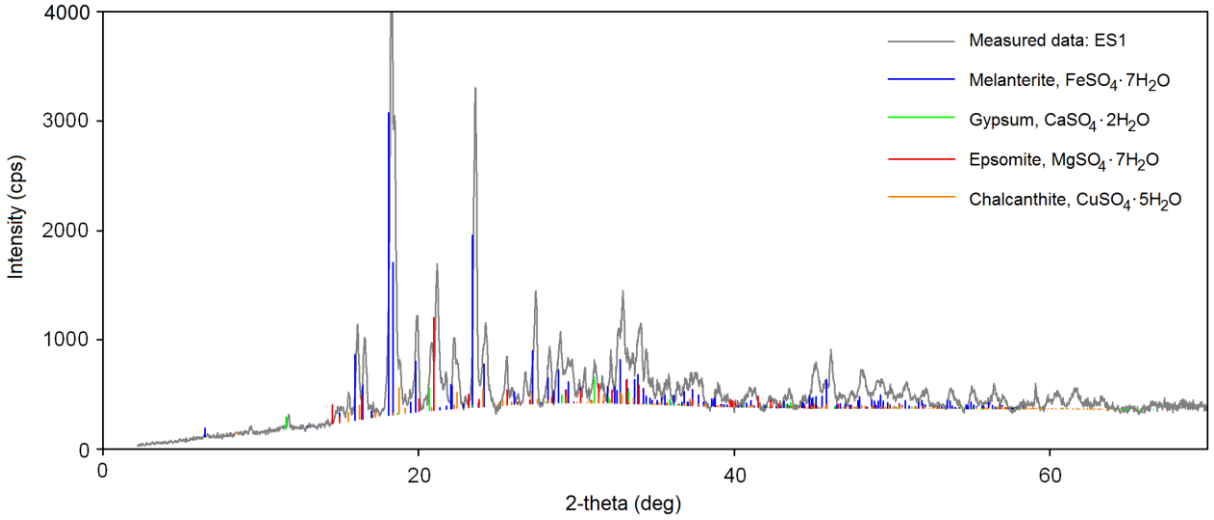

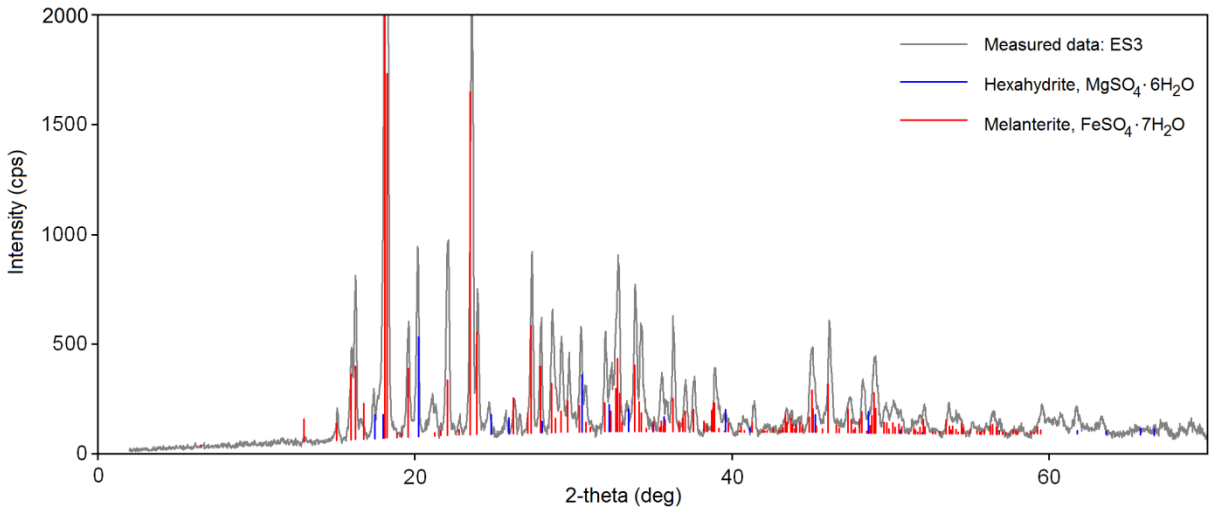

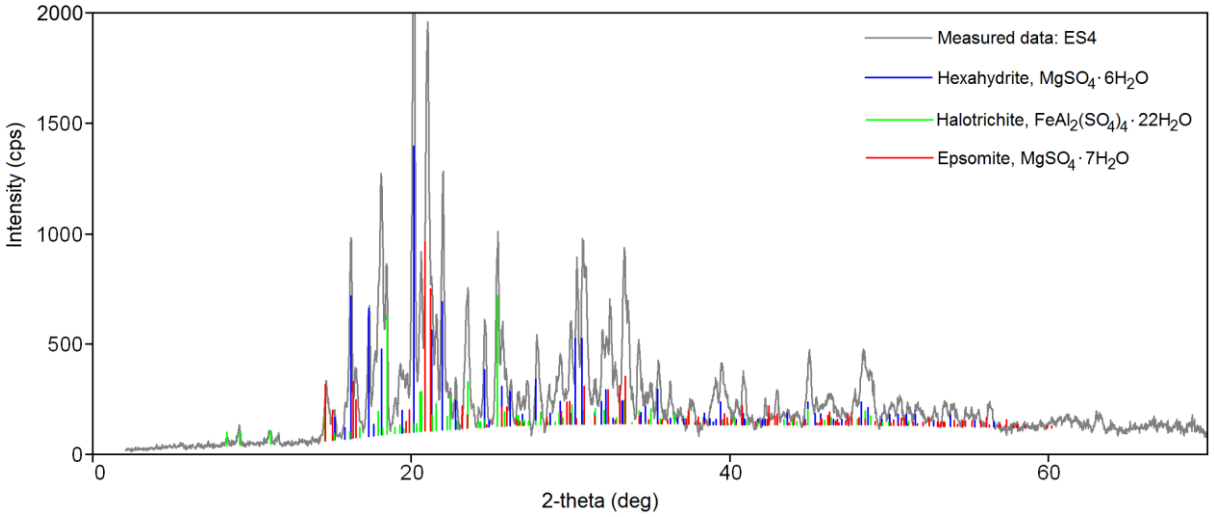
Measured data: ES4
Hexahydrite, $MgSO_4 \cdot 6H_2O$
Halotrichite, $FeAl_2(SO_4)_4 \cdot 22H_2O$
Epsomite, $MgSO_4 \cdot 7H_2O$
Intensity (cps)
2-theta (deg)

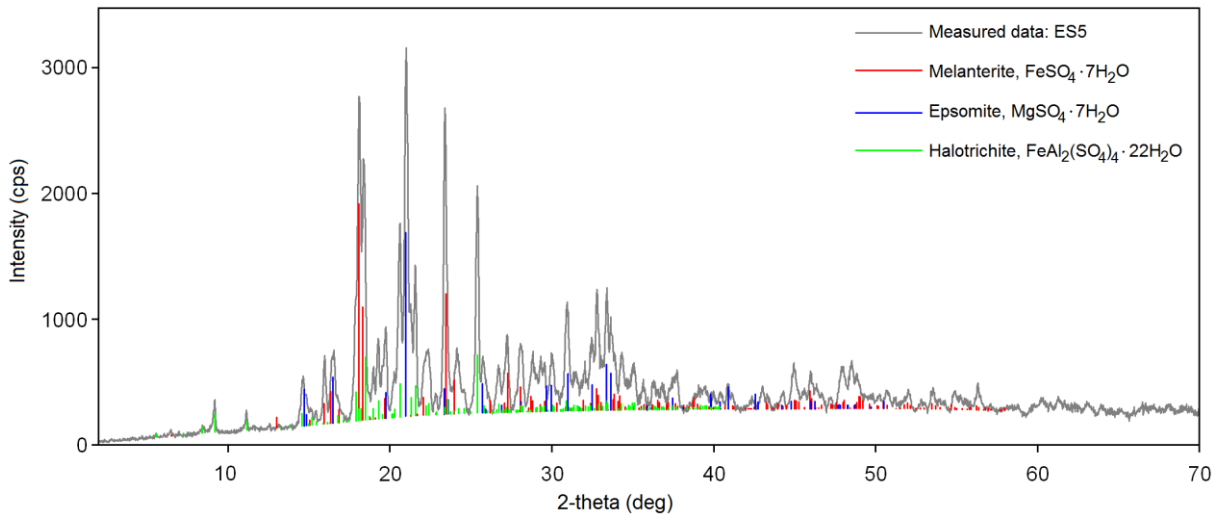
Measured data: ES5
Melanterite, $FeSO_4 \cdot 7H_2O$
Epsomite, $MgSO_4 \cdot 7H_2O$
Halotrichite, $FeAl_2(SO_4)_4 \cdot 22H_2O$
Intensity (cps)
2-theta (deg)